PREPARATION OF POLYELECTROLYTES NANOENCAPSULATED PHASE CHANGE MATERIAL FOR SMART TEXTILES

YUWANDA IAMPHAOJEEN

A THESIS SUBMITTED IN PARTIAL FULFILLMENT
OF THE REQUIREMENT FOR THE DEGREE OF
DOCTOR OF PHILOSOPHY IN NANOSCIENCE AND NANOTECHNOLOGY
COLLEGE OF NANOTECHNOLOGY
KING MONGKUT'S INSTITUTE OF TECHNOLOGY LADKRABANG
2016

การเตรียมแคปซูลพอลิอิเล็กโทรไลต์ระดับนาโนห่อหุ้มวัสดุเปลี่ยนสถานะสำหรับสิ่งทออัจฉริยะ

PREPARATION OF POLYELECTROLYTES NANOENCAPSULATED PHASE CHANGE MATERIAL FOR SMART TEXTILES

ยุวันดา เอี่ยมเผ่าจีน
Yuwanda Iamphaojeen

วิทยานิพนธ์นี้เป็นส่วนหนึ่งของการศึกษาตามหลักสูตรปริญญาปรัชญาดุษฎีบัณฑิต
สาขาวิชานาโนวิทยาและนาโนเทคโนโลยี
วิทยาลัยนาโนเทคโนโลยีพระจอมเกล้าลาดกระบัง
สถาบันเทคโนโลยีพระจอมเกล้าเจ้าคุณทหารลาดกระบัง
พ.ศ.2559
KMITL-2016-NT-D-001-003

หัวข้อวิทยานิพนธ์	การเตรียมแคปซูลพอลิอิเล็กโทรไลต์ระดับนาโนห่อหุ้มวัสดุเปลี่ยน-สถานะสำหรับสิ่งทออัจฉริยะ
นักศึกษา	นางสาว ยุวันดา เอี่ยมเผ่าจีน
รหัสประจำตัว	54670104
ปริญญา	ปรัชญาดุษฎีบัณฑิต
สาขาวิชา	นาโนวิทยาและนาโนเทคโนโลยี
พ.ศ.	2559
อาจารย์ที่ปรึกษา	ผศ.ดร.ปุณณมา ศิริพันธ์โนน

บทคัดย่อ

พอลิอิเล็กโทรไลต์นาโนแคปซูลที่บรรจุด้วย *n*-octadecane (PEL-en-Oc) ถูกเตรียมและตรึงลงบนผ้าฝ้ายอย่างง่ายด้วยกระบวนการสารละลายอย่างอ่อนที่อุณหภูมิห้อง เพื่อสร้างสมบัติการปรับเปลี่ยนอุณหภูมิตามสภาวะแวดล้อม (Thermo-regulating) ให้กับผ้าฝ้าย พอลิอิเล็กโทรไลต์ (PEL) 2 ชนิดที่ถูกใช้เป็นวัสดุเปลือกเพื่อห่อหุ้ม *n*-octadecane ได้แก่ พอลิไดอัลลิลไดเมทิลแอมโมเนียมคลอไรด์ (PDDA) และ พอลิสไตรีนซัลโฟนิกแอซิด (PSS) ในขั้นแรกอิมัลชันของ *n*-octadecane และโซเดียมโดเดซิลซัลเฟต (Oc-SDS) ถูกเตรียมโดยคลื่นเสียงความเข้มสูง จากนั้นจะถูกนำไปผสมกับพอลิอิเล็กโทรไลต์เพื่อสร้างชั้นเปลือกพอลิอิเล็กโทรไลต์ด้วยตนเองเคลือบบนหยดของ Oc-SDS โดยระบบการห่อหุ้มแคปซูล 2 ระบบได้ถูกพัฒนาขึ้น ได้แก่ PDDA แคปซูลห่อหุ้ม *n*-octadecane (PDDA-en-Oc) และมัลติเลเยอร์ PDDA และ PSS แคปซูลห่อหุ้ม *n*-octadecane (PSS(PDDA-en-Oc) หรือ PDDA(PSS(PDDA-en-Oc)) ซึ่งระบบดังกล่าวสามารถสร้างนาโนแคปซูลที่มีโครงสร้างเปลือกและแกนลักษณะทรงกลม (Globular core-shell structure) ได้สำเร็จ ซึ่งนาโนแคปซูล PDDA-en-Oc มีค่าความร้อนแฝง (Latent heat) อยู่ในช่วง 99 - 152 จูลต่อกรัม โดยมีขนาดอนุภาคเฉลี่ยอยู่ในช่วง 101 - 256 นาโนเมตร ขนาดอนุภาคเฉลี่ยของนาโนแคปซูล PDDA-en-Oc เพิ่มขึ้นเมื่อเพิ่มความเข้มข้นของ PDDA จาก 1 ถึง 14 มิลลิโมลาร์ เนื่องจากการก่อตัวของ PDDA ที่มีการจัดเรียงรูปร่าง (Conformation) และความหนาของชั้นเปลือกที่แตกต่างกัน นอกจากนี้การเพิ่มความเข้มข้นของ PDDA จะช่วยปรับปรุงประสิทธิภาพในการห่อหุ้ม *n*-octadecane เป็นผลให้ปริมาณของนาโนแคปซูล PDDA-en-Oc เพิ่มขึ้น ยิ่งปริมาณแคปซูลเพิ่มสูงขึ้นจะส่งผลให้ค่าความร้อนแฝงที่เกิดขึ้นขณะเปลี่ยนสถานะของ *n*-octadecane ยิ่งมากขึ้น ประสิทธิภาพในการห่อหุ้มเป็นแคปซูล จะมีค่าสูงสุดที่ 65.99 % เมื่อใช้ PDDA 10 มิลลิโมลาร์ในกระบวนการห่อหุ้ม โดยแคปซูลจะมีค่าความร้อนแฝงสูงสุดประมาณ 151.97 จูลต่อกรัม นาโนแคปซูลที่มีเปลือกหลายชั้นจะแสดงประจุบนพื้นผิวที่แตกต่างกันขึ้นกับชนิดของพอลิอิเล็กโทรไลต์ที่

เป็นเปลือกชั้นนอกสุด การเพิ่มจำนวนชั้นของเปลือกในกระบวนการห่อหุ้มสามารถเพิ่มเสถียรภาพทางความร้อนของนาโนแคปซูล PSS(PDDA-en-Oc) และ PDDA(PSS(PDDA-en-Oc)) ได้ อย่างไรก็ตามขนาดอนุภาคเฉลี่ยและปริมาณค่าความร้อนแฝงของนาโนแคปซูลที่มีเปลือกห่อหุ้มเป็น 2 และ 3 ชั้น (นาโนแคปซูล PSS(PDDA-en-Oc) และ PDDA(PSS(PDDA-en-Oc)) ตามลำดับ) มีค่าน้อยกว่านาโนแคปซูล PDDA-en-Oc ที่มีเปลือกห่อหุ้ม 1 ชั้น ชั้นของพอลิอิเล็กโทรไลต์ที่เป็นเปลือกห่อหุ้ม *n*-octadecane สามารถรักษาวัสดุแกน *n*-octadecane ระหว่างการเปลี่ยนสถานะได้อย่างมีประสิทธิภาพ

นาโนแคปซูล PEL-en-Oc ที่เตรียมได้จากขั้นตอนก่อนหน้าสามารถถูกตรึงลงบนผ้าฝ้ายที่ถูกทำให้มีประจุบวกได้สำเร็จโดยใช้ ระบบการแช่อย่างง่าย 2 ระบบ ได้แก่ (1) การเคลือบสลับด้วยสารยึดติด PSS และนาโนแคปซูล PDDA-en-Oc ที่เปลือกชั้นนอกสุดมีประจุบวก และ (2) การเคลือบโดยตรงด้วยนาโนแคปซูล PSS(PDDA-en-Oc) ที่เปลือกชั้นนอกสุดมีประจุลบ โดยในระบบที่ใช้ PSS และ PDDA-en-Oc จะปรับความเข้มข้นของสารยึดติด PSS ในช่วง 1 – 50 มิลลิโมลาร์ ยิ่งเพิ่มความเข้มข้นของ PSS ปริมาณของ PDDA-en-Oc นาโนแคปซูลที่ถูกตรึงลงบนผ้าฝ้ายจะยิ่งเพิ่มขึ้น ส่วนในระบบนาโนแคปซูล PSS(PDDA-en-Oc) เมื่อตรึงนาโนแคปซูลที่เตรียมโดยใช้ PSS เข้มข้น 10 มิลลิโมลาร์ในการสร้างเปลือกชั้นนอกสุดให้มีประจุลบลงบนผ้า พบว่ายิ่งเพิ่มระยะเวลาแช่ที่นานมากขึ้นจะส่งผลให้ปริมาณของนาโนแคปซูล PEL-en-Oc ที่ตรึงบนพื้นผิวผ้าฝ้ายมากขึ้น นอกจากนี้การเพิ่มปริมาณของนาโนแคปซูล PEL-en-Oc ที่ถูกตรึงลงบนพื้นผิวของผ้าฝ้ายสามารถทำได้โดยการแช่สลับตัวอย่างผ้าฝ้ายในระบบสารยึดติด PSS/นาโนแคปซูล PDDA-en-Oc หรือระบบนาโนแคปซูล PEL-en-Oc ที่เปลือกชั้นนอกสุดที่มีประจุตรงกันข้ามกัน

ผ้าฝ้ายที่ถูกตรึงด้วยนาโนแคปซูล PEL-en-Oc แสดงสมบัติการปรับเปลี่ยนอุณหภูมิ โดยยังสามารถรักษาสมบัติการหายใจได้ (Breathability) ของผ้าฝ้ายตั้งต้นไว้ได้ เมื่อปริมาณของนาโนแคปซูล PEL-en-Oc นาโนแคปซูลที่ถูกตรึงลงบนผ้าฝ้ายเพิ่มขึ้นจะแสดงสมบัติการปรับเปลี่ยนอุณหภูมิได้ยาวนานขึ้น ผ้าฝ้ายที่ถูกตรึงด้วย PSS และนาโนแคปซูล PDDA-en-Oc จำนวน 5 รอบ สามารถลดอุณหภูมิบนพื้นผิวได้สูงที่สุด นั่นคือ ประมาณ 2.5 องศาเซลเซียสเป็นเวลามากกว่า 10 นาที เมื่ออุณหภูมิแวดล้อมมีค่าประมาณ 50 องศาเซลเซียส ยิ่งไปกว่านั้นตัวอย่างนี้ยังสามารถรักษาปริมาณ PDDA-en-Oc ที่ถูกตรึงไว้ได้ถึง 77 เปอร์เซ็นต์จากปริมาณเริ่มต้นภายหลังผ่านการซักล้างเป็นจำนวน 15 รอบ

คำสำคัญ : วัสดุเปลี่ยนสถานะ, พอลิอิเล็กโทรไลต์, การสร้างแคปซูลระดับนาโน, สิ่งทออัจฉริยะ

Thesis Title	Preparation of polyelectrolytes nanoencapsulated phase change material for smart textiles
Student	Miss Yuwanda Iamphaojeen
Student ID	54670104
Degree	Doctor of Philosophy
Program	Nanoscience and Nanotechnology
Year	2016
Thesis Advisor	Asst. Prof. Dr. Punnama Siriphannon

ABSTRACT

Polyelectrolyte encapsulated *n*-octadecane (PEL-en-Oc) nanocapsules were facilely prepared and immobilized on cotton fabrics *via* soft solution processing at ambient temperature in order to generate thermo-regulating property. Two types of polyelectrolytes (PEL), i.e cationic poly(diallyldimethyl-ammonium chloride) (PDDA) and anionic poly(4-styrenesulfonic acid) (PSS), were used as shell forming materials to encapsulate *n*-octadecane. Firstly, an emulsion of *n*-octadecane and sodium dodecyl sulfate (Oc-SDS) was prepared by high intensity sonication and then mixed with the polyelectrolytes to create the self-assembled PEL shell coated on the Oc-SDS primary droplets. Two encapsulation systems were developed, i.e. PDDA encapsulated *n*-octadecane (PDDA-en-Oc) and multilayer PDDA and PSS encapsulated *n*-octadecane ((PSS(PDDA-en-Oc) or PDDA(PSS(PDDA-en-Oc))), in which they successfully produced the nanocapsules with globular core-shell structure. The PDDA-en-Oc nanocapsules possessed the latent heat value in the range of 99 – 152 J/g with the average particle size in the range of 101 – 256 nm. The average particle size of PDDA-en-Oc increased with increasing of PDDA concentration from 1 to 14 mM due to the formation of different PDDA conformation and shell thickness. In addition, the increase of PDDA concentration could improve the efficiency of *n*-octadecane encapsulation, bringing about the increase PDDA-en-Oc nanocapsules quantity. The higher amount of encapsulated nanocapsules, the higher latent heat quantity was obtained during the phase transition of *n*-octadecane. The highest encapsulation efficiency was obtained at about 65.99 % when the 10 mM PDDA was used in the encapsulation process, in which it possessed the highest latent heat of

about 151.97 J/g. The nanocapsules with multilayer shell possessed different surface charges depending on the type of outermost polyelectrolyte shell. The increase of number of shell layer used in encapsulation process could enhance the thermal stability of (PSS(PDDA-en-Oc) and PDDA(PSS(PDDA-en-Oc)) nanocapsules. However, the average particle size and latent heat quantity of nanocapsules with double and triple shell layers (i.e. (PSS(PDDA-en-Oc) and PDDA(PSS(PDDA-en-Oc)) nanocapsules, respectively) were lower than those of PDDA-en-Oc single shell nanocapsules. The polyelectrolyte shell could effectively preserve the *n*-octadecane core material during the phase transitions.

The as-prepared PEL-en-Oc nanocapsules were successfully immobilized on the cationized cotton fabrics using two facile soaking systems, i.e. (1) stepwise coating with the PSS binder and PDDA-en-Oc nanocapsules having positively charged outermost shell, and (2) direct coating with the PSS(PDDA-en-Oc) nanocapsules having negatively charged outermost shell. In the PSS and PDDA-en-Oc system, the concentration of PSS binder was varied in the range of 1 – 50 mM. The higher PSS concentration, the higher quantity of PDDA-en-Oc nanocapsules was immobilized on the cotton fabrics. In the PSS(PDDA-en-Oc) system, the nanocapsules produced by using 10 mM PSS for creating the negatively charged outermost shell were used for immobilization. The longer soaking time, the higher quantity of PSS(PDDA-en-Oc) was obtained on the cotton fabrics. In addition, the increase of quantity of PEL-en-Oc nanocapsules immobilized on the cotton fabric could be obtained by stepwise soaking the cotton samples in the system of PSS binder/PDDA-en-Oc nanocapsules or the system of PEL-en-Oc nanocapsules having oppositely charged outermost shell.

The PEL-en-Oc immobilized cotton fabrics exhibited the thermo-regulating property, while preserved the breathability of starting cotton fabric. The prolonged duration of thermo-regulating action was obtained when increasing the quantity of PEL-en-Oc immobilized on the cotton fabric. The cotton sample immobilized with 5 cycles of PSS and PDDA-en-Oc nanocapsules exhibited the highest reduction of surface temperature, i.e. ~2.5 $^{\circ}$C for longer than 10 min when the surrounding temperature was about 50 $^{\circ}$C. In addition, this sample could retain about 77 % of original quantity of immobilized PDDA-en-Oc after 15 washing cycles.

Keywords : Phase change material, Polyelectrolyte, Nanoencapsulation, Smart textiles

Acknowledgments

I would like to take this opportunity to express my sincere thanks to my thesis advisor, Asst. Prof. Dr. Punnama Siriphannon for her invaluable help. She is the best advisor in my mind. She teaches and advises me not only the research methodologies but also many other methodologies in life. I would not have achieved these successes without all the support from her.

In addition, I would like to express my sincere gratitude to Assoc. Prof. Dr. Taweechai Amornsakchai, Asst. Prof. Dr. Apiluck Eiad-Ua, Asst. Prof. Dr. Darinee Phromyothin and Dr. Tosapol Maluangnont for reading and criticizing this thesis.

Special thanks to Royal Golden Jubilee Ph.D. program (RGJ) of the Thailand research fund (TRF) and Thai government's budget for fiscal year 2016 for financial support, Research Institute of Textile Chemistry and Physics, University of Innsbruck, AUSTRIA for cooperation, and Synchrotron Light Research Institute, Thailand for the XPS analysis.

Finally, I am very thankful to my teachers, my family and my friends for all their support throughout the Ph.D. period.

Miss Yuwanda Iamphaojeen

Contents

Contents (Cont.)

Contents (Cont.)

List of Tables

List of Tables (Cont.)

List of Figures

List of Figures (Cont.)

List of Figures (Cont.)

List of Figures (Cont.)

Abbreviations

Oc	:	*n*-octadecane
SDS	:	Sodium dodecyl sulfate
PDDA	:	Poly(diallyldimethylammonium chloride)
PSS	:	Poly(4-styrenesulfonic acid)
CHTAC	:	3-chloro-2-hydroxypropyl trimethyl ammonium chloride
MB	:	Methylene Blue
EO	:	Eosin B
PEL	:	Polyelectrolyte
Oc-SDS	:	SDS encapsulated *n*-octadecane, *n*-octadecane nanoemulsion
PEL-en-Oc	:	Polyelectrolyte encapsulated *n*-octadecane
PEL-en-colOc	:	Polyelectrolyte encapsulated colored *n*-octadecane
PDDA-en-Oc	:	PDDA encapsulated *n*-octadecane
PDDA-en-colOc	:	PDDA encapsulated colored *n*-octadecane
PSS(PDDA-en-Oc)	:	PSS encapsulated PDDA-en-Oc (Double polyelectrolyte shell layer encapsulated *n*-octadecane)
PDDA(PSS(PDDA-en-Oc))	:	PDDA encapsulated PSS(PDDA-en-Oc) (Triple polyelectrolyte shell layer encapsulated *n*-octadecane)
Cat-cot	:	Cationized cotton
Cat-cot/PSS	:	PSS coated on Cat-cot
Cap+	:	Nanocapsules with positively charged outermost shell
colCap+	:	Colored nanocapsules with positively charged outermost shell
Cap-	:	Nanocapsules with negatively charged outermost shell
colCap-	:	Colored nanocapsules with negatively charged outermost shell
Cat-cot/PSS/Cap+	:	Cap+ immobilized on Cat-cot/PSS
Cat-cot/Cap-	:	Cap- immobilized on Cat-cot
Cat-cot/(PSS/Cap+)	:	Multi-cycle of PSS and Cap+ immobilized on Cat-cot
Cat-cot/(Cap-/Cap+)	:	Multi-cycle of Cap- and Cap+ immobilized on Cat-cot

Abbreviations (Cont.)

DLS	: Dynamic light scattering
TEM	: Transmission electron microscopy
DSC	: Differential scanning calorimetry
TGA	: Thermogravimetric analysis
FE-SEM	: Field emission scanning electron microscopy
XPS	: X-ray photoelectron spectrometry
UV-Vis	: UV-Visible spectrophotometry
EKA	: Electrokinetic analysis
IR	: Infrared
WVTR	: Water vapor transmission rate

Chapter 1
Introduction

1.1 Background

Since a textile is one of the basic human needs for livelihood; therefore, the demand for textile products rapidly increases with the massive growth of human population, leading to the highly competitive markets. Some competitive strategies are either through lowering prices and/or through creating the value-added products. Textile finishing process is one of the most common and attractive method to create the value-added textile products with various special properties obtained from finishing agents, e.g. fragrances [1-3], skin softener [4], flame retardants [5-6], phase change material [7-9], insect repellents [10-11], and antimicrobials [12-14], etc. However, the textile finishing processes always commonly use high concentration of finishing agents in order to deliver enough finishing agents to textile products. The increase of finishing agent concentration in the treatment processes bring about the remaining of the excess chemicals after treatment, in which the extravagant use of finishing agents increases not only the production costs, but also the toxic residues in the water effluents.

From the above mentioned limitation of general finishing processes, this research aims to create the value-added products by immobilization of phase change materials (PCMs) on cotton fabric in order to create thermo-regulating textile and development the efficient process for PCM finishing using less amount of chemicals. The thermo-regulating textile is an intelligent textile that can maintain the core body temperature during the extreme temperature changes. Since the rapidly change in climatic environments between outdoors and indoors, from hot to cold conditions can cause a serious effect on human health [15]. One of the possible ways to protect human from heat-related illness, especially in case of sudden change in temperature, is the usage of thermo-regulating textiles.

The PCMs work by melting and crystallization at the specific temperatures. When the PCMs change state from solid to liquid, the PCMs absorb large quantities of latent heat from the surrounding area. Conversely, the PCMs release large quantities of latent heat to the surrounding area when they change state from liquid

to solid. The suitable PCMs for thermo-regulating clothes should be non-toxic, non-corrosive, non-flammable, chemical inert, ease of availability and changing phase at temperature between 15 and 35 °C. One of the most preferred PCMs for clothing are linear chain hydrocarbons known as paraffin waxes (or *n*-alkanes, C_nH_{2n+2}), e.g. *n*-hexadecane, *n*-heptadecane, *n*-octadecane, *n*-eicosane, etc., due to their high latent heat values and appropriate phase change temperatures [16].

Among large number of techniques for incorporating the PCMs to fabric, the commonly used technique is encapsulation PCMs by thin shell materials and then immobilization of PCMs capsules on fabrics. The encapsulation could make PCMs easy-to-use and handle, prevent leakage and loss of PCMs in frequent phase transition process, enhance the thermal and mechanical stabilities of the PCMs and protect PCMs from the outside environments.

In this study, the effective method for PCM encapsulation and immobilization on cotton fabric has been proposed *via* the electrostatic interaction of polyelectrolyte. Firstly, the *n*-octadecane PCM was nanoencapsulated by polyelectrolyte using polyelectrolyte multilayer emulsion technique in order to create charged *n*-octadecane nanocapsules. The nanocapsules could increase the heat-transfer areas between the PCM and environment and reduce the amount of chemical reagent used for thermo-regulating action. The cotton fabrics were subsequently coated with the *n*-octadecane nanocapsules using layer-by-layer (LbL) technique, resulting in the immobilization of *n*-octadecane nanolayers on the cotton fabric. The PCM nanolayer finishing was considered to preserve the original properties of cotton fabric, i.e. soft touch and comfortable to wear, while exhibit the thermo-regulating property with long-lasting performance. In addition, the proposed processes were simple and eco-friendly because they used low amount of non-toxic chemicals and low energy consumption, resulting in the reduction of residual chemicals and production costs. Therefore, these processes of nanocapsule formation and immobilization could fulfill the development of eco-friendly textile finishing.

1.2 Objective of study

1. To prepare the PEL-en-Oc nanocapsules and immobilize the PEL-en-Oc nanocapsules on cotton fabric.

2. To investigate the effect of PEL-en-Oc preparation parameters on characteristics and thermal properties of PEL-en-Oc nanocapsules.

3. To investigate the effect of immobilization conditions on characteristics, thermo-regulating and some physical properties of treated fabrics.

1.3 Scope of study

1. Preparation of SDS encapsulated *n*-octadecane (Oc-SDS) using various conditions as follows:

- Oc concentration : 2.5, 5, 7.5, 10 and 15 ml/L
- Sonication time : 5, 10, 15, 20 and 30 min.

2. Preparation of polyelectrolyte encapsulated *n*-octadecane (PEL-en-Oc)

2.1 Single layer of PEL-en-Oc (PDDA-en-Oc) using various concentrations of PDDA solution, i.e. 1, 2, 4, 6, 8, 10, 12 or 14 mM

2.2 Multilayers of PEL-en-Oc (PSS(PDDA-en-Oc), PDDA(PSS(PDDA-en-Oc)))

3. Characterization of PEL-en-Oc nanocapsules by various techniques, i.e. transmission electron microscope (TEM), dynamic light scattering (DLS), differential scanning calorimetry (DSC) and thermogravimetric analysis (TGA) in order to determine the formation mechanism of polyelectrolyte along the Oc-SDS micelles surface

4. Immobilization of PEL-en-Oc nanocapsules on cationized cotton fabrics.

4.1 Stepwise soaking in PSS solution and PDDA-en-Oc emulsion using various concentrations of PSS solution, i.e. 1, 5, 10, 20, 30, 40 and 50 mM.

4.2 Direct soaking in PSS(PDDA-en-Oc) emulsion using various soaking time, i.e. 5, 10, 15, 20 and 30 min.

5. Multi-cycle immobilization of PEL-en-Oc nanocapsules on cationized cotton fabric.

5.1 Stepwise soaking in PSS solution and PDDA-en-Oc emulsion using various PSS/PDDA-en-Oc treatment cycles, i.e. 1 - 5 cycles.

5.2 Stepwise soaking in PSS(PDDA-en-Oc) and PDDA-en-Oc emulsion using various nanocapsule layers, i.e. 1 - 5 layers.

6. Characterization of treated fabric by various techniques, i.e. field emission scanning electron microscope (FE-SEM), X-ray photoelectron spectrometer (XPS), electrokinetic analyzer (EKA), UV-Visible spectrophotometer (UV-Vis), and colorimeter

in order to determine the formation mechanism of PEL-en-Oc nanocapsules on cotton fabric.

7. Determination of the amount of PEL-en-Oc nanocapsules on treated fabric and thermo-regulating property of treated fabrics by various techniques, i.e. UV-Vis, colorimeter and infrared thermography camera.

8. Determination of the breathability and washing durability.

1.4 Expected results

1. High efficiencies and eco-friendly methods for PCM encapsulation and immobilization on cotton fabric which can create the value-adding of textile products and reduce the amount of toxic residual chemicals and energy consumption were obtained.

2. The concept and knowledge of the facile encapsulation method developed in this research can be applied not only the PCM finishing agent, but also the others oil based finishing agents.

3. The concept and knowledge of the effective and eco-friendly method for immobilization of finishing agent, which can preserve the original properties of natural fiber while exhibit special properties with long-lasting performance, can be applied to the other treatment processes in textile industry.

Chapter 2
Theory and Literature reviews

2.1 Thermo-regulating textiles

The thermo-regulating textile is an intelligent textile that can maintain the core body temperature during the extreme temperature changes. Since the rapidly change in climatic environments between outdoors and indoors, from hot to cold conditions can cause a serious effect on human health [15]. One of the possible ways to protect human from heat-related illness, especially in case of sudden change in temperature, is the usage of thermo-regulating textiles which have been developed by incorporating phase change materials (PCMs) into the fabric. The PCMs work by melting and crystallization at a specific temperature. When the PCMs change state from solid to liquid, the PCMs absorb large quantities of latent heat from the surrounding area. Conversely, the PCMs release large quantities of latent heat to the surrounding area when they change state from liquid to solid.

The benefits of PCMs incorporated textiles are as follows [17] :

- Cooling and heating effects occur through the heat absorption and emission of the PCMs.
- Thermo-regulating effect from either heat absorption or heat emission of the PCMs can keep the temperature of a surrounding area almost constant
- Thermal barrier effect from either heat absorption or heat emission of the PCMs can regulate the heat flux from the human body into the environment and adopts it to the thermal needs (i.e. activity level, ambient temperature).

2.1.1 Phase change materials (PCMs) for textile products

The first application of PCMs was developed in the early 1980s by NASA in aerospace field in order to improved the thermal protection and against the extreme temperature fluctuations in the outer space [18]. From the original application of astronauts' suits, nowadays the PCMs incorporated textiles are in the market place for general consumer products as given below [19-26].

- Casual clothing, e.g. shirt, T-shirt, underwear, jackets, etc.
- Bedding and accessories, e.g. pillows, mattress cover, blankets, sleeping bag, etc.
- Sportswear, e.g. active wear, gloves for ice climbing and snowboard, underwear for cycling and running, etc.
- Medical applications, e.g. surgical clothing, patient bedding materials, bandages and products to regulate patient temperature in intensive care units, incontinence products, etc.
- Shoe and accessories, e.g. ski boots, golf shoes, mountaineering boots, race car drivers' boots, etc.
- Automotive textiles, e.g. seat cover, automobile interior, etc.
- Building textile materials, e.g. architectural structural embedded in concrete, in roof and in others material, etc.

For the applications in thermo-regulating textile, the PCMs should exhibit the phases transition within a temperature range that make human feel comfortable, i.e. T_m = 18–36 °C, therefore; they are suitable for making all-season protective outfits [27]. A large number of PCMs with melting temperature in this temperature range have been reported, in which these materials possess various phase change temperature, latent heat (ΔH) and heat storage capacities. The main categorizations of PCMs are inorganic and organic PCMs as given below [26,28,29].

2.1.1.1 Organic phase change materials

The commonly used organic PCMs are paraffins and fatty acids.

A. Paraffins

The paraffins mainly consist of straight chain *n*-alkanes, i.e. $CH_3–(CH_2)_n–CH_3$, in which they are non-toxic, non-corrosive, inexpensive, chemically stable, abundant sources of raw material. They have wide range of melting temperature depending on the number of carbon atoms, therefore; they would be convenient for various usages. The melting points of paraffin waxes increase with the increase of their chain length due to the increase of the induced dipole attractions between *n*-alkane chains [30-36].

Polyethylene glycol (PEG) is a group of commercial paraffin waxes with high energy storage densities, wide range of melting temperatures and

inexpensive price. The repeating unit of PEG is oxyethylene $(-O-CH_2-CH_2-)_n$ with each end of chains incorporating with hydroxyl group. The melting temperature of PEG increases with the increase of molecular weight of PEG due to the lowering of segmental mobility [37-40].

B. Fatty acid

The general formula of all fatty acids are given by $CH_3(CH_2)_{2n}\cdot COOH$. The fatty acids have high latent heat of fusion values in comparison with other paraffins. Moreover, the fatty acids show the reproducibility of freezing and melting without supercooling and they are also mild corrosive. However, the main disadvantage of fatty acid is their costs, which are 2–2.5 times higher than the technical grade paraffins [41-48].

Some common organic PCMs for thermo-regulating textile applications are listed in Table 2.1 [26,28-48].

Table 2.1 Thermal properties of some common organic PCMs

Organic PCMs	Chemical formula	T_m (°C)	ΔH_m (J/g)
A. Paraffin wax			
n-Hexadecane	$CH_3(CH_2)_{14}CH_3$	18 – 19	237
n-Heptadecane	$CH_3(CH_2)_{15}CH_3$	22	171
n-Octadecane	$CH_3(CH_2)_{16}CH_3$	28	242
n-Nonadecane	$CH_3(CH_2)_{17}CH_3$	32 – 33	222
n-Eicosane	$CH_3(CH_2)_{18}CH_3$	36 – 37	247
n-Heneicosane	$CH_3(CH_2)_{19}CH_3$	39 – 41	201
n-Docosane	$CH_3(CH_2)_{20}CH_3$	42 – 45	157
PEG M_w ~600	$(-O-CH_2-CH_2-)_n$	22.2	108.4
PEG M_w ~1000		32	149.5
PEG M_w ~1500		46.5	176.3
B. Fatty acid			
Acetic acid	CH_3COOH	16.7	184
Capric acid	$CH_3(CH_2)_8\cdot COOH$	36	152
Eladic acid	$C_8H_7C_9H_{16}\cdot COOH$	47	218

2.1.1.2 Inorganic phase change materials

The commonly used inorganic PCMs are salt hydrates. The inorganic salt hydrates are solid compounds containing '*n*' water molecules in their structures. The salt hydrates have some attractive properties, i.e. high latent heat of fusion per unit volume, high thermal conductivity, non-flammability, their availability and moderate costs compared to the organic PCMs. On the other hand, the salt hydrates have some disadvantages, i.e. incongruent melting and supercooling. The incongruent melting causes the phase separation because the *n* moles of water are insufficient to dissolve one mole of salt, resulting in the supersaturated solution at the melting temperature. The solid salts settle down to the bottom of the container due to their high densities and they cannot recombine with water during the reverse freezing process, resulting in the reduction of phase transition cycles of PCMs. The supercooling is a phenomenon that liquid turns into a solid below its normal crystallization temperature due to its weak nucleation property. Some salt hydrates are listed in Table 2.2 [26,29,49-54].

Table 2.2 Thermal properties of some salt hydrates PCMs

Salt hydrates PCMs	T_m (°C)	ΔH_m (J/g)
$FeBr_3 \cdot 6H_2O$	21.0	105
$Mn(NO_3)_2 \cdot 6H_2O$	25.5	148
$FeBr_3 \cdot 6H_2O$	27.0	105
$CaCl_2 \cdot 12H_2O$	29.8	174
$LiNO_3 \cdot 2H_2O$	30.0	296
$LiNO_3 \cdot 3H_2O$	30.0	189
$Na_2CO_3 \cdot 10H_2O$	32.0	267
$Na_2SO_4 \cdot 10H_2O$	32.4	241
$KFe(SO_4)_2 \cdot 12H_2O$	33.0	173
$CaBr_2 \cdot 6H_2O$	34.0	138
$LiBr_2 \cdot 2H_2O$	34.0	124
$Zn(NO_3)_2 \cdot 6H_2O$	36.1	134
$FeCl_3 \cdot 6H_2O$	37	223
$Mn(NO_3)_2 \cdot 4H_2O$	37.1	115

Table 2.2 (continued)

Salt hydrates PCMs	T_m (°C)	ΔH_m (J/g)
$Na_2HPO_4 \cdot 12H_2O$	40	279
$CoSO_4 \cdot 7H_2O$	40.7	170
$KF \cdot 2H_2O$	42	162
$MgI_2 \cdot 8H_2O$	42	133
$CaI_2 \cdot 6H_2O$	42	162
$K_2HPO_4 \cdot 7H_2O$	45	145
$Zn(NO_3)_2 \cdot 4H_2O$	45	110
$Mg(NO_3) \cdot 4H_2O$	47	142
$Ca(NO_3) \cdot 4H_2O$	47	153
$Fe(NO_3)_3 \cdot 9H_2O$	47	155

2.1.2 Encapsulation of PCMs

Before incorporating the PCMs to fibers and/or fabrics, the PCMs would be encapsulated in thin shell materials, in which they were easy-to-use and handle. In addition, the encapsulation could prevent leakage and loss of PCMs in frequent phase transition process, enhance the thermal and mechanical stabilities of the PCMs, protect PCMs from the outside environments and increase heat-transfer area [55-57].

Encapsulation is a process of enclosing particles or droplets with a continuous film to produce capsules. Capsules consist of two main parts i.e. core and shell materials, as show in Fig. 2.1. The core material contains active ingredient, while the shell material covers the core material.

The shape of the capsule is mainly depended on the nature of the core material and/or the deposition process of the shell material. For example, the capsule may have irregular shape if the core material is a solid or crystalline material. But, the capsule may have a regular shape with simple spherical capsule containing a single droplet if the core material is a liquid. Figure 2.2 shows the general form of capsules [58].

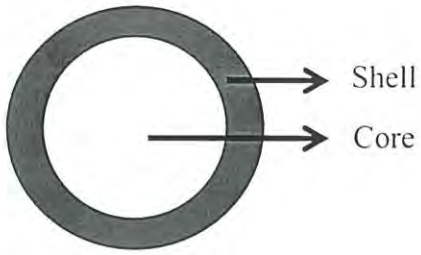

Figure 2.1 General capsule structure

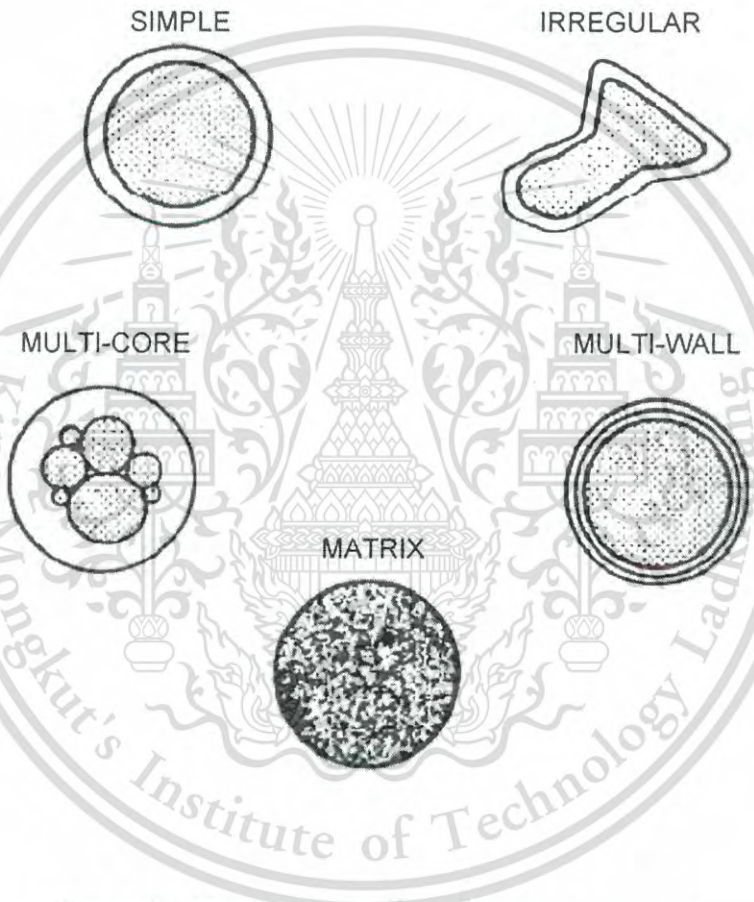

Figure 2.2 Morphologies of various microcapsules

There are two main methods for PCMs encapsulation, i.e. physical and chemical methods. The physical methods (e.g. spray drying, solvent evaporation, centrifugal extrusion, etc.) result in relatively large and rough surface capsules in comparison with the chemical methods [59]. From this point of view, the chemical methods have been, therefore, studied and developed by various research groups using different encapsulation systems and several kinds of capsule shell [60-100].

Some literature reviews are shown below.

Cho J.S. *et al.* [68] fabricated the microcapsules containing phase change material for thermally adaptable fiber application. The microcapsules of about 1 μm in diameter were prepared using the interfacial polycondensation method from toluene-2,4-diisocyanate (TDI) and diethylenetriamine (DETA) monomers in the emulsion system. Octadecane and poly(ethylene glycol) nonyl phenyl ether (NP-10) were used as phase change material and emulsifier, respectively. Polyurea microcapsules were formed not only by reaction between TDI and DETA but also by reaction of TDI with hydrolyzed TDI at the interface. The TDI was reacted with DETA in the weight ratio of 3:1. Some portion of the NP-10 nonionic surfactant having hydroxyl groups could react with the TDI to form urethane. The efficiency of octadecane encapsulation increased with the decreasing of the core content.

Zhang H. and Wang X. [78] fabricated resorcinol-modified melamine–formaldehyde encapsulated *n*-octadecane by *in situ* polymerization using sodium salt of styrene-maleic anhydride copolymer (SMA), sodium dodecyl sulfate (SDS), or polyvinyl alcohol (PVA) with weight average molecular weight of 22,000 as emulsifiers. The microcapsules fabricated by using SMA emulsifier with the core/shell weight ratio of 75/25 had average particle size below 20 μm with the latent heat of 146.5 J/g and encapsulation efficiency of about 92%, in which they were higher than those of the others. In addition, the confinement effect of *n*-octadecane inside the microcapsules also resulted in the significant decreasing in the latent heat of phase change (214.6 J/g).

Wei L. *et al.* [79] studied the effects of dropping rate of MF prepolymer on the surface morphology, dispersibility and thermal stability of the microcapsules fabricated by *in situ* polymerization using melamine–formaldehyde (MF) resin as shell and *n*-octadecane as core. The flocculation of microcapsules and their surface roughness decreased with the decreased in dropping rate of the MF prepolymer. However, the thermal stability regularly increased with the decreasing of the dropping rate. The average diameter of microcapsules was about 2.2 μm with narrow size distribution. The latent heat of the microcapsules containing 59 wt% *n*-octadecane was 144 J/g.

Zhang X.X. *et al.* [80] studied the effects of stirring rate, emulsifier content and cyclohexane content on diameters, morphology, phase change properties and thermal stabilities of the microcapsules containing *n*-octadecane with

melamine-formaldehyde shell prepared by *in situ* polymerization. The diameters of the microcapsules decreased with the increase of stirring rate, emulsifier content and cyclohexane content. The diameters showed slight effect on the melting behaviour of microcapsules, but significant effect on the crystallization behavior. Two crystallization peaks were observed from the DSC when the diameters of the microcapsules were decreased. The thermal stability of microcapsule increased with the increase of stirring rates and emulsifier content. The cyclohexane content had no significant effect on the thermal stability of microcapsule. The microcapsules fabricated with stirring rate of 6000 rpm and TA emulsifier content of 20 g had a mean particle size of 2.4 μm with latent heat of 172 J/g.

Fang Y. *et al.* [81] synthesized the PCM nanocapsules containing *n*-octadecane with polystyrene shell by ultrasonic-assisted mini-emulsion *in situ* polymerization. The nanocapsules were regular spherical shape with the particle size ranged from 100 nm to 123 nm. The phase change temperature of nanoencapsulated PCM was very closer to that of *n*-octadecane, and its latent heat was about 124.4 J/g.

Sarı A. *et al.* [89] studied on the preparation and characterization of polymethylmetracrylate (PMMA) microcapsules containing *n*-octacosane as phase change material for thermal energy storage. The microcapsules were prepared by emulsion polymerization. The DSC results showed that the latent heat of fusion of the microencapsulates was 86.4 J/g. TGA analysis indicated that the microcapsules had good thermal stability. Based on the results, it was concluded that the PMMA microencapsuled *n*-octacosane have good energy storage potential.

Chen Z-H. *et al.* [90] synthesized the nanocapsules containing *n*-dodecanol phase change material as core and polymethyl methacrylate (PMMA) as shell by mini-emulsion polymerization with polymerizable emulsifier DNS-86 and co-emulsifier hexadecane (HD). The effects of polymerizable emulsifier and co-emulsifier on the properties of nanocapsules were studied. The results showed that the thermal properties of nanocapsules were greatly affected by the methods of HD addition and the amounts of DNS-86 and HD. The addition of HD into water phase was helpful for the encapsulation of n-dodecanol. When the mass ratios of DNS-86 to *n*-dodecanol and the mass ratios of HD to *n*-dodecanol were 3% and 2%, respectively, the latent heat of phase change and the encapsulation efficiency of

nanocapsules reached to the maximum values of 98.8 J/g and 82.2%, respectively. Spherical nanocapsules with mean diameter of 150 nm with the phase change temperature of 18.2 °C were obtained, in which they possessed good potential for energy storage.

You M. *et al.* [99] synthesized the microcapsules containing *n*-octadecane using styrene (St)-divinybenzene (DVB) copolymer shells by suspension-like polymerization. The effects of stirring rates and monomers/*n*-octadecane mass ratios on the average diameter and phase change properties of microcapsules were investigated. The average diameters of microcapsules decreased with the increase of stirring rate. When the monomers/*n*-octadecane mass ratio of 1:1 was used, the enthalpy of microcapsule reached the highest value of 126 J/g. The thermal decomposition temperature of microcapsule was about 230 °C, which is higher than that of microcapsule using melamine-formaldehyde shell.

Sánchez L. *et al.* [100] fabricated the microcapsules containing various PCMs (i.e. paraffin wax PRS®, tetradecane, PEG 800, PEG 1000, Rubitherm® RT27, Rubitherm® 20 and nonadecane) with a polystyrene shell by suspension polymerization. The paraffin wax PRS®, tetradecane, Rubitherm® RT27, Rubitherm® 20, nonadecane could be encapsulated by this method and formed as core-shell structure. However, the PEG could not be encapsulated because of its hydrophilic nature. It could be observed that the diameter, the latent heat of phase change and the amount of microcapsules were varied depend on the kind of PCM used in the preparation.

2.2 The encapsulation of PCMs by self-assembled polyelectrolyte

Since the chemical polymerization techniques commonly performed in the high energy consumption systems and used toxic chemicals, therefore; they are considered to be the main drawbacks of the encapsulation of PCMs through the chemical polymerization. To overcome the mentioned disadvantages, a soft solution technique for PCMs nanoencapsulation by self-assembled polyelectrolyte has been proposed in this research. The self-assembled polyelectrolyte nanoencapsulation is considered to be simple technique that performs in an aqueous system, using low amount of non-toxic chemicals and low reaction temperature, leading to the environmentally friendly technique.

The self-assembly of polyelectrolyte encapsulation can be performed by stepwisely assembled polyelectrolyte layer on the droplet of oil-in-water emulsion *via* electrostatic interaction as shown in Fig. 2.3 [101]. Firstly, a primary emulsion is prepared by high-shear agitating the oil phase within the aqueous phase containing the charged hydrophilic emulsifier, resulting in the formation of charged emulsifier-coated oil droplets dispersed within an aqueous continuous phase. Then, an oppositely charged polyelectrolyte is added to the primary emulsion, resulting in the secondary emulsion that contains oil droplet coating by two-layer of emulsifier-polyelectrolyte interface. This step can be repeated to form oil droplets coated with three or more layers interfaces [101-103]. If more than one layer of polyelectrolyte is coated on the droplets, the inner layer of polyelectrolyte tends to be more densely packed and have more limited motion than the outermost layer [103].

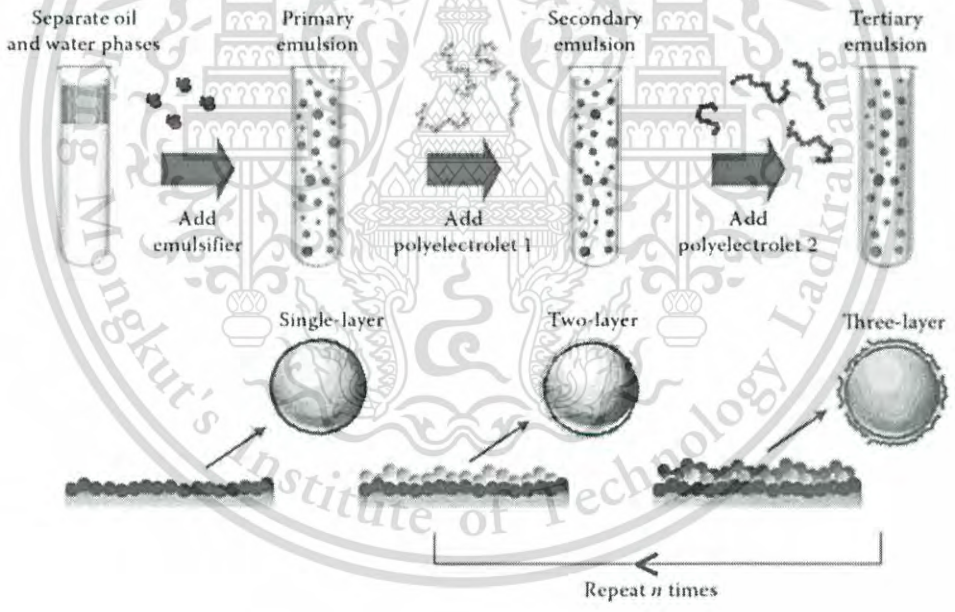

Figure 2.3 Schematic representation of PCMs encapsulation by self-assembled polyelectrolyte

2.2.1 Emulsion

An emulsion is a dispersion of one liquid phase (the dispersed or internal phase) in another immiscible phase (the continuous or external phase), typically created by rupturing the dispersed phase down to tiny droplets through mechanical

agitation devices. According to the mode of dispersion, the emulsions can be commonly classified as given below [101,104,105].

(1) Oil-in-water (O/W system), or direct emulsion; i.e. a system consisting of oil droplets dispersed in an aqueous phase.

(2) Water-in-oil (W/O system), or inverse emulsion; i.e. a system consisting of water droplets dispersed in an oil phase.

(3) Multiple phases emulsion, e.g. W/O/W, O/W/O, etc.

The emulsion of oil and water can form by mechanical agitation devices, but this emulsion is thermodynamically unstable systems because the interaction between water and oil molecules is unfavorable, resulting in the rapid phase separation of oil layer (lower density) on top of water layer (higher density). However, the emulsion that is kinetically stable (metastable) for a period of time can form by adding substances known as emulsifiers and/or thickening agents prior to the mechanical agitation process [101,104-106].

2.2.2 Emulsifier

Emulsifiers are amphiphilic molecules with both hydrophilic head group and hydrophobic (lipophilic) tail as shown in Fig. 2.4 [107], which adsorb to the surface of oil droplets during mechanical agitation process, forming a protective membrane that prevents the aggregation of oil droplet. The hydrophilic head groups align themselves within the water phase, while the hydrophobic tails align in the oil phase resulting in the formation of micelle or reverse micelle [101,104,105,108-110] as shown in Fig. 2.5 [108].

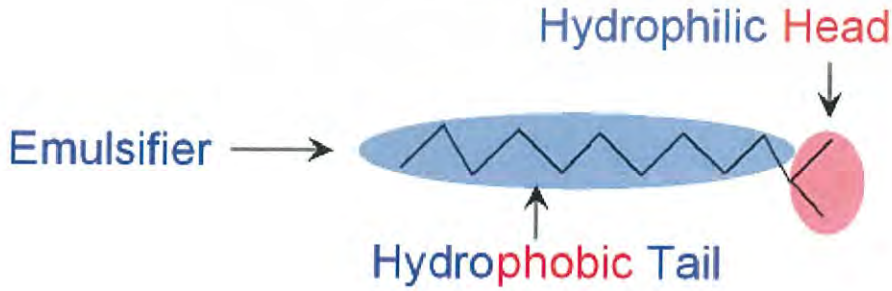

Figure 2.4 Schematic representation of emulsifier structure

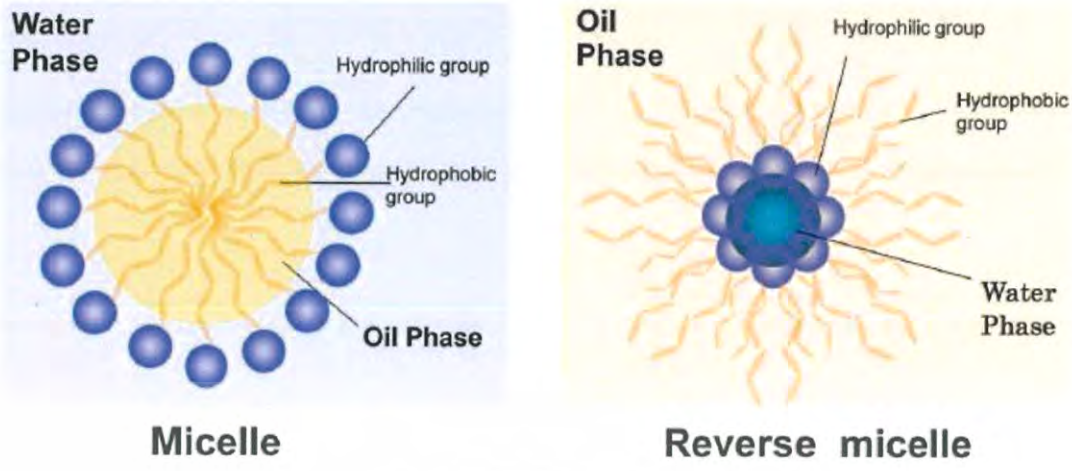

Figure 2.5 Schematic representation of micelle and reverse micelle structures

A. Micelles

Since the emulsifiers possess the hydrophilic part together with the hydrophobic part, in which their properties greatly diverse depended on their concentrations. In diluted solution, the emulsifiers align themselves at the oil/water interface as shown in Fig. 2.6 (Left side) [109]. The micelles or reverse micelles are formed by the assembling of excess emulsifier molecules as shown in Fig. 2.6 (Right side) [109]. The emulsifier concentration at which micelle or reverse micelles start to form is called critical micelle concentration (CMC).

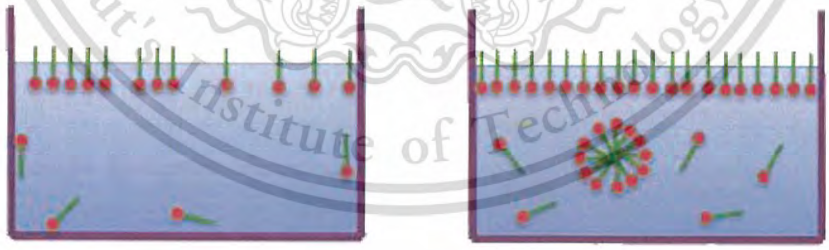

Figure 2.6 Schematic representation of emulsifier solution lower than CMC (Left side) and at CMC (Right side)

The properties of the emulsifer solution are abrupt change when the emulsifier concentration reaches the CMC, e.g. surface tension, electrical conductivity, turbidity, osmotic pressure, etc., as shown in Fig. 2.7 [110].

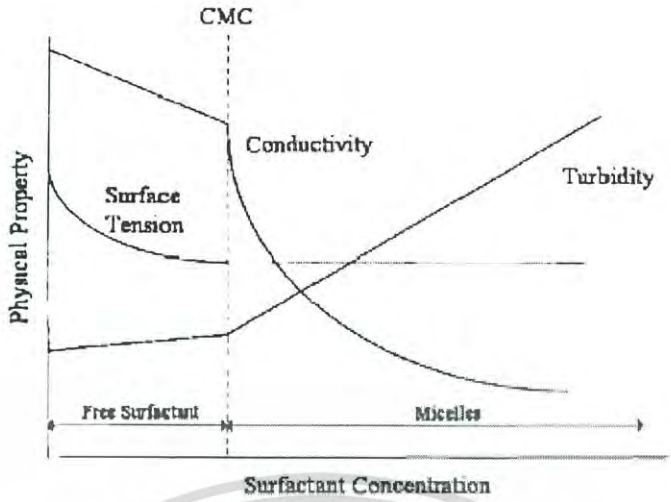

Figure 2.7 Changes of the solution at various emulsifier concentrations

B. Emulsifier classification

The most common emulsifier classification based on the nature of the hydrophilic group is as follows.

- Anionic: hydrophilic portion possesses a negative charge.
- Cationic: hydrophilic portion possesses a positive charge.
- Non-ionic: hydrophilic portion possesses no charge.
- Zwitter-ionic: hydrophilic portion possesses both negative and positive functional groups.

In addition, the emulsifier can be classified by another rule as given below.

- Hydrophile-Lipophile Balance (HLB)

The HLB is an empirical expression for the relationship between the hydrophilic and hydrophobic groups of emulsifiers. The emulsifiers which have HLB in the range of 8 to 18 are suitable for oil-in-water emulsion system, while the emulsifiers which have HLB in the range of 4 to 6 are suitable for water-in-oil emulsion system.

2.2.3 Polyelectrolytes

Polyelectrolytes are polymers with electrolyte repeating units. When the polyelectrolytes dissolve or swell in a highly polar solvent such as water. The electrolyte groups will dissociate, resulting in the charged polymers. The

polyelectrolytes are also commonly termed as polyions due to their charges arise from many ionized functional groups positioned along the chain contour. Electrostatic interactions between the ionized groups and the presence of small electrolyte ions in the solution make the properties of polyelectrolyte system distinct from the conventional polymer systems [111]. Some important and common chemical structures of polyelectrolytes are illustrated in Table 2.3 [112]

Table 2.3 Chemical structures of some important polyelectrolytes

Name	Repeat unit
Poly(acrylic acid)	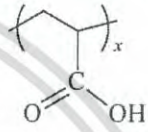
Poly(4-styrenesulfonic acid)	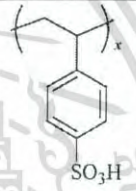
Poly(2-vinyl-pyridine)	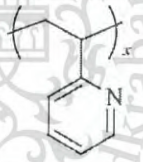
Poly(lysine)	
Poly(methacrylic acid)	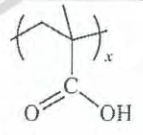
Poly(diallyldimethylammonium chloride)	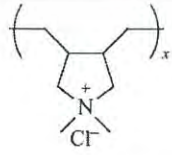
Poly(dimethylaminoethyl acrylate)	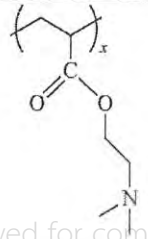

Table 2.3 (continued)

Name	Repeat unit
Poly(ethyleneimine)	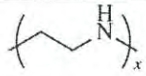
(6,6-ionene)	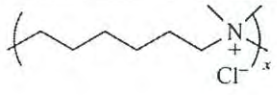
Poly(glutamic acid)	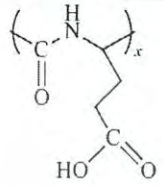
Poly(acrylamide-*co*-acrylic acid)	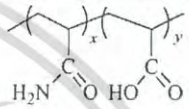
Hyaluronic acid	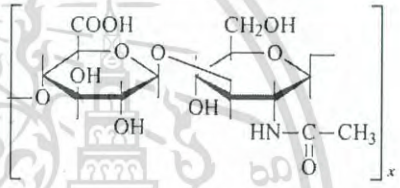
Chitosan	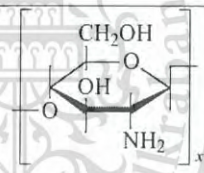
Carboxymethyl cellulose	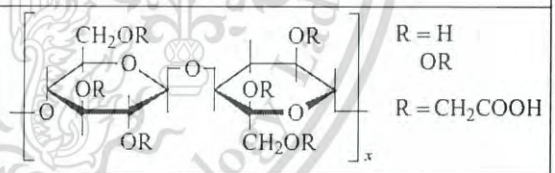
DNA (single stranded)	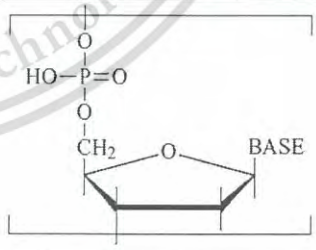
Poly(vinyl sulfate)	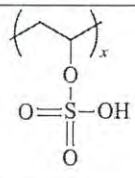

2.2.3.1 Effect of polyelectrolyte concentration on stability of polyelectrolyte coated emulsion droplets

The polyelectrolyte adsorption can lead to emulsion stability due to the electrostatic repulsion between the polyelectrolyte coated droplets. The repulsive interactions between the polyelectrolyte coated droplets should be strong enough to prevent the droplet aggregation. There should be sufficient amount of polyelectrolyte to saturate all droplet surfaces and the polyelectrolyte molecules should be adsorbed onto the droplet surfaces more rapidly than the droplet–droplet collisions because both positive and negative patches on the droplet surfaces can promote droplet aggregation (Bridging flocculation). On the other hand, the exceed of the polyelectrolyte concentration can promote "Depletion flocculation". The high concentration of polyelectrolyte in the bulk and a low concentration between the droplet causes the difference in osmotic pressure, therefore, the solvent molecules will be excluded from the space between two approaching droplets, causing them to flocculate. These flocculation phenomena are the main problems of this technique due to the formation of the permanent particle aggregates (*flocs*), in which they occur during the preparation. However, the amount of polyelectrolyte needed to saturate the surfaces depends on the polyelectrolyte characteristics, e.g. chain length, chain conformation, charge density, and flexibility, etc. [102-103].

2.2.3.2 Factors affecting the properties of polyelectrolyte layer

As previously mentioned, the polyelectrolytes differ from the conventional polymers because the presence of charges on their structures. The conformations of polyelectrolytes in the solution media and/or at the substrate surfaces change by various factors, e.g. polyelectrolyte characteristic, polyelectrolyte concentration, ionic strength, pH, solvent quality, temperature, etc. Brief descriptions of these factors affect the properties of polyelectrolytes are given below [102,112-118].

- Concentrations and characteristics of polyelectrolyte

Figure 2.8 [116] shows the polyelectrolyte behavior when using various polyelectrolyte concentrations with different charge density.

When the concentrations of polyelectrolytes are low corresponded to low charge density, the polyelectrolytes tend to adsorb onto the

surfaces with opposite charges, in which the adsorbed amount is high and the adsorbed layer is thick as shown in Fig. 2.8 diagram (a).

When the polyelectrolyte possesses more charge density as sketched in Fig. 2.8 diagram (b), the adsorbed amount of polyelectrolyte is lower and the adsorbed layer is much thinner due to the intra-molecular interactions dominated over the inter-molecular ones, thus, the strong intra-molecular electrostatic repulsion between different segments of the same chain led to the adsorb layer tends to be flat and spread out. Moreover, the strong attractive force between polyelectrolyte chains and oppositely charged groups on the surface after the adsorption causes them come into close proximity, resulting in the formation of thin layer on adsorb surface.

Polyelectrolytes typically do not adsorb onto similarly charged surfaces when polyelectrolyte concentration is low because of the electrostatic repulsion between polyelectrolyte and surface as show in Fig. 2.8 diagram (c).

On the upper part of the diagram (d) in Fig. 2.8, it can be seen that the polyelectrolyte is adsorbed on the solid surface consisting the opposite charges when using high polyelectrolyte concentration with low charge density. The bottom part of diagram (d) shows that the polyelectrolyte with more charge density exhibits similar behavior as the upper diagram due to the strong screening of electrostatic interactions.

Diagram (e) describes the behavior of polyelectrolyte at intermediate concentration. Either electrostatic interaction on the upper part or segment–surface interaction energy on the bottom part of diagram (e) can dominate. In the bottom part of diagram (e), the polyelectrolyte adsorbs to similar charged surfaces by aligning charges as far away from the surface as possible [111,112,115].

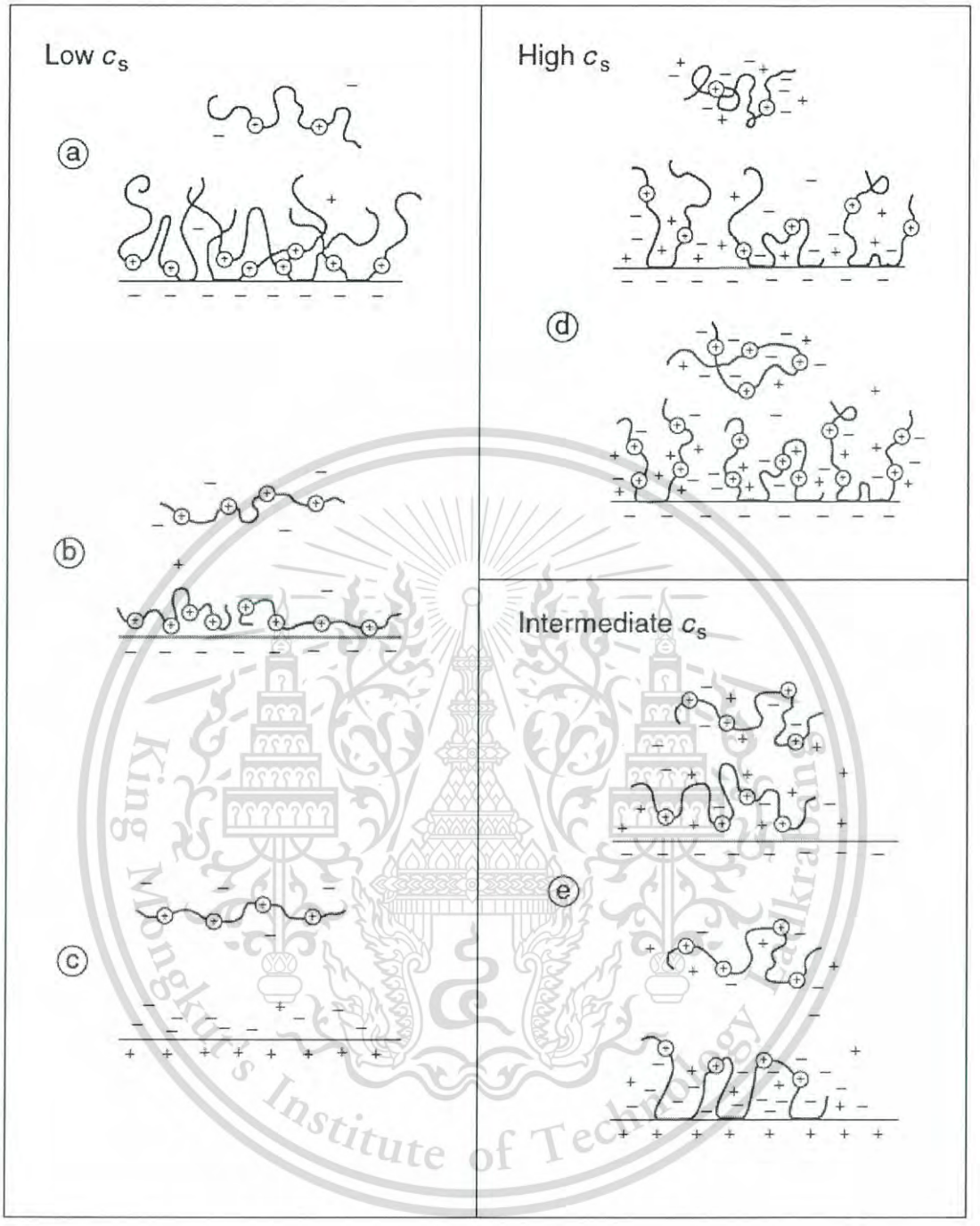

Figure 2.8 Schematic representations of polyelectrolyte adsorption on the substrate surface using various polyelectrolyte concentrations, C_s = Polyelectrolyte concentration

In addition, the thickness of adsorbed polyelectrolyte also depends on the polyelectrolyte chain length corresponded to its conformation. In case of the polyelectrolyte lies flat along the substrate surface, the chain length of

polyelectrolyte has a slight impact on the interfacial thickness. Therefore, the thickness of adsorbed layer can be determined by the width of the polyelectrolyte chain. On the other hand, in case of the polyelectrolyte adsorbs onto the surface with the coil conformation, the chain length of polyelectrolyte has a large impact on the interfacial thickness.

- Ionic strength

The ionic strength refers to the concentration of ions in solution that can determine the strength and range of intra- and inter-molecular electrostatic interactions which can change the polyelectrolyte layer formation, structure and thickness. When the ionic strength of the solution increases, the magnitude and range of electrostatic interactions between polyelectrolyte and substrate surface will decrease due to the accumulation of counter-ions around the surfaces which commonly refers to the electrostatic screening.

The electrostatic screening increases with the increase of the ion concentration and/or the valency of counter-ions in the solution. Multivalent counter-ions (e.g., Ca^{2+}, Fe^{2+}, Fe^{3+}) are much stronger than monovalent counter-ions (e.g., Na^{+}, Cl^{-}, K^{+}) and the lower concentrations of multivalent counter-ions can screen more charges than monovalent counter-ions. Moreover, the surface charges and charge density of polyelectrolytes can be bind and/or change by multivalent counter-ions.

In addition, the change of ionic strength after the formation of polyelectrolyte layer can change the characteristics of polyelectrolyte layer (e.g. the permeability of polyelectrolyte layer into small molecules, interfacial porosity, etc.,). The permeability of polyelectrolyte layer into the small molecules in solution can be increased through the weak electrostatic interactions between polyelectrolyte molecules in different layers by increasing the ionic strength. Moreover, the solution of sufficiently high ionic strength can cause the detachment of one or more polyelectrolyte layers from the adsorbed surfaces by weakening electrostatic interactions [117-119].

- pH

The polyelectrolyte conformation in solution can be changed by adjusting the pH especially in the case of weak polyelectrolytes. The strong polyelectrolytes can dissociate in the wide pH range, but the dissociation of weak polyelectrolytes generally depend on the solution pH. Therefore, the charge density of weak polyelectrolytes can be tuned by varying the pH of solution.

The electrostatic interactions, i.e. between the substrate surface and the adsorbed polyelectrolyte, between the adsorbed polyelectrolytes and between the adsorbed and non-adsorbed polyelectrolytes, can change by varying the pH solution, in which they will have the effect on the characteristics of polyelectrolyte layer (e.g. thickness, packing, interface integrity, etc., [120-122].

- Solvent quality and temperature

The quality of solvent can affect the polyelectrolyte conformation. The polyelectrolytes posses extended structure in good solvent due to the strong interactions between the polyelectrolyte chains and the solvent molecules. On the other hand, the poor solvent causes the increase of interaction among the polyelectrolyte chains but the decrease of polymer–solvent interactions, resulting in the contracting of the polyelectrolyte chains [117,123].

The temperature can also affect the polyelectrolyte conformation due to the change of solvent viscosity, bringing about the modification of solvent–polyelectrolyte interactions.

- Substrate characteristics

The characteristics of substrate especially the polarity are one of the most important factor that can effect on the properties of the next formed layer.

2.3 Incorporation of PCM capsule into fabric by coating process

The encapsulated PCM can be incorporated to the fabric by applying the coating composition to fabric substrate using various coating processes, e.g. knife over roll, screen printing, pad-dry-cure, dip coating, etc. The coating composition has been prepared by dispersing the PCM capsules in a solution containing polymer binder and/or other additives. For the textiles applications, the suitable polymer binder should have the glass transition temperature (T_g) in the range of -30 °C to +12 °C, e.g. polyacrylic, polyurethane, etc., for making soft and flexible film with sufficient toughness to maintain the strength of the binding systems [124].

In addition, the factors affecting the durability and thermal properties of the final coated products depend upon the composition of the polymeric binder, the binder/PCM capsules mass ratio, the type and mechanical stability of the shell material, the curing temperature and other process coating conditions. From this point of view, the coating processes have been, therefore, studied and developed by various research groups as follow.

Sánchez P. *et al.* [7] fixed the polystyrene microcapsules containing paraffin wax on the textile substrate by coating technique. In this study, 345 g of various binders (i.e. TEXPRINT ECOSOFT N10® and WST SUPERMOR®) per m^2 of fabric were applied in order to fix the PCM microcapsules on the textile substrate curing at 95 °C for 11 min. The fabric coated with the 35 wt% of microcapsules using WST SUPERMOR® binder showed the energy storage capacity of 7.6 J/g. After durability testing, the loss of microcapsules was clearly observed for all fabric samples.

Koo K. *et al.* [9] impregnated the PCM microcapsules dispersed in polyurethane on the fabric by dual-type coating method, i.e. wet coating and dry coating using curing temperature at 160 °C for 90 sec. The thermal release capacities of the dual-coated fabrics containing 10, 20, and 30 wt% of microcapsules were respectively 2.23, 3.15, and 3.21 J/g. The study results confirmed that the thermal regulation performance of the dual-coated fabrics was obtained. The durability of the dual-coated fabrics was investigated by water entry pressure (WEP). The WEP value tended to retain over 80% of its original value after 10 cycles over.

Shin Y. *et al.* [27] added the melamine–formaldehyde microcapsules containing eicosane on the polyester knit fabrics by conventional pad–dry–cure process using polyurethane binder. The fabric samples were impregnated by the aqueous solution

containing of 12.5, 25, 50, and 100 wt% of microcapsules and 3 wt% polyurethane binder at 300% wet pick up, dried at 80 °C for 8 min, and cured at 130 °C for 10 min. The fabric samples possessed the heat storage capacities of 0.91–4.44 J/g, depended on the microcapsules concentration. After 5 laundering, they could be retained about 40% of their heat storage capacity.

Alay S. *et al.* [91] added the poly(methyl methacrylate)/*n*-hexadecane microcapsules to the woven fabrics by conventional pad-cure method using polyurethane binder. The cotton, cotton/polyester blend and microfiber polyester fabrics were impregnated with the solution containing 50 g/L of microcapsules and 100 g/L of binder, in which they were cured at 160 °C for 3 min. The enthalpies of PCM microcapsules treated fabrics were in the range of 3.14 J/g to 10.02 J/g. After once laundering, the microcapsules were present on the fabric surface.

Salaün F. *et al.* [125] incorporated the melamine–formaldehyde microcapsules containing the mixture of *n*-alkane on the fabric by padding process cured at 150 °C for 4 min using different mass ratios of polyurethane binder to microcapsules. It was observed from DSC data that the main endothermic peaks of microcapsules shifted to higher temperatures due to the effect of polymeric binder. Furthermore, the thermo-regulating response depended on the weight of the surface-deposited binder and the mass ratio of binder to microcapsules.

The usage limitations of some techniques mentioned above were their high processing cost, high treatment temperature and the usage of organic solvents and/or toxic chemical reagents.

2.4 Layer-by-layer (LbL) dip coating technique

To overcome the disadvantages of mentioned above, the PCM capsules were immobilized on the fabric substrate by Layer-by-layer (LbL) technique using the polyelectrolyte self-assembly. The advantages of LbL technique are this technique can be performed using low concentrations of non-toxic chemical reagents and low treatment temperature, resulting in cost- and energy-saving and eco-friendly process. Moreover, the thickness of deposition layer on fabrics can be finely controlled at a nano-scale that can maintain various conventional properties (e.g. fabric softness, flexibility, breathability and moisture transport properties, mechanical strength). In addition, the electrostatic interaction makes a good adhesion between the fabric

surface/polyelectrolyte and polyelectrolyte/polyelectrolyte, in which the surface functionality can be directly and flexibly altered by choosing the appropriate polyelectrolytes [12,126-131].

This method is performed by alternating immersion of the substrate into two or more coating solutions containing oppositely charged species as shown in Fig. 2.9 [126].

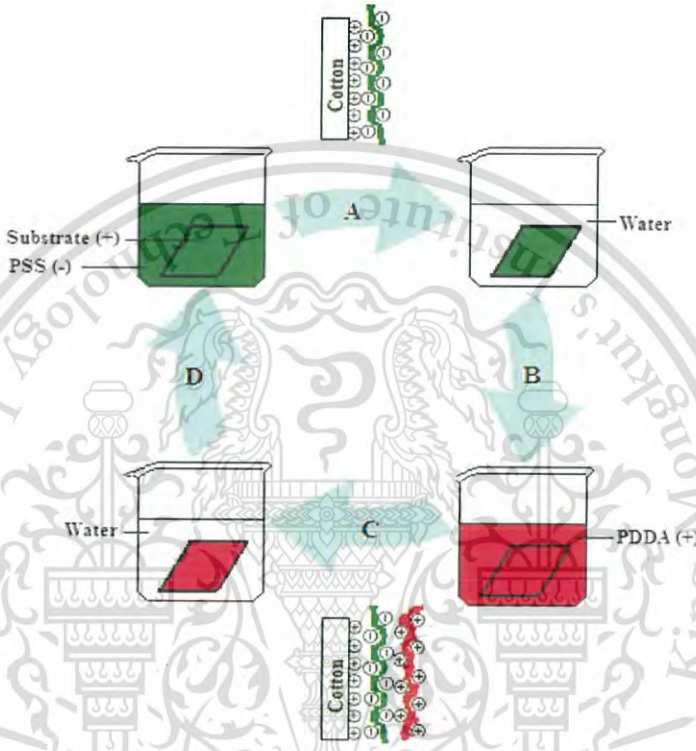

Figure 2.9 Schematic representation of LbL dip coating technique

According to the advantages of LbL technique, therefore; the LbL technique for textiles surface coating has been studied and developed by various research groups as follow.

Iamphaojeen Y. and Siriphannon P. [12] studied on the immobilization of ZnO nanoparticles on the cotton fabrics using poly(4-styrenesulfonic acid) (PSS). The cotton fabrics were firstly cationized using 3-chloro-2-hydroxypropyl trimethylammonium chloride (CHTAC) solution. The surfaces of cationized cotton were coated using LbL technique by stepwise dipping the cationized cotton into a solution of anionic PSS polyelectrolyte and $Zn(NO_3)_2 \cdot 6H_2O$ solution. The coating procedure was repeated 2, 4 and 6 times to obtain the PSS/Zn^{2+} multilayers coated

on the cotton fabrics. The treated cotton fabrics were hydrothermal treated in NH_4OH solution at 90 °C for 24 hours, resulting in the immobilization of ZnO nanocrystals on the cotton fabrics. The SEM, XRF and XPS characterized data revealed the accomplishment of ZnO immobilization on the surfaces of the treated cotton fabrics. The higher number of PSS/Zn^{2+} coating layers on the fabrics, the more hydrothermal grown ZnO nanoparticles could be obtained, resulting in the higher UV protection factor (UPF) when testing along the AATCC 183-2004 standard test method. All cotton fabrics with the ZnO immobilized on the surfaces were classified according to the AS/NZS 4399:1996 standard in the range of "VERY GOOD" UV protection category. The ZnO immobilized cotton fabrics with the six PSS/Zn^{2+} coating layers could inhibit the growth of *Staphylococcus aureus* when testing along the AATCC 147-2004 standard test method.

Wang Q. and Hauser P.J. [126] investigated two simple characterization methods for electrostatic self-assembly deposition of two typical polyelectrolytes, i.e. poly(4-styrenesulfonic acid) (PSS) and poly(diallyldimethylammonium chloride) (PDDA) on cotton fabrics. Dyeing of the PSS/PDDA assembled cotton fabrics with anionic direct red 80 and cationic methylene blue showed the regular and observable ''odd – even'' oscillations in terms of color depth (K/S value), which could be utilized for the assessment of the variation of surface electric property of the cotton substrate due to the alternate fabrication of PSS and PDDA. A linear increase in UV absorbance at wavelengths of 226 and 261 nm of the treated cotton fabrics further revealed that the growth of these LbL multilayers could be recorded by monitoring the UV spectra of the assembled cotton specimens.

Hyde K. *et al.* [127] reported the effect of surface cationization on the conformal deposition of alternating nanolayers of poly(4-styrenesulfonic acid) (PSS) and poly(allylamine hydrochloride) (PAH) on the cotton fibers. The variations in the cationization degree were achieved by manipulating the molar ratio of 3-chloro-2-hydroxy propyl trimethyl ammonium to NaOH. The experimental results indicated that the deposition process was not significantly influenced by the degree of cotton cationization. The buildup of further polyelectrolyte layers was found to be less sensitive to variations in the cationic character of the substrates once a critical number of alternating layers was deposited.

Ugur S.S. *et al.* [128] fabricated the ZnO nanoparticle–based multilayer nanocomposite films on cationized cotton fabrics *via* LbL molecular self-assembly technique. The cotton fabrics were pretreated with 2,3-epoxypropyl trimethylammonium chloride (EPTAC) by pad-batch method in order to create the cationic surface charge. The positively charged cotton fabrics were deposited by alternating nanolayers of anionic ZnO colloid solution and cationic ZnO colloid solution. The nano-ZnO films deposited cotton fabrics exhibited the excellent antimicrobial activity against *Staphylococcus aureus* bacteria. The results also showed that the coated fabrics with nano-ZnO multilayer films enhanced the protection of cotton fabrics from UV radiation. The tensile strength data of weft and warp yarns before and after deposition of nano-ZnO multilayer film by LbL process were not significant difference. It can be concluded that the nano-ZnO multilayer film prepared by the LbL process on the cotton fabrics did not cause any significant damage to the structure of the yarns.

Joshi M. *et al.* [129] deposited the nano-coating onto the cotton textile substrate using LbL self-assembly approaches. Chitosan, a natural biopolymer with polycationic characteristic, was used as a polyelectrolyte together with poly(4-styrenesulfonic acid) (PSS) anionic polyelectrolyte. The effect of ultrasonication during the intermediate washing steps was studied. The results showed that the ultrasonication during the washing steps could improve the uniformity of polyelectrolyte bilayers deposited onto the fiber surfaces. The use of this novel method for depositing the chitosan imparted the antimicrobial properties to the fabric without adverse affecting its flexibility, feel, or breathability.

Ali S.W. *et al.* [130] evaluated the effect of different process parameters on the amount of polyelectrolyte adsorbed on the cotton textile substrate *via* sequential adsorption of negatively charged poly(4-styrenesulfonic acid) (PSS) and positively charged poly(allylamine hydrochloride) (PAH) using LbL self-assembly nanocoating process. The amount of adsorbed polyelectrolyte was evaluated by measuring the color value (K/S) of methylene blue adsorbed cotton sample. At higher temperature, the amount of polyelectrolyte adsorbed as the multilayers was higher. The increase of PSS and PAH depositions was obtained with the increase of electrolyte (NaCl) concentration. The amounts of PSS and PAH adsorptions increased upto 0.03 M of PSS and 0.01 M of PAH concentrations, respectively. The dipping

time of 5 min was sufficient to obtain the maximum deposition of the polyelectrolyte multilayers.

Wang Q. and Hauser P.J. [131] studied a new approach for UV protection of cotton fabrics based on electrostatic self-assembly (ESA) technique. Three fluorescent brightening agents (FBAs) and poly(diallyldimethylammonium chloride) (PDDA) were stepwisely fabricated on the cationized cotton fabrics through the direct LbL deposition technique. Dyeing of the modified cotton fabrics with the anionic dyes showed the regular and identifiable "odd–even" changes in color depth (K/S value), indicating the variation of surface polarities of the cotton substrates due to the alternate deposition of FBA and PDDA. The stepwise increases in ultraviolet protection factor (UPF) of the treated cotton fabrics further revealed the growth of these LbL deposition multilayers. The modified cotton fabrics could obtain the excellent UV protection ratings of UPF > 40 after several bilayer coating of FBA/PDDA, depending on the type of FBAs. The excellent washing durability of the $(FBA/PDDA)_n$ multilayers coated cotton was obtained, indicating the good adhesion between the multilayer coatings and the cotton surfaces.

Chapter 3

Experimental

3.1 Materials

1. *n*-octadecane ($CH_3(CH_2)_{16}CH_3$, Oc; 99 %), AR grade, Merck
2. Sodium dodecyl sulfate ($CH_3(CH_2)_{11}SO_4Na$, SDS), AR grade, Ajax Finechem
3. Poly(diallyldimethylammonium chloride) (PDDA; M_w~100,000-200,000, 20 wt% in water), AR grade, Sigma Aldrich
4. 3-chloro-2-hydroxypropyl trimethyl ammonium chloride (CHTAC), AR grade, Sigma Aldrich
5. Sodium hydroxide (NaOH), AR grade, Carlo Erba
6. Poly(4-styrenesulfonic acid) (PSS; M_w~75,000, 18 wt% in water), AR grade, Sigma Aldrich
7. Methylene blue, AR grade, Sigma Aldrich
8. Eosin B, AR grade, Acros Organics
9. Sudan red 7B, For microscopy, Merck
10. Baby liquid detergent, D-nee

3.2 Apparatus

1. High intensity ultrasonic processor, Sonics&Materials Inc., Vibra-Cell VC505
2. Dynamic light scattering analyzer (DLS), Beckman Coulter Inc., DelsaNano C
3. Transmission electron microscope (TEM), JEOL, JSM 5600 LV
4. Differential scanning calorimeter (DSC), Mettler Toledo, DSC 3
5. Thermogravimetric analyzer (TGA), Perkin Elmer, Pyris1
6. Field emission scanning electron microscope (FE-SEM), Hitachi, SU8020
7. X-ray photoelectron spectrometer (XPS), Siam Photon Laboratory
8. UV-Visible spectrophotometer (UV-Vis), Thermo Scientific, Helios Omega
9. Electrokinetic analyzer (EKA), Anton Paar
10. Colorimeter, HunterLab, MiniScan XE Plus
11. Infrared thermography camera, FLIR, C2
12. Freeze dryer, Labogene, Coolsafe 110-4
13. Magnetic stirrer, IKA

3.3 Experimental procedure

The experimental procedure was divided into 2 main parts as follows;

3.3.1 Preparation of polyelectrolyte encapsulated *n*-octadecane (PEL-en-Oc)

1) Preparation of SDS encapsulated *n*-octadecane (Oc-SDS) primary emulsion

The Oc-SDS primary emulsions were obtained by dispersing *n*-octadecane (Oc) in 20 ml of 10 mM sodium dodecyl sulfate (SDS) solution and then treated by high intensity ultrasonic processor operating at a frequency of 20 kHz and power output of 500 W for various periods of treatment times. In order to obtain the most effective condition, the preparation was performed using various conditions, i.e.

- Oc concentration : 2.5, 5, 7.5, 10 and 15 ml/L
- Sonication time : 5, 10, 15, 20 and 30 min

2) Encapsulation of Oc-SDS primary emulsions by polyelectrolyte

2.1) Single layer (positively charged polyelectrolyte)

The as-prepared Oc-SDS primary emulsions were mixed with 1, 2, 4, 6, 8, 10, 12 or 14 mM of PDDA solution with slow agitating in order to obtain the positively charged PDDA polyelectrolyte encapsulated *n*-octadecane (PDDA-en-Oc) nanocapsules. The volume ratio of SDS : PDDA was fixed at 1 : 1.

2.2) Multilayer

The PEL-en-Oc nanocapsules with multilayer shells were prepared by stepwise adding PDDA and PSS solutions into the as-prepared Oc-SDS primary emulsion, resulting in the formation of PDDA-en-Oc, PSS(PDDA-en-Oc) or PDDA(PSS(PDDA-en-Oc)) nanocapsules with single, double and triple shell layers, respectively. The volume ratio of SDS : PDDA : PSS was fixed at 1 : 1 : 1.

3.3.2 Characterization of PEL-en-Oc nanocapsules

- Transmission electron microscopy (TEM)

Morphologies of the PEL-en-Oc nanocapsules were directly observed by transmission electron microscope. Before observing in TEM microscope, the PEL-en-Oc emulsion was dropped onto a TEM copper grid and then dried at room temperature.

- Dynamic light scattering analysis (DLS)

Mean droplet diameters and zeta potential (ζ) values of all Oc-SDS and PEL-en-Oc emulsions were directly measured by DLS. The measurement was performed three times for each sample to obtain a mean value.

- Differential scanning calorimetry (DSC)

The as-prepared PEL-en-Oc nanocapsules were frozen overnight and then freeze-dried using freeze dryer at -100 °C for 48 hr before characterized by DSC. Thermal properties of starting materials and samples before and after encapsulation by PEL, i.e. latent heat (ΔH) and phase change temperature (T_m, T_c), were analyzed by DSC using a heating rate of 5 °C/min in the temperature range of 0–50 °C under nitrogen atmosphere (flow rate of N_2 = 20 mL/min). The integrated areas under the endothermic and exothermic DSC peaks respectively corresponded to the latent heat of melting (ΔH_m) and latent heat of crystallization (ΔH_c), in which they were used to calculate the encapsulation efficiency [78] as expressed in equation (3.1):

$$\%\ \text{Encapsulation efficiency} = \frac{\Delta H_{m,capsules} + \Delta H_{c,capsules}}{\Delta H_{m,PCM} + \Delta H_{c,PCM}} \times 100 \quad (3.1)$$

where $\Delta H_{m,capsules}$ and $\Delta H_{c,capsules}$ are the latent heat of melting and crystallization of PEL-en-Oc nanocapsules, respectively; $\Delta H_{m,PCM}$ and $\Delta H_{c,PCM}$ are the latent heat of melting and crystallization of *n*-octadecane, respectively.

- Thermogravimetric analysis (TGA)

The as-prepared PEL-en-Oc nanocapsules were frozen overnight and then freeze-dried using freeze dryer at -100 °C for 48 hr before characterized by TGA. Thermal stabilities of starting materials and samples before and after encapsulation by PEL were analyzed by TGA using a heating rate of 10 °C/min in the temperature range of 50 – 500 °C under nitrogen atmosphere (flow rate of N_2 = 20 mL/min).

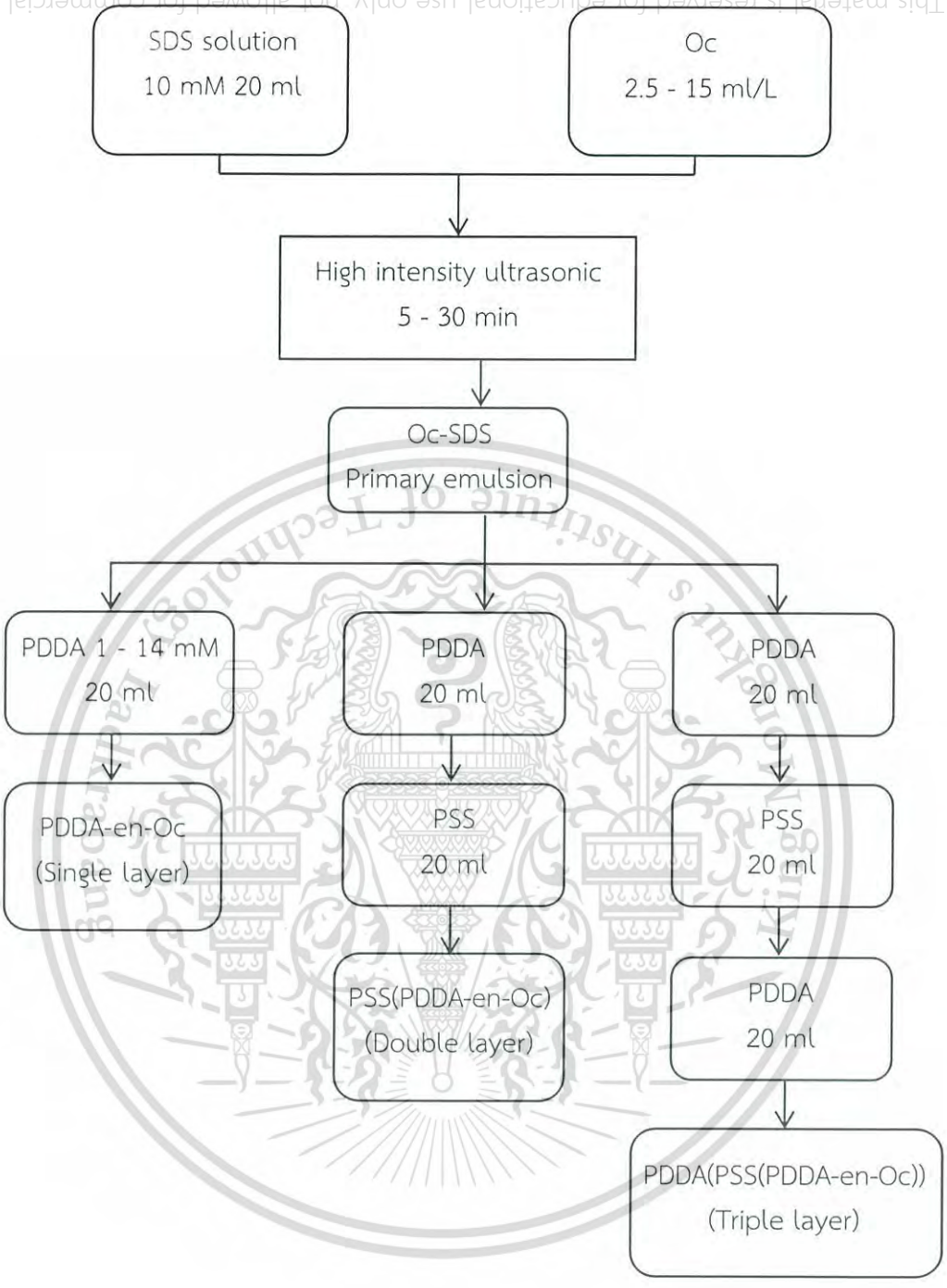

Figure 3.1 Preparation procedure of polyelectrolyte encapsulated *n*-octadecane

3.3.2 Immobilization of PEL-en-Oc nanocapsules on fabric

The PEL-en-Oc nanocapsules were immobilized on the cotton fabrics.

Prior to immobilization, the cotton fabrics were cationized in order to create the positive surfaces. An aqueous solution of cationizing agent was prepared by dissolving 50 g of 3-chloro-2-hydroxypropyl trimethylammonium chloride (CHTAC) and 18 g of NaOH in 1 L of deionized water. The desized cotton fabrics (~5 g) were soaked in the cationizing solution with slowly stirred at room temperature for 24 hr. The fabrics were neutralized with dilute acetic acid, then washed several times with deionized water and dried at ambient conditions.

The immobilization of PEL-en-Oc nanocapsules on the cationized fabrics were carried out as follows;

1) Stepwise soaking in PSS solution and PDDA-en-Oc emulsion

The cationized cottons with rectangular shape (4 cm x 4 cm) were firstly immersed into 20 ml of negatively charged PSS solution followed by rinsing in deionized water for 5 min (Cat-cot/PSS) and then immersed into positively charged PDDA-en-Oc emulsion followed by the same rinsing procedure to obtain the self-assembled PDDA-en-Oc nanocapsules coated on cotton fabrics as shown schematically in Fig. 3.2. PDDA concentration was varied, i.e. 1, 5, 10, 20, 30, 40 and 50 mM

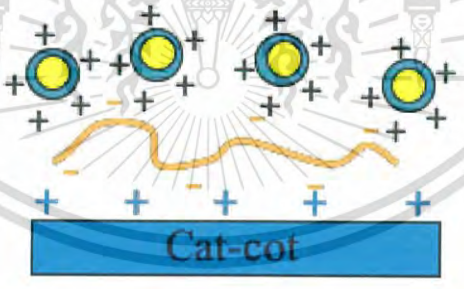

Figure 3.2 Schematic model of PEL-en-Oc nanocapsule immobilized on cotton fabrics by stepwise soaking in PSS solution and PDDA-en-Oc emulsion

2) Direct soaking in PSS(PDDA-en-Oc) emulsion

The cationized cottons with rectangular shape (4 cm x 4 cm) were directly immersed into the negatively charged PSS(PDDA-en-Oc) emulsion followed by rinsing in deionized water for 5 min in order to obtain the self-assembled PSS(PDDA-en-Oc) nanocapsules coated on cotton fabrics as schematically shown in Fig. 3.3. Soaking time was varied, i.e. 5, 10, 15, 20 and 30 min.

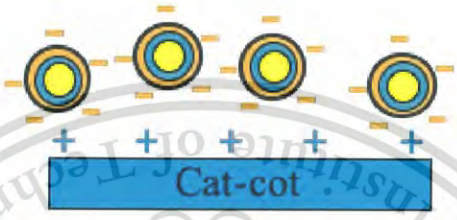

Figure 3.3 Schematic model of PEL-en-Oc nanocapsule immobilized on cotton fabrics by direct soaking in the PSS(PDDA-en-Oc) emulsion

3.3.3 Multi-cycle immobilization of PEL-en-Oc nanocapsules on fabric

In order to increase the immobilized content of nanocapsules on the cotton fabrics, the fabric samples were treated by following methods:

1) Stepwise soaking in PSS solution and PDDA-en-Oc emulsion

The cationized cottons with rectangular shape (4 cm x 4 cm) were firstly immersed into the 20 ml of negatively charged PSS solution followed by rinsing in deionized water for 5 min and then immersed into the positively charged PDDA-en-Oc emulsion followed by the same rinsing procedure. The treatment was repeated in the range of 1 - 5 cycles in order to increase the immobilized content of nanocapsules on the cotton fabrics as schematically shown in Fig. 3.4.

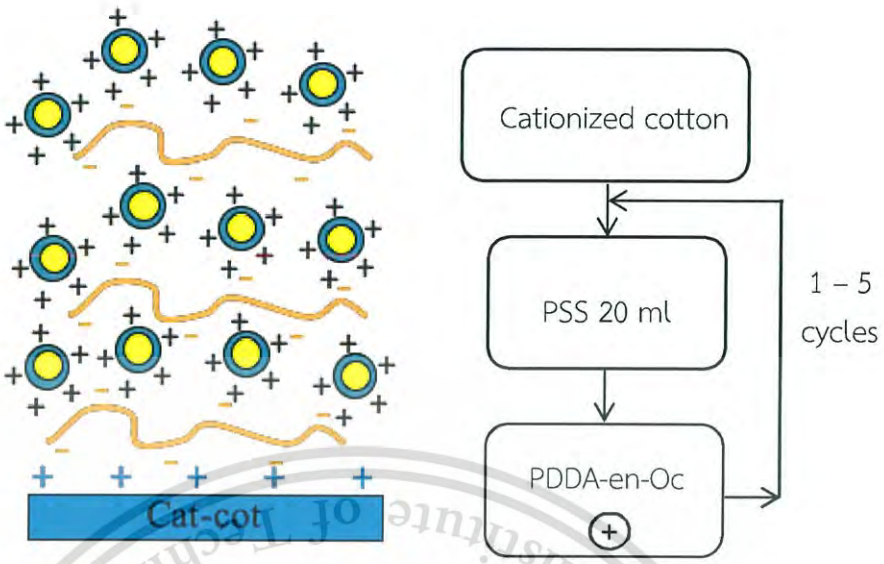

Figure 3.4 Schematic model of multi-cycle immobilization of PEL-en-Oc nanocapsules by stepwise soaking in PSS solution and PDDA-en-Oc emulsion

2) Stepwise soaking in PSS(PDDA-en-Oc) and PDDA-en-Oc emulsion

The cationized cottons with rectangular shape (4 cm x 4 cm) were firstly immersed into the negatively charged PSS(PDDA-en-Oc) emulsion followed by rinsing in deionized water for 5 min and then immersed into the positively charged PDDA-en-Oc emulsion followed by the same rinsing procedure. The treatment was repeated in the range of 1 - 5 nanocapsule layers in order to increase the immobilized content of nanocapsules on the cotton fabrics as schematically shown in Fig. 3.5.

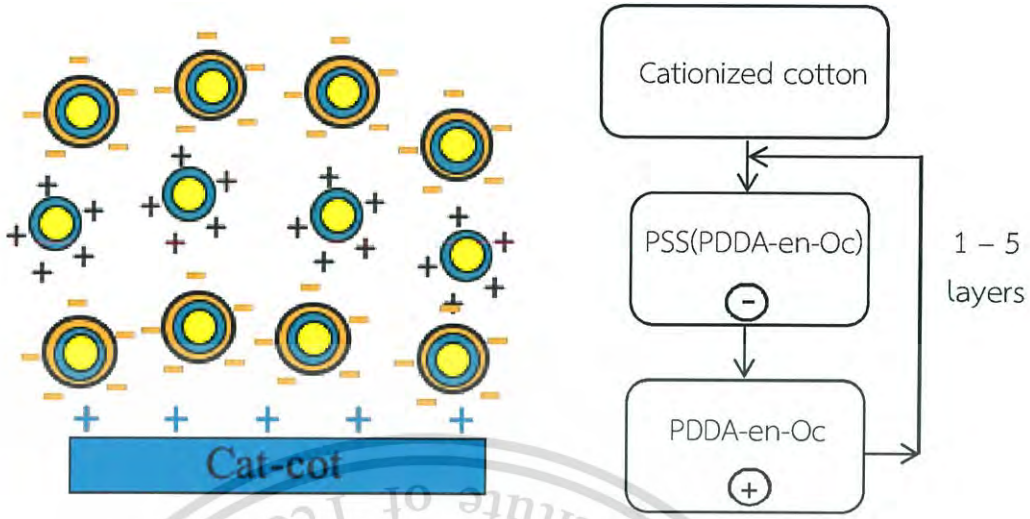

Figure 3.5 Schematic model of multi-cycle immobilization of PEL-en-Oc nanocapsules by stepwise soaking in PSS(PDDA-en-Oc) and PDDA-en-Oc emulsion

3.3.4 Characterization of PEL-en-Oc nanocapsules immobilized on fabric

- Field emission scanning electron microscopy (FE-SEM)

The cotton fabrics before and after immobilization of PEL-en-Oc nanocapsules were analyzed by field emission scanning electron microscope (FE-SEM). Before FE-SEM observing, the surfaces of the samples were coated with platinum.

- X-ray photoelectron spectrometry (XPS)

The chemical states of neat and treated cotton samples were characterized by X-ray photoelectron spectrometer (XPS).

- Electrokinetic analysis (EKA)

The cotton samples before and after immobilization of PEL-en-Oc nanocapsules were analyzed by electrokinetic analyzer (EKA) in order to measure the streaming potential as a function of pH. The zeta potential of cotton sample was calculated from the Helmholtz–Smoluchowski equation (3.2) [132]:

$$\text{Zeta potential} = \frac{U_p \eta L}{\varepsilon \varepsilon_0 Q R \Delta P} \qquad (3.2)$$

where U_p is the streaming potential (mV) ; ΔP is the pressure difference (Pa); η is the viscosity (Pa·s); L is the capillary length (m); Q is the capillary cross-section (m^2); *R* is the electric resistance (Ω); ε is the dielectric constant (F/m); and ε_0 is the electric permittivity of vacuum (F/m).

- Dye adsorption determination

Dye adsorption behavior of cotton samples was studied using 2 different kinds of dye i.e. methylene blue and eosin B. The 1 cm x 1 cm of cotton samples were soaked in 10 mL of 10 mg/L methylene blue solution and/or 50 mg/L eosin B solution at ambient condition for 24 hr. After 24 hours, the cotton samples were separated from the dye solution. The adsorbencies of the dye solutions were determined by UV-Visible spectrophotometer at λ_{max} 664.5 nm and 530 nm for methylene blue and eosin B, respectively. The measurement was performed three times for each sample to obtain a mean value. The methylene blue and eosin B concentrations were determined by linear regression equation from the standard calibration curves, i.e. y = 0.1477x - 0.0029 and y = 0.0581x + 0.0121, respectively, where x is the concentrations; and y is the adsorbance values. The dye uptake onto cotton fibers was calculated from the differences between the adsorbance of dye concentration before and after adsorption onto the cotton fabrics. The quantity of dye adsorbed by the fabric was expressed in mg/g.

- Color measurement of colored PEL-en-Oc immobilized on cotton fabric

The presence of PEL-Oc-cap immobilized on cotton fabric was confirmed by facile color detection method. Prior to PEL encapsulation, Sudan red 7b was dissolved in *n*-octadecane with the initial concentration of 1,000 mg/L in order to obtain the PEL colored *n*-octadecane nanocapsules (PEL-colOc-cap). The PEL-colOc-cap was immobilized on the cotton sample and then analyzed by colorimeter at λ_{max} 530 nm. The color strength (K/S value) was calculated using the Kubelka-Munk equation (3.3) [133]:

$$\frac{K}{S} = \frac{(1-R)^2}{2R} \qquad (3.3)$$

where K is the sorption coefficient (cm^{-1}); S is the scattering coefficient (cm^{-1}); and R is the reflectance of the cotton sample.

- Determination of thermo-regulating property

The neat cotton and treated cotton samples containing different quantity of PEL-en-Oc nanocapsules were used for evaluating the thermo-regulating property. All cotton samples were chilled at 5 °C for 3 min. After that, they were taken out from chilling system, kept in the chamber at temperature of about 50 °C and monitored their temperature change during 1 – 10 min from the thermal images. The thermal images were recorded using digital infrared thermography camera (FLIR, C2). In addition, the thermal images of neat and treated cotton samples after taking out from the chilling system for 1 min were used for calculation their temperature differences (ΔT) as described in Appendix A.3.

- Determination of breathability

The breathabilities of neat and treated cotton samples were determined from the water vapor transmission rate (WVTR). All cotton samples were sealed over the test tubes containing 10 ml of deionized water and recorded their initial weights. Then, the cotton sealed test tubes were kept in the oven at 50 °C for 24 hr. After that, the cotton sealed test tube were taken out from the oven weighed to determine their weight losses. The WVTR in $g/m^2/day$ was calculated using equation (3.4) [134].

$$WVTR = \frac{24M}{At} \tag{3.4}$$

where M is the loss in mass of water in the test tube (g); A is the area of test tube (m^2); and t is the time used in the measurement (hr).

- Washing durability of the treated fabrics

The washing durability testing of PEL-en-Oc nanocapsules immobilized on cotton fabric was determined after washing the PEL-colOc-cap immobilized cotton in the simulated washing system. The PEL-colOc-cap immobilized cotton was soaked in 100 ml of 7.5 ml/L detergent solution (Baby liquid detergent, D-nee) under vigorous stirring for 20 min followed by rinsing twice in distilled water under stirring for 5 min. After 5, 10 and 15 simulated washing and rinsing cycles, the sample was

dried at ambient condition. The relative amount of PEL-colOc-cap remained on the fabric was indirectly determined by K/S values as described in color measurement section. The reduction percentages of their K/S values after washing and rinsing for 5, 10 and 15 cycles were calculated using equation (3.5).

$$\% \text{ Reduction} = (K/S_{before} - K/S_{after})/K/S_{before} \times 100 \quad (3.5)$$

where K/S_{before} is the K/S value of treated cotton sample before washing; K/S_{after} is the K/S value of treated cotton sample after washing and rinsing.

Chapter 4

Results and Discussion

4.1 Encapsulation of Oc-SDS primary emulsions by polyelectrolyte

The encapsulation of *n*-octadecane was performed by generating primary emulsion of *n*-octadecane in water using high intensity ultrasonic processor with various conditions in order to obtain the most effective condition. The as-prepared Oc-SDS primary emulsion was mixed with various concentrations of PDDA solution in order to produce the positively charged PDDA polyelectrolyte encapsulated *n*-octadecane (PDDA-en-Oc) nanocapsules. In addition, the alternative encapsulation of *n*-octadecane with multilayer polyelectrolyte shells were prepared by stepwise adding PDDA and PSS solutions into the as-prepared Oc-SDS primary emulsion in order to obtained the single, double and triple polyelectrolyte shell layers coated on Oc-SDS micelles. The effects of preparation conditions on properties of the as-prepared PDDA-en-Oc nanocapsules were described below.

4.1.1 Preparation of SDS encapsulated *n*-octadecane (Oc-SDS) primary emulsion

A primary emulsion of *n*-octadecane was obtained by dispersing *n*-octadecane in sodium dodecyl sulfate (SDS) solution and then treated by high intensity ultrasonic processor. The critical micelle concentration (CMC) of sodium dodecyl sulphate (SDS) in pure water at 25 °C is 8.2 mM, [135] therefore; the 10 mM of SDS solution was used in this research.

The primary emulsions were prepared by using various *n*-octadecene concentration and sonication time in order to determine the optimum condition having no excess free *n*-octadecene fraction. The physical appearances of the as-prepared primary emulsions were shown in Fig. 4.1. The emul-$Sx_1Ocx_2\_tx_3$ is the Oc-SDS primary emulsion, where x_1 refers to SDS concentration (mM) used in the synthesis, x_2 refers to *n*-octadecane concentration (ml/L) of used in the synthesis and x_3 refers to sonication time (min) used in the synthesis. It can be seen that there had no excess free of *n*-octadecene in the primary emulsions prepared by using 2.5 - 10 ml/L *n*-octadecene and sonication for longer than 10 min. However, when the

primary emulsion were prepared by using higher *n*-octadecene concentration than 10 ml/L, the sonication time should be extended to 30 min which was adequate to break down all *n*-octadecene into nanodroplets and subsequently enclosed the *n*-octadecene nanodroplets by the SDS molecules as Oc-SDS micelles.

From the above mentioned results, the primary emulsion used for further encapsulation by polyelectrolytes was prepared by using 10 ml/L *n*-octadecene and sonicating for 10 min.

Figure 4.1 Physical appearances of primary emulsions prepared by using various *n*-octadecene concentrations and sonication treatment times

4.1.2 Effect of PDDA polyelectrolyte concentration

- *Size and Zeta potential*

Figure 4.2 and Table 4.1 show the average particle size and zeta potential of Oc-SDS primary emulsion and PDDA-en-Oc nanocapsules. It can be seen that the average particle size and zeta potential of Oc-SDS was about 101 nm and (-74.87) mV, respectively. The negative zeta potential of Oc-SDS indicated the successful formation of negatively charged SDS micelles encapsulated the *n*-octadecane droplet after high intensity ultrasonic treatment for a short period of time.

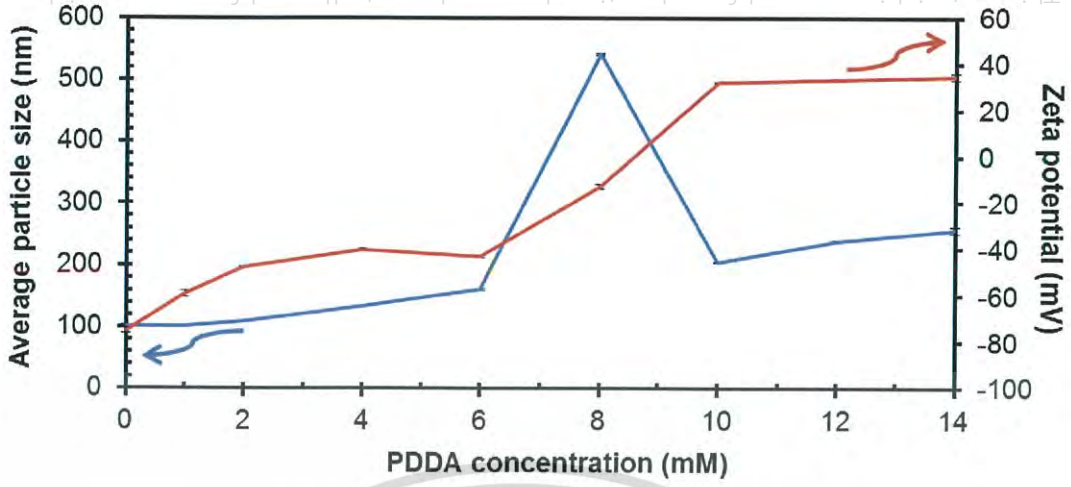

Figure 4.2 Size and zeta potential of Oc-SDS and PDDA-en-Oc nanocapsules using various PDDA concentrations

When the Oc-SDS primary emulsion was mixed with 1 mM PDDA solution, the zeta potential of PD1-en-S10Oc10_t10 nanocapsules changed to (-59.09) mV due to the electrostatic attraction between negatively charged Oc-SDS micelles and positively charged PDDA chains, resulting in the partial charge compensation.

From these results, the formation mechanism of PDDA-en-Oc nanocapsules was proposed as schematically shown in Fig.4.3. The *n*-octadecane phase was broken down to nanodroplets by cavitation interaction of high-intensity ultrasound with liquids. The *n*-octadecane nanodroplets were then spontaneously encapsulated with the SDS molecules, forming as oil-in-water micelles with negatively charged surface of sulfate functional groups. In the second step, the PDDA solution was added into the as-prepared Oc-SDS emulsion, the positive charges of PDDA repeating units could ionically interacted with the negative micelles, resulting in the self-assembly of PDDA shell coated on the Oc-SDS micelles (PDDA-en-Oc).

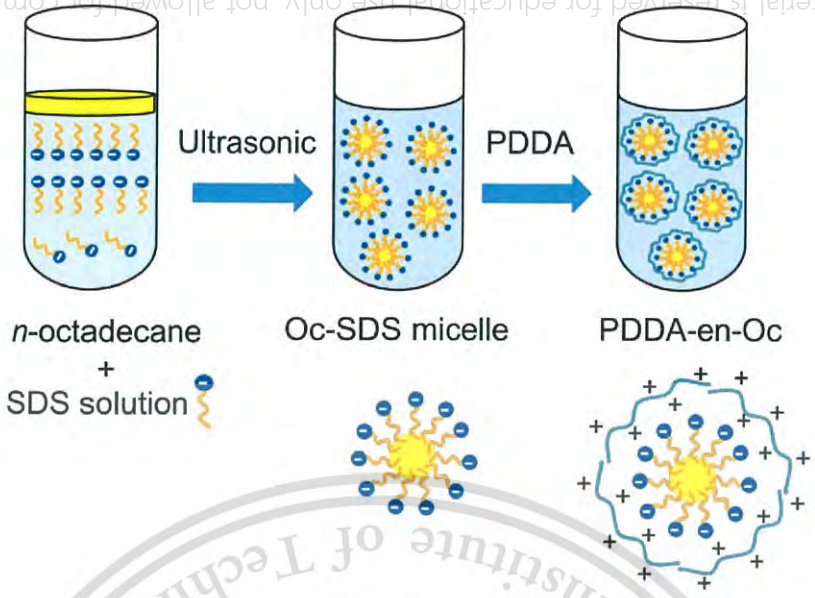

Figure 4.3 Schematic representation of PDDA-en-Oc formation

The average particle size and zeta potential of PDDA-en-Oc nanocapsules increased with the increase of PDDA concentration, implying the formation of thicker PDDA shell. These results were attributed to the effect of PDDA concentration on its chain conformation during the shell forming step. When the PDDA concentration was 1 mM, the PDDA is a strong polyelectrolyte fully charged in aqueous solution, the intrachain interactions dominated over the interchain ones in dilute condition [136], thus, the strong intrachain electrostatic repulsion between different segments of the same PDDA chain led to the chain stretching along the adsorbing surface. It was, therefore, the formation of relatively thin layer of PDDA shell covered on the Oc-SDS micelles as schematically shown in Fig. 4.4(a).

Considering the increase of PDDA concentration from 1 to 6 mM, the concomitant increases of PDDA-en-Oc particle sizes and their zeta potential values were attributed to the dominant effects of increasing the adsorbed PDDA amount and/or changing the PDDA chain conformation on the Oc-SDS micelles as schematically shown in Fig. 4.4(b). The increase of polyelectrolyte concentration brought about the reductions of polyelectrolyte effective charge and its size because of the counterion condensation, resulting in the random coil conformation of PDDA molecules in solution, so they tended to adsorb on the surfaces of Oc-SDS droplets as thick shell layer.

Table 4.1 Size, polydispersity index (PDI) and zeta potential values of Oc-SDS and PDDA-en-Oc capsules using various PDDA concentrations

Samples	PDDA concentration (mM)	Size (nm)	PDI	Zeta potential (mv)
emul-S10Oc10_t10	0	101.00 ± 3.08	0.147 ± 0.022	-74.87 ± 1.27
PD1-en-S10Oc10_t10	1	101.37 ± 0.84	0.147 ± 0.015	-59.09 ± 1.38
PD2-en-S10Oc10_t10	2	108.90 ± 0.56	0.146 ± 0.011	-47.69 ± 0.29
PD4-en-S10Oc10_t10	4	134.17 ± 0.42	0.175 ± 0.007	-40.29 ± 0.52
PD6-en-S10Oc10_t10	6	160.63 ± 1.69	0.188 ± 0.006	-43.29 ± 0.25
PD8-en-S10Oc10_t10	8	541.13 ± 1.55	0.198 ± 0.054	-12.94 ± 0.93
PD10-en-S10Oc10_t10	10	204.43 ± 1.19	0.143 ± 0.014	31.94 ± 0.22
PD12-en-S10Oc10_t10	12	238.17 ± 1.50	0.140 ± 0.006	33.38 ± 0.55
PD14-en-S10Oc10_t10	14	255.97 ± 5.61	0.159 ± 0.014	34.54 ± 1.45

* Remarks : - emul-$Sx_1Ocx_2\_tx_3$ is Oc-SDS primary emulsion.

- PDx_4-en-$Sx_1Ocx_2\_tx_3$ is PDDA-en-Oc nanocapsule.
- x_1 refers to the concentration (mM) of SDS used in the synthesis.
- x_2 refers to the concentration (ml/L) of *n*-octadecane used in the synthesis.
- x_3 refers to sonication time (min) used in the synthesis.
- x_4 refers to the concentration (mM) of PDDA used in the synthesis.

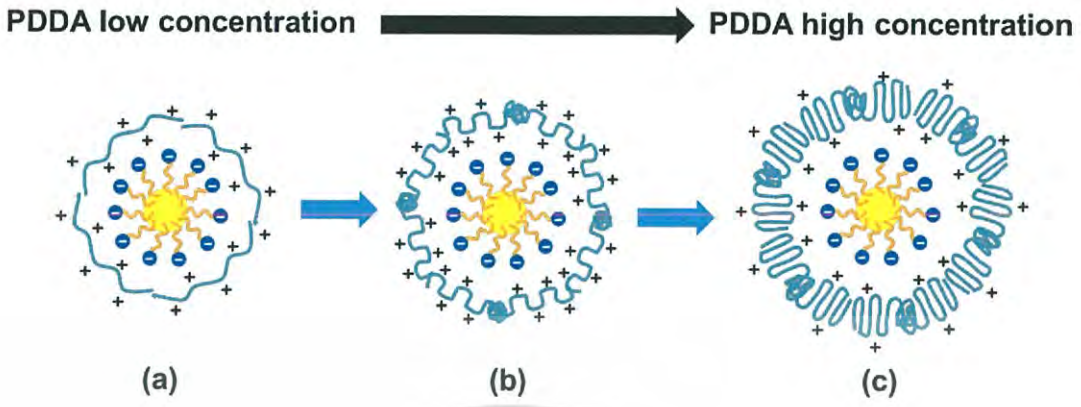

Figure 4.4 Schematic models of PDDA-en-Oc capsules created in the encapsulation system using various PDDA concentrations

When the PDDA solution used in the treatment was increase from 4 to 6 mM, the zeta potential value of the PD6-en-S10Oc10_t10 nanocapsules was decreased from (-40) to (-43) mV. This result was inconsistent with the hypothesis above owing to the formation of some tiny aggregates. The presence of tiny aggregates in the PD6-en-S10Oc10_t10 sample brought about the error of zeta potential value. When the PDDA concentration used in encapsulation was increased from 6 to 8 mM, the average particle size of PD6-en-S10Oc10_t10 sample was drastically increased from 160.63 to 541.13 nm simultaneously with the increase of zeta potential value close to zero. These results were considered to be because the formation of large aggregates known as flocculation in the PD6-en-S10Oc10_t10 sample. It was, therefore, the largest particle size of 541.13 nm was obtained in the PD8-en-S10Oc10_t10 sample.

When the PDDA concentration used in the encapsulation process was increased from 8 to 10 mM, the zeta potential values would changed from (-12.94) to (31.94) mV due to the charge compensation between positively charged PDDA and negatively charged Oc-SDS micelles. The highly positive or negative zeta potential value brought about the stable emulsion system without the occurring of flocculation process. It was, therefore, the average particle size of PDDA-en-Oc would drastically decreased from 541.13 to 204.43 nm. In addition, the average particle size of PDDA-en-Oc nanocapsules using 10 mM was higher than the

PDDA-en-Oc nanocapsules using 1 - 6 mM due to the dominant effect of increasing the adsorbed PDDA amount and/or the changing the PDDA chain conformation on the Oc-SDS micelles as mentioned above.

The average particle size of PDDA-en-Oc would drastically increased from 204.43 to 255.97 nm, while their zeta potential values would slightly changed in the range of (31.94) – (34.54) mV, when the PDDA concentration used in the encapsulation was higher than 10 mM. These results were considered to be due to the formation of electrostatic blob conformation of PDDA on the Oc-SDS micelles, bringing about the drastic increase of shell thickness but nevertheless the reduction of effective surface charge number [112] as schematically shown in Fig. 4.4(c).

Figure 4.5 shows the TEM micrographs of PD4-en-S10Oc10_t10 nanocapsules. It can be seen that the nanocapsules were relatively globular shape with core-shell structure, in which the *n*-octadecane core was a pale circular part encapsulated in the dark part of PDDA shell.

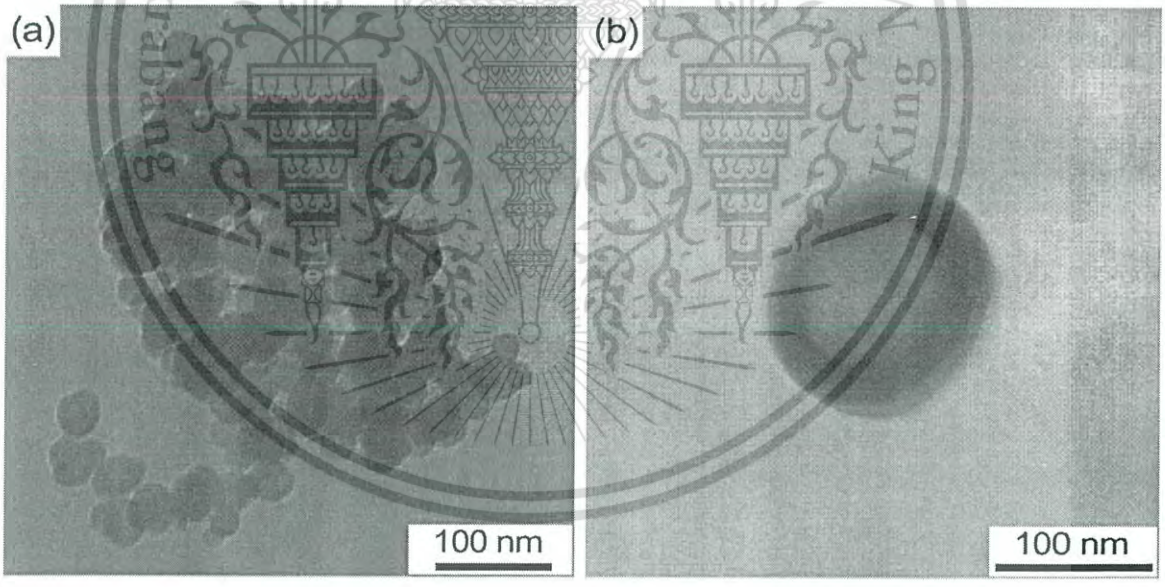

Figure 4.5 TEM micrographs of PD4-en-S10Oc10_t10 nanocapsules

- *DSC*

Figure 4.6 shows the DSC thermograms of the starting *n*-octadecane, mixture of PDDA and SDS (PDDA+SDS) and PDDA-en-Oc nanocapsules. The integrated areas under the endothermic and exothermic DSC peaks respectively corresponded to the latent heat of melting (ΔH_m) and latent heat of crystallization

(ΔH_c) of *n*-octadecane were determined. The melting temperature (T_m), crystallization temperature (T_c), latent heat of phase transitions and encapsulation efficiency of all the samples are summarized in Table 4.2.

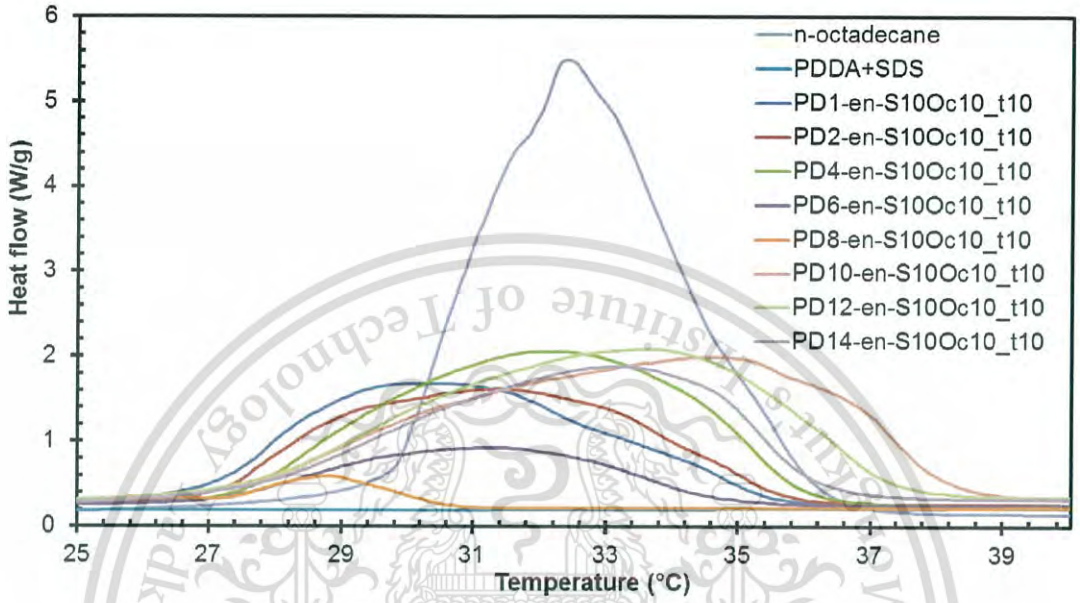

Figure 4.6 DSC thermograms of *n*-octadecane, mixture of PDDA and SDS (PDDA+SDS) and PDDA-en-Oc nanocapsules using various PDDA concentrations

In Fig. 4.6, the heating thermograms of the starting *n*-octadecane respectively revealed an endothermic peak at about 28 °C corresponding to T_m of *n*-octadecane. Since the PDDA and SDS are shell forming materials used in the encapsulation process, therefore, the thermal behavior of PDDA+SDS was investigated. It was found that the thermogram of PDDA+SDS mixture shows no peak in the temperature range of 25 – 40 °C, implying that there is no phase transition of the capsule shell within the phase transition temperature range of *n*-octadecane.

After encapsulation of *n*-octadecane, all PDDA-en-Oc capsules exhibited the phase transitions at temperatures very close to T_m of the neat *n*-octadecane as shown in Fig. 4.6. These thermal properties of PDDA-en-Oc nanocapsules insisted the presence of *n*-octadecane in the as-prepared capsules. The smaller diameter of PDDA-en-Oc nanocapsules, the faster heat absorption were obtained in the DSC thermograms, owing to the higher surface area to volume ratio of PDDA-en-Oc capsules. In addition, the dissolution of SDS hydrophobic tails in the

n-octadecane encapsulated in the PDDA shell might cause the melting point depression of *n*-octadecane.

The latent heat values (ΔH_m and ΔH_c) of all PDDA-en-Oc capsules significantly lower than those of the starting *n*-octadecane due to the shielding effect of capsule shell. When the PDDA concentration in the encapsulation process was increased, the ΔH_m and ΔH_c of PDDA-en-Oc capsules gradually increased as summarized in Table 4.2. These results were considered to be because the encapsulation efficiency was improved with the increase of PDDA concentration, resulting in the increase of PDDA-en-Oc quantity. However, the values of latent heat and encapsulation efficiency drastically decreased when the 6 and 8 mM of PDDA concentration was used in the encapsulation process. These results might be because the PD6-en-S10Oc10_t10 and PD8-en-S10Oc10_t10 emulsion could generate the unstable emulsion system as previously mentioned. The unstable emulsion system induced the formation of aggregates know as flocculation, resulting in the reduction of encapsulation efficiency.

When the PDDA solutions with higher concentration (> 10 mM) were used, the ΔH_m and ΔH_c of PDDA-en-Oc capsules gradually decreased due to the formation of thick layer of PDDA on the Oc-SDS micelles. The thicker layer of PDDA shell, the higher of shielding effect were obtained, resulting in the lower latent heat values of PDDA-en-Oc capsules.

The increase of PDDA concentration used in the encapsulation process played an important role in the conformation of PDDA molecules formed as the capsules' shell, resulting in the dominant influence on the shell thickness and capsule size. The smaller PDDA encapsulated *n*-octadecane capsules with the thinner capsule shell exhibited the faster heat absorption of phase transition processes. In addition, the increase of PDDA concentration could improve the efficiency of *n*-octadecane encapsulation, resulting in the increase of quantity of PDDA encapsulated *n*-octadecane capsules. The higher amount of encapsulated capsules, the higher latent heat quantity was obtained during the phase transitions of PDDA encapsulated *n*-octadecane.

Table 4.2 Thermal properties of *n*-octadecane and PDDA-en-Oc capsules using various PDDA concentrations

Samples	PDDA conc. (mM)	$T_{m,onset}$ (°C)	$T_{m,peak}$ (°C)	ΔH_m (J/g)	$T_{c,onset}$ (°C)	$T_{c,peak}$ (°C)	ΔH_c (J/g)	Encapsulation efficiency (%)
n-octadecane	0	29.6	32.44	232.3	27.42	24.8	236.77	n/a
PD1-en-S10Oc10_t10	1	26.86	24.08	98.5	25.38	30.53	101.55	42.65
PD2-en-S10Oc10_t10	2	26.98	31.39	115.57	25.33	24.59	119.41	50.09
PD4-en-S10Oc10_t10	4	27.34	32.09	124.44	25.82	23.37	124.38	53.05
PD6-en-S10Oc10_t10	6	26.90	31.28	43.88	25.11	22.68	38.54	17.57
PD8-en-S10Oc10_t10	8	26.84	28.77	15.47	25.08	21.12	14.10	6.30
PD10-en-S10Oc10_t10	10	27.20	34.66	151.97	26.08	25.74	157.59	65.99
PD12-en-S10Oc10_t10	12	27.41	33.58	137.78	25.54	25.36	142.49	59.75
PD14-en-S10Oc10_t10	14	27.37	33.17	109.99	25.92	25.06	113.54	47.65

4.1.3 Encapsulation of Oc-SDS primary emulsions by multilayer polyelectrolyte

- *Size and Zeta potential*

Figure 4.7 and Table 4.3 show the average particle size and zeta potential values of sample before and after encapsulation with polyelectrolyte multilayers. The zeta potential results revealed the successful coating of stepwise assembled polyelectrolytes on the surfaces of *n*-octadecane droplets, in which the average particle sizes of PEL-en-Oc nanocapsules were in the range of 154 – 204 nm.

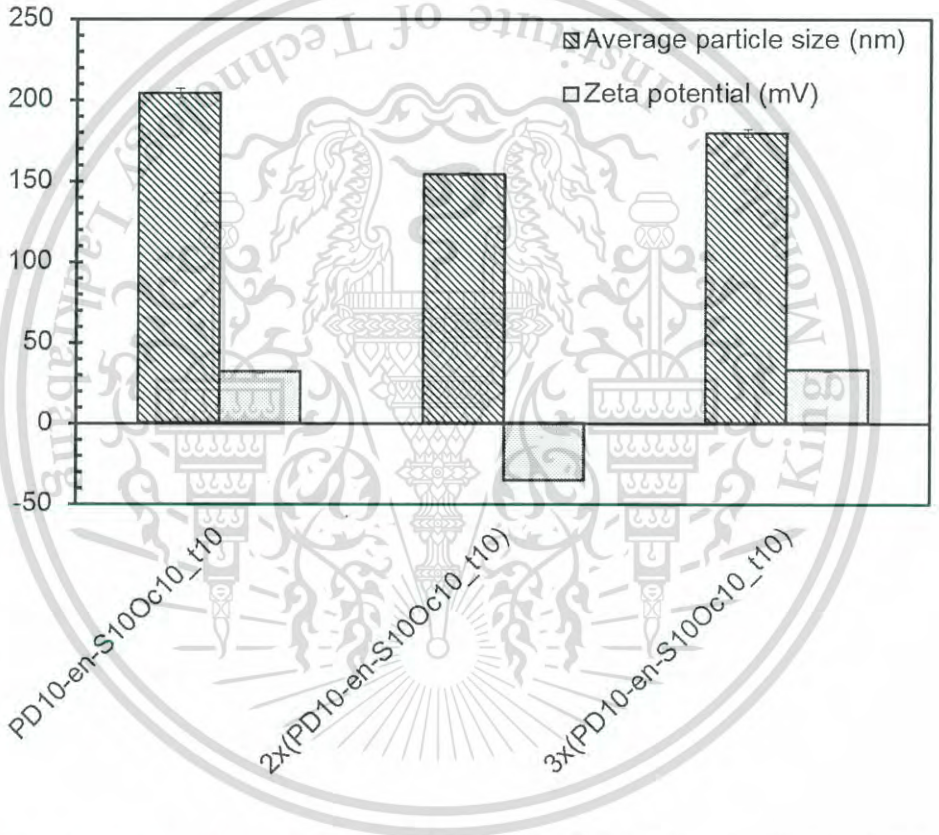

Figure 4.7 Size and zeta potential of Oc-SDS, PDDA-en-Oc and PEL-en-Oc capsules with multilayer shells

When the PD10-en-S10Oc10_t10 nanocapsules were mixed with the PSS solution to formed 2x(PD10-en-S10Oc10_t10), the zeta potential of the resulting product changed to (-35.48) mV due to the formation of negatively charged PSS outermost shell layer. On the other hand, the average particle size of 2x(PD10-en-S10Oc10_t10) product reduced to 154.33 nm because of the shrinking of polyelectrolyte doubled layer shell. The shrinkage of doubled layer (PSS/PDDA

shell) was considered to be because the hydrodynamic volume of PSS was less than PDDA molecule [137]. When the PSS molecules interacted with PDDA shell coated on the Oc-SDS micelles, the PSS molecules was induced the shrinking of PSS/PDDA shell layer.

Table 4.3 Size, polydispersity index (PDI) and zeta potential values of Oc-SDS, PDDA-en-Oc and PEL-en-Oc capsules with multilayer shell

Samples	NO. of PEL layer	Size (nm)	PDI	Zeta potential (mV)
emul-S10Oc10_t10	0	101.00 ± 3.08	0.147 ± 0.022	-74.87 ± 1.27
PD10-en-S10Oc10_t10	1	204.43 ± 1.19	0.143 ± 0.014	31.94 ± 0.22
2x(PD10-en-S10Oc10_t10)	2	154.33 ± 2.31	0.168 ± 0.018	-35.48 ± 1.00
3x(PD10-en-S10Oc10_t10)	3	179.80 ± 3.40	0.110 ± 0.017	33.05 ± 2.31

*Remarks : - $yx(PDx_4\text{-en-}Sx_1Ocx_2\_tx_3)$ is PEL-en-Oc capsules with multilayer shell.
- y refers to the number of polyelectrolyte layer used in the synthesis.

When the PDDA solution was mixed with the 2x(PD10-en-S10Oc10_t10) nanocapsules to create the 3x(PD10-en-S10Oc10_t10) product, the larger average particle size of 179.80 nm was obtained with the positive zeta potential value (33.05 mV).

From these results, the polyelectrolyte shell formation was proposed as shown in Fig. 4.8. The strong polyelectrolyte PDDA is fully charged in aqueous solution. However, the concentrated PDDA solution brought about the reductions of polyelectrolyte effective charge because of the counterion condensation, resulting in a random coil conformation of PDDA in solution. It was, therefore, the random coil PDDA molecules tended to adsorb to the Oc-SDS surfaces as a thick shell layer. When the 2x(PD10-en-S10Oc10_t10) nanocapsules was prepared by adding the PSS solution into the PD10-en-S10Oc10_t10 nanocapsules, the lower hydrodynamic volume of PSS brought about the shrinking of polyelectrolyte shell layer, therefore, the polyelectrolyte shell thickness coated on Oc-SDS micelles was decreased. Thus, the average particle size of 2x(PD10-en-S10Oc10_t10) and 3x(PD10-en-S10Oc10_t10) samples would decreased.

When the PDDA solution was mixed with the 2x(PD10-en-S10Oc10_t10) nanocapsules, the PDDA molecules with random coil conformation in solution were adsorbed on the surface of 2x(PD10-en-S10Oc10_t10) *via* the electrostatic interaction between positively charged PDDA and negatively charged nanocapsules, forming as 3x(PD10-en-S10Oc10_t10). The average particle size of 3x(PD10-en-S10Oc10_t10) was, therefore, higher than that of the 2x(PD10-en-S10Oc10_t10).

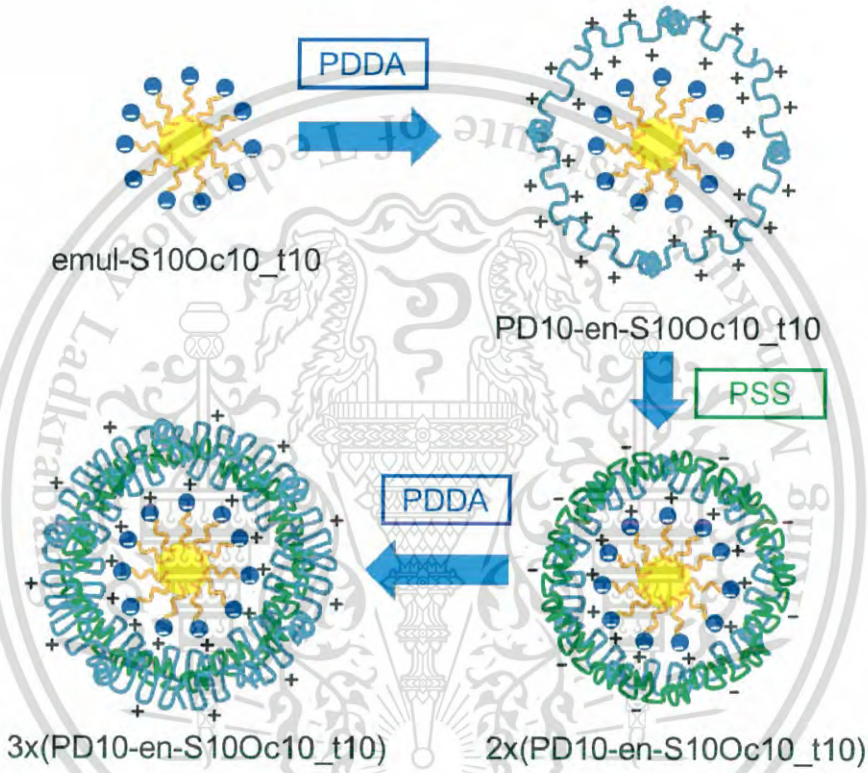

Figure 4.8 Schematic models of PEL-en-Oc capsules created in the encapsulation system using various number of polyelectrolyte layers

- *DSC*

Figure 4.9 shows the DSC thermograms of the starting *n*-octadecane, and PEL-en-Oc nanocapsules sample. All PEL-en-Oc capsules exhibited the phase transitions in the temperatures range very close to the neat *n*-octadecane. These thermal properties of PDDA-en-Oc capsules insisted the presence of *n*-octadecane in the as-prepared nanocapsules. The fastest heat absorption were obtained in the PD10-en-S10Oc10_t10 sample owing to the lowest packing density of its polyelectrolytes/capsules' shell.

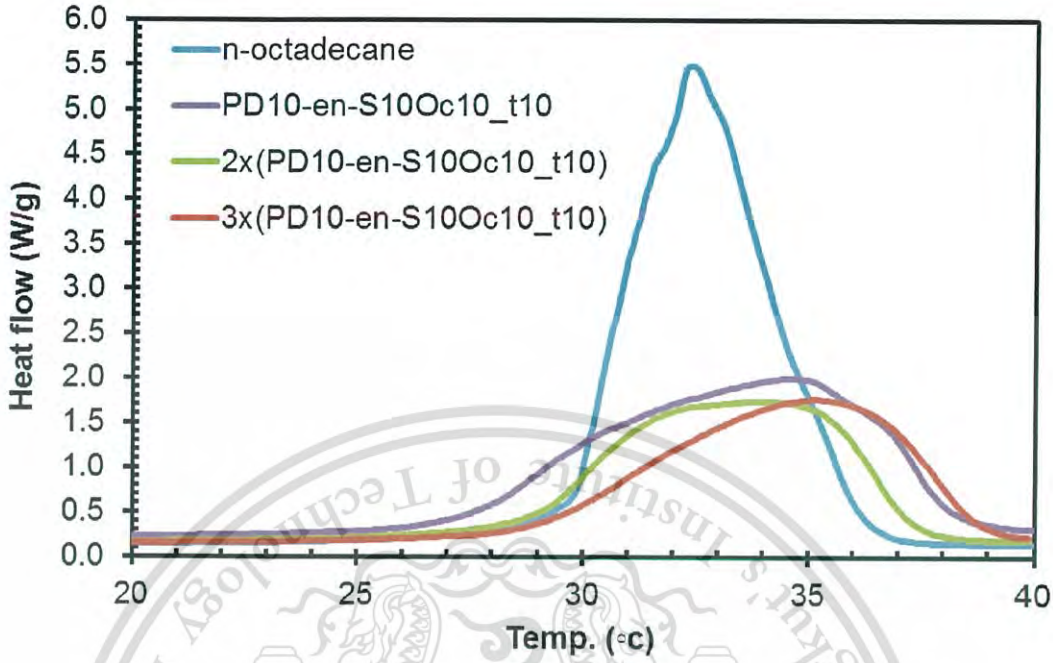

Figure 4.9 DSC thermograms of neat *n*-octadecane, PD10-en-S10Oc10_t10, 2x(PD10-en-S10Oc10_t10) and 3x(PD10-en-S10Oc10_t10) nanocapsules

The melting temperature (T_m), crystallization temperature (T_c), latent heat of phase transitions and encapsulation efficiency of all PEL-en-Oc nanocapsules samples are summarized in Table 4.4. The latent heat of all capsules significantly decreased from those of the starting *n*-octadecane due to the shielding effect of capsule shell. However, the latent heat values of 2x(PD10-en-S10Oc10_t10) sample was similar to that of the 3x(PD10-en-S10Oc10_t10). These results were because the 2x(PD10-en-S10Oc10_t10) sample possessed the highest packing density of polyelectrolytes shell layers, while the 3x(PD10-en-S10Oc10_t10) sample possessed higher shell thickness. The higher packing density and/or the thicker of polyelectrolytes shell layers, the higher shielding effect of capsule shell would be obtained in the nanocapsules.

Table 4.4 Thermal properties of *n*-octadecane, PD10-en-S10Oc10_t10, 2x(PD10-en-S10Oc10_t10) and 3x(PD10-en-S10Oc10_t10)

Samples	NO. of PEL layer	$T_{m,onset}$ (°C)	$T_{m,peak}$ (°C)	ΔH_m (J/g)	$T_{c,onset}$ (°C)	$T_{c,peak}$ (°C)	ΔH_c (J/g)
n-octadecane	0	29.6	32.44	232.3	27.42	24.8	236.77
PD10-en-S10Oc10_t10	1	27.2	34.66	151.97	26.08	25.74	157.59
2x(PD10-en-S10Oc10_t10)	2	28.69	34.01	118.13	27.09	23.75	122.67
3x(PD10-en-S10Oc10_t10)	3	28.83	35.16	118.16	26.09	22.51	127.03

4.1.4 Thermo-regulating property of PEL-en-Oc nanocapsules

The thermal-regulating property of PDDA-en-Oc nanocapsules was determined by measuring the latent heat of nanocapsules under multiple heating-cooling cycles from the DSC thermograms. Figure 4.10 shows the DSC thermograms of PD10-en-S10Oc10_t10 nanocapsules detected during 1 – 4 cycles of heating-cooling scan. It can be seen that there are no significant change of heating and cooling thermograms even after several thermal treatment cycles, indicating the as-prepared nanocapsules could maintain the thermal properties of *n*-octadecane core material. The presence of polyelectrolyte shell could effectively protect the loss of *n*-octadecane during thermal events, therefore, the PDDA-en-Oc nanocapsules could perform the thermo-regulating behavior.

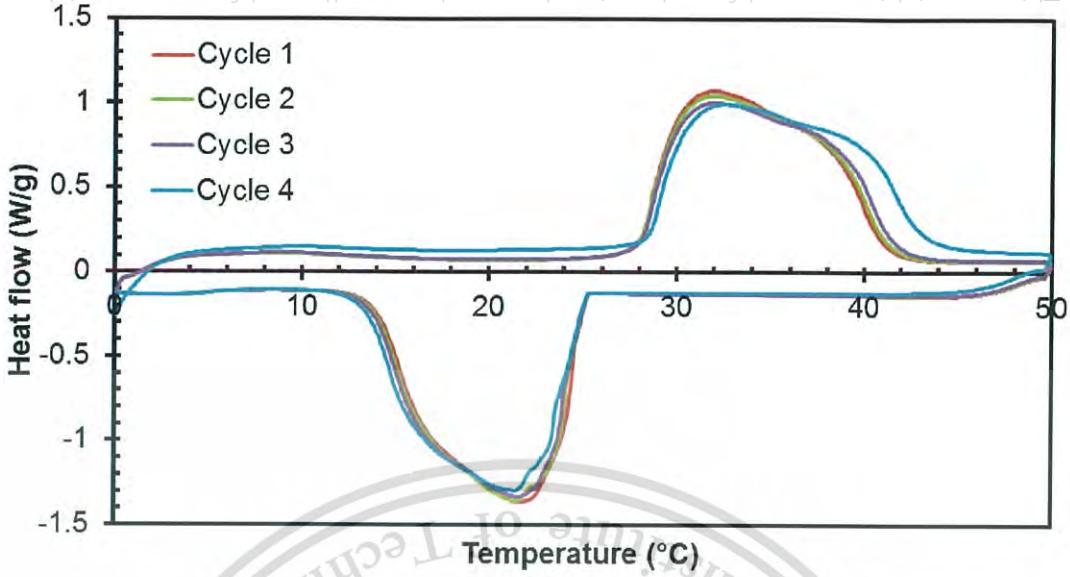

Figure 4.10 DSC thermograms of PD10-en-S10Oc10_t10 nanocapsules under multiple heating-cooling cycles

4.1.5 Thermal stability of PEL-en-Oc

Figure 4.11 shows the TGA thermograms of the starting *n*-octadecane and PDDA-en-Oc nanocapsules. The neat *n*-octadecane completely decomposed in the temperature range of about 153.7 °C (onset) – 180 °C (endset). All PEL-en-Oc nanocapsules displayed two significant steps of weight losses. The first weight loss was observed in the range of 163 – 180 °C (onset), corresponding to the decomposition of *n*-octadecane core material due to the softening and cracking of polyelectrolyte shell at the elevated temperature [138]. It was found that the initial decomposition temperature of *n*-octadecane leaked out from the nanocapsules was obviously higher than that of the neat *n*-octadecane, indicating the enhancement of thermal stability by the polyelectrolyte encapsulation. The second degradation step in the range of 250 – 330 °C was attributed to the decomposition of polyelectrolyte shell.

The decomposition temperature of *n*-octadecane was increase with the increase of the number of polyelectrolyte shell layer due to the effect of different polyelectrolyte chain movement in the capsule shell. The 3x(PD10-en-S10Oc10_t10) nanocapsules possessed the highest thermal stability due to the strong interaction of triple polyelectrolyte layers coated on the Oc-SDS micelle. The triple shell layer might be more difficult to move than the single and double polyelectrolyte shell

layers, therefore, the leakage of *n*-octadecane from the 3x(PD10-en-S10Oc10_t10) nanocapsules was retarded.

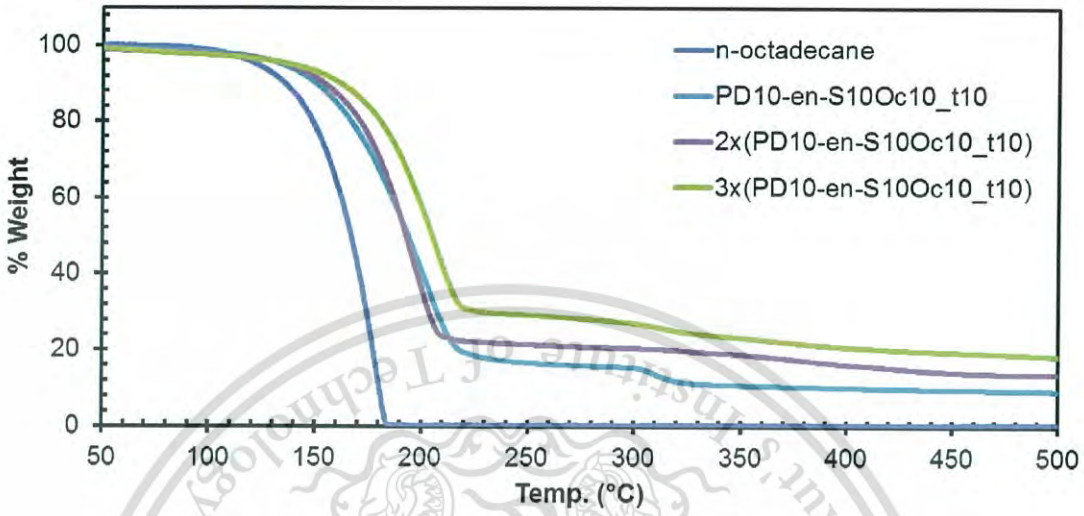

Figure 4.11 TGA thermograms of neat *n*-octadecane, PD10-en-S10Oc10_t10, 2x(PD10-en-S10Oc10_t10) and 3x(PD10-en-S10Oc10_t10) nanocapsules

In addition, the formation of char was obtained in all PEL-en-Oc samples after TGA analyses, in which it was non-combustible products of SDS and polyelectrolyte shell forming materials. The char yield increased with the increased of the number of polyelectrolyte layer.

4.2 Immobilization of PEL-en-Oc nanocapsules on fabric

Prior to the immobilization of nanocapsules, the cotton fabrics were cationized in order to create the positive functional groups on their surfaces. The positive functional groups would further electrostatic react with the oppositely charged polyelectrolytes and/or *n*-octadecane nanocapsules, resulting in the well attachment of the *n*-octadecane nanocapsules on the cotton surface.

In the cationization process, the CHTAC reacted with NaOH to form 2,3-epoxypropyl trimethyl ammonium chloride (EPTAC), which would react further with the hydroxyl groups of cellulose, producing the cationized cotton fabric [127] as shown in Fig. 4.12.

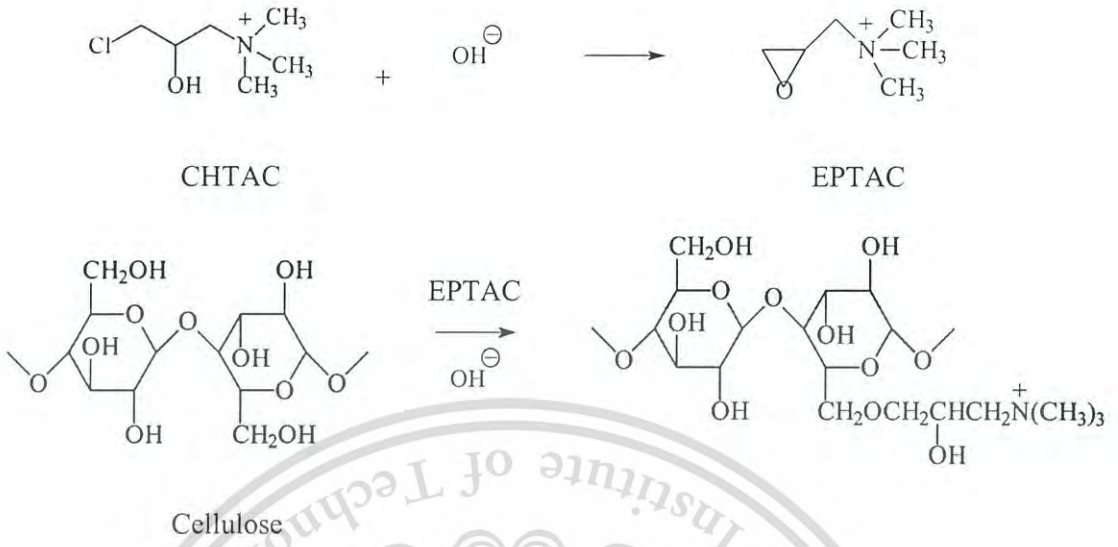

Figure 4.12 Cationization of cellulose

The cationized cotton fabrics were treated with various procedures in order to immobilize the *n*-octadecane nanocapsules on cotton fabrics, i.e. (1) stepwise soaking in PSS solution and nanocapsules with positively charged outermost shell and (2) direct soaking in nanocapsules with negatively charged outermost shell.

In addition, the cationized cotton samples were multi-cycle treated by various methods in order to increase the immobilized content of nanocapsules on the cotton fabrics, i.e. (1) stepwise soaking in PSS solution and nanocapsules with positively charged outermost shell and (2) stepwise soaking in nanocapsules with negatively and positively charged outermost shell.

The effects of immobilization conditions on properties of the *n*-octadecane nanocapsules immobilized cotton fabrics were described below.

4.2.1 Stepwise soaking in PSS solution and nanocapsules with positively charged outermost shell

Since the PDDA-en-Oc nanocapsules possessed the positive sites on their surface, the cationized cotton fabrics would initially coated with the PSS polyelectrolytes in order to act as the negative binder on cotton surface for further immobilization of PDDA-en-Oc. When the cationized cotton was immersed into the PSS solution, the electrostatic interaction between the cationized cellulose and the

anionic polyelectrolyte led to the self-assembled formation of PSS nanolayer on the cationized cotton surface (Cat-cot/PSS). After alternate soaking in the nanoemulsion containing the PDDA-en-Oc, the positively charged nanocapsules could interact with the negatively charged PSS, resulting in the immobilized nanocapsules on the cotton fabric (Cat-cot/PSS/Cap+).

(1) Characterization of PDDA-en-Oc nanocapsules immobilized cotton

Figure 4.13 shows the FE-SEM image of PD4-en-S10Oc10_t10 on the carbon tape. It can be seen that the PDDA-en-Oc nanocapsules were uniform globular in shape, having a size smaller than 100 nm.

Figure 4.13 FE-SEM image of PD4-en-S10Oc10_t10 dropped on carbon tape

Figure 4.14 shows the surface morphologies of the cotton fabrics before and after immobilization with the PD4-en-S10Oc10_t10 (Cap4+) nanocapsules. The surface morphologies of neat cotton and cationized cotton (Cat-cot) were respectively smooth and slightly rough as shown in Fig. 4.14(a) and 4.14(b). In Fig. 4.14(c), the surface of PSS coated cationized cotton (Cat-cot/PSS) was quite rough due to the deposition of anionic PSS layer on the Cat-cot surface. After treating the Cat-cot/PSS in the PDDA-en-Oc nanoemulsion, the globular particles of PDDA-en-Oc were observed on the treated fabric surface as shown in Fig. 4.14(d), indicating the successful immobilization of PDDA-en-Oc on the cotton fabric.

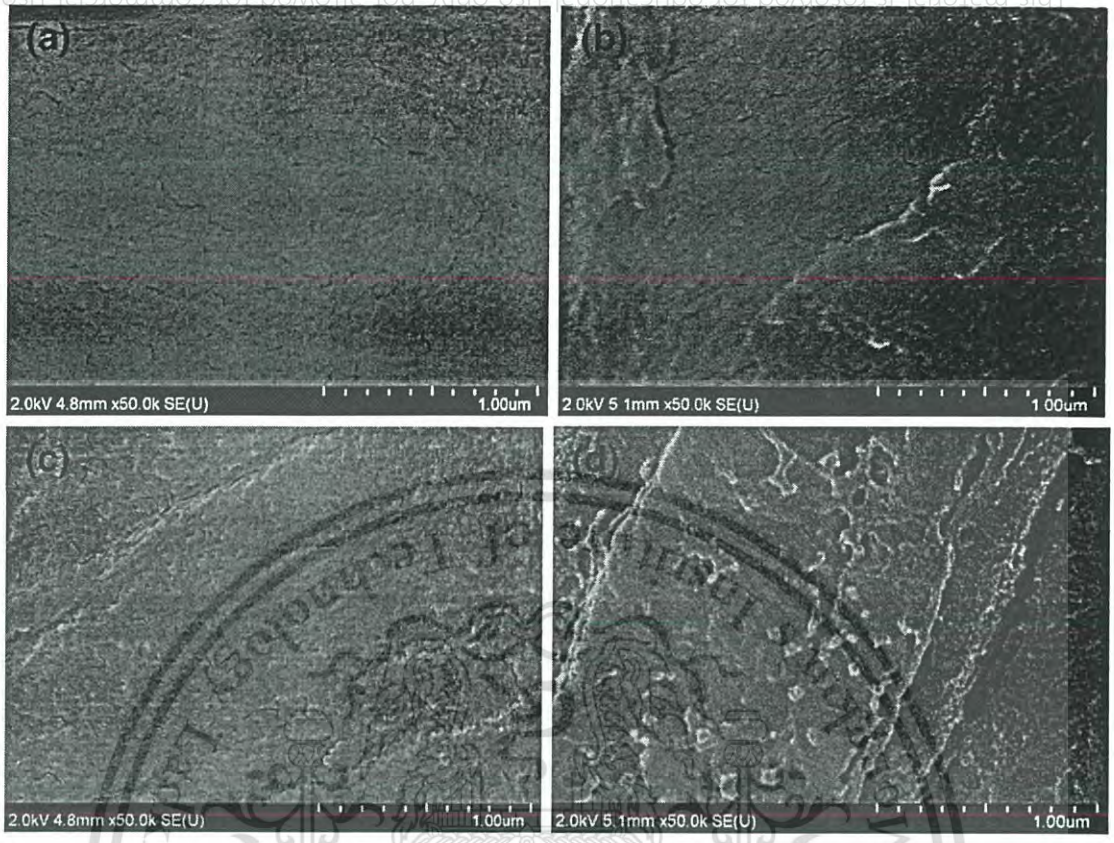

Figure 4.14 FE-SEM images of (a) neat cotton, (b) Cat-cot, (c) Cat-cot/PSS and (d) Cat-cot/PSS/Cap4+

Figure 4.15 shows the values of zeta potential of cotton samples before and after treatments as a function of pH determined from the electrokinetic analyzer (EKA). In the pH range of 3 – 11, the zeta potential of neat cotton was about (-4) to (-13) mV due to the dissociation of carboxylic group (–COOH), in which it was obtained when the $-CH_2OH$ in the cotton was oxidized [139]. After cationization, the presence of quaternary ammonium ions (NR_4^+) on the Cat-cot sample resulted in the positive zeta potential.

When the Cat-cot sample was coated with the PSS layer, the Cat-cot/PSS sample showed the negative zeta potential in the whole pH range due to the presence of sulfonate anions (SO_3^-) from the PSS molecules. The positive zeta potential was obtained when the Cat-cot/PSS was soaked in the PD4-en-S10Oc10_t10 emulsion, forming as the Cat-cot/PSS/Cap4+. This result was due to the deposition of the positively charged PDDA-en-Oc on the treated cotton fabric, indicating the successful immobilization of PDDA-en-Oc nanocapsules *via*

electrostatic interaction between negatively charged PSS on the Cat-cot/PSS surface and the positively charged PDDA-en-Oc shell.

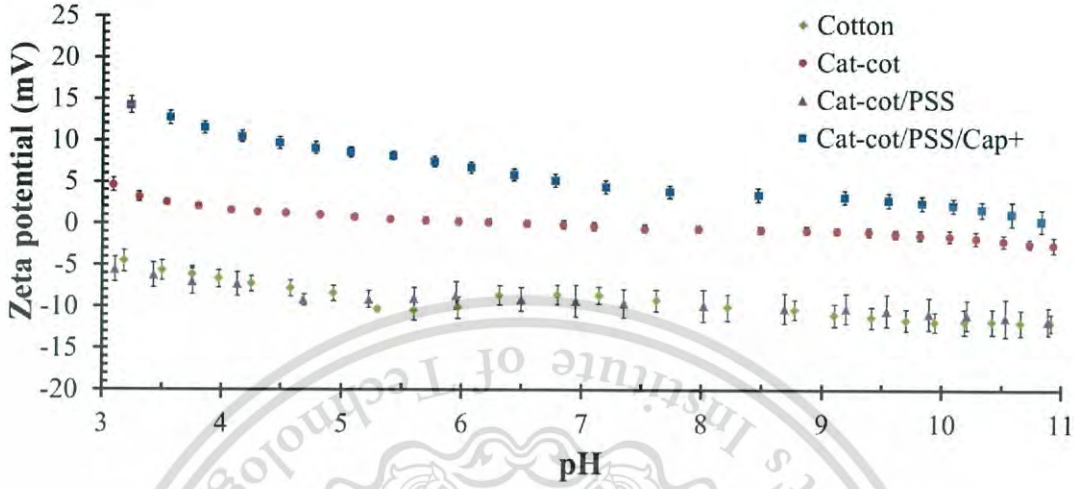

Figure 4.15 EKA results of Cotton, Cat-cot, Cat-cot/PSS and Cat-cot/PSS/Cap4+

In addition, the XPS was used to investigate the chemical changes of the cotton surface after treatment. The chemical state of the cotton before and after treatment were analyzed by XPS as shown in Fig. 4.16(a). The XPS spectrum of a cotton sample showed peaks at 281.91 eV and 528.91 eV, corresponding to the signals of carbon (C1s) and oxygen (O1s), respectively. These signals came from the cellulose, which is the main component of cotton. When the cotton was cationized, a trace amount of nitrogen (N1s), generated during the cationization process, was detected at 398.91 eV together with the signals of C1s and O1s of the cotton.

After the cationized cotton was treated with the PSS, the signal of sulfur (S2p) originated from PSS was observed at 165 eV in the XPS spectrum. However, the signals of C1s, O1s and N1s from the cationized cotton were still remain. These results indicated the formation of PSS nanolayer on the surface of cationized cotton.

After immobilation of nanocapsules on the treated cotton, the amine group from PDDA shell would interacted with the free sulfonate group of the PSS binder layer. From this point of view, the changes of S2p and N1s trace signals were determined as shown in Fig. 4.16(b) and 4.16(c). Table 4.5 show the peak intensities of N1S, O1s and S2p and the peak intensity ratios of N/O and S/O of cotton samples

before and after each treatment step. It can be seen that the N/O and S/O peak intensity ratios of nanocapsule immobilized cotton (Cat-cot/PSS/Cap4+) were higher than those of the starting samples (Cotton and Cat-cot). The increment of N1s signal was attributed to the integration of signals from the PDDA shell of nanocapsules and the cationized cotton. In addition, the increment of S2p signal was attributed to the integration of signals from the SDS shell of nanocapsules and the PSS treated cationized cotton. These results could insist the presence of *n*-octadecane nanocapsules immobilized on the cotton surface.

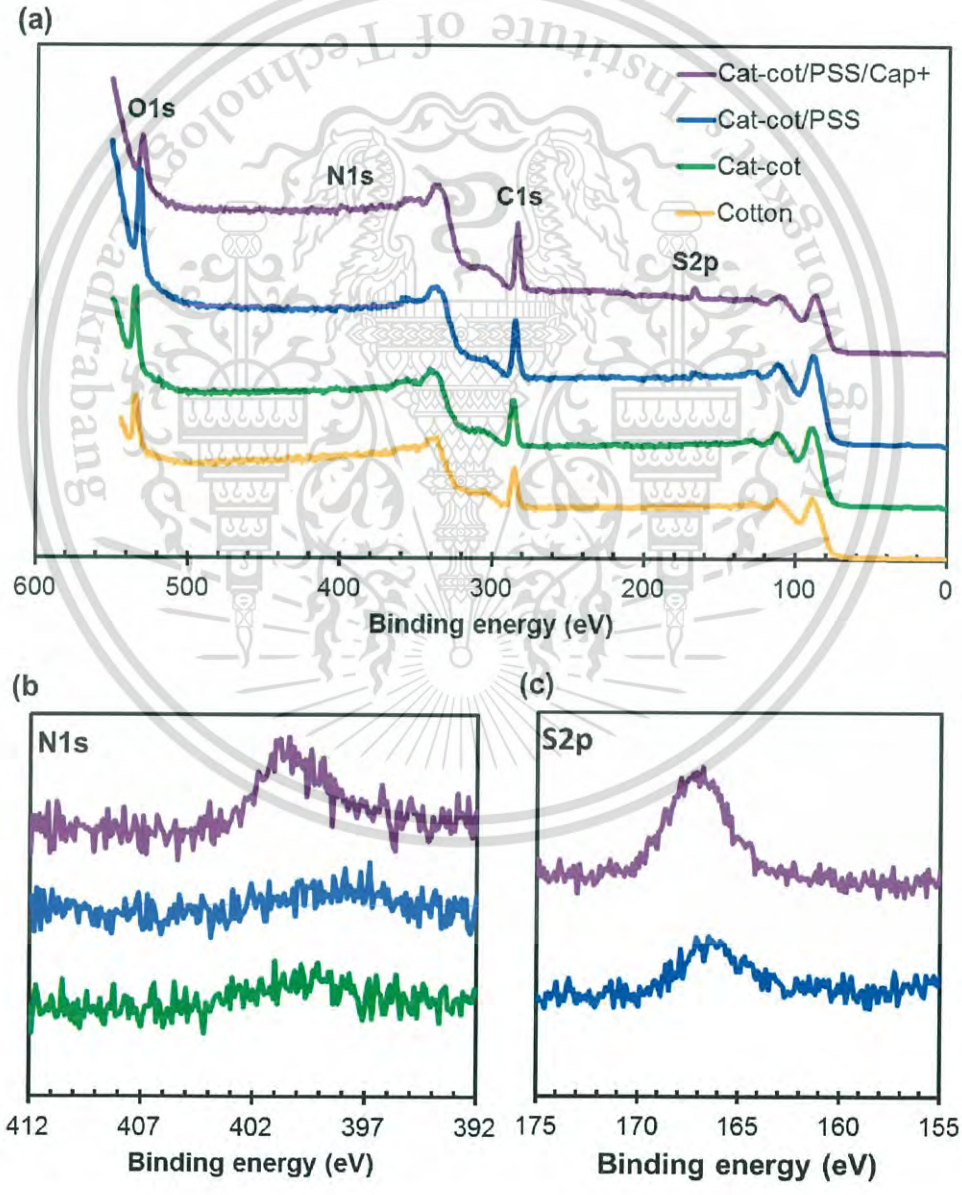

Figure 4.16 XPS spectra of Cotton, Cat-cot, Cat-cot/PSS and Cat-cot/PSS/Cap4+ : (a) low resolution spectra, (b) N1s and (c) S2p high resolution spectra

Table 4.5 XPS peak intensities of N1S, O1s and S2p and the peak intensity ratios of N/O and S/O of cotton samples before and after various treatment steps

Sample	Peak intensity (CPS)			Intensity ratio	
	N1s	O1s	S2p	N/O	S/O
Cotton	n/a	6.11	n/a	-	-
Cat-cot	0.44	8.95	n/a	0.05 : 1	-
Cat-cot/PSS	0.39	9.24	0.51	0.04 : 1	0.06 : 1
Cat-cot/PSS/Cap4+	0.58	4.37	0.76	0.13 : 1	0.17 : 1

(2) Effect of PSS concentration

In order to study the effect of PSS concentration used in the treatment system, the cationized cotton was firstly treated with 1 - 50 mM PSS solution and then soaked in the PD4-en-S10Oc10_t10 (Cap4+) emulsion. The quantities of immobilized nanocapsules and surface properties of Cat-cot/PSS/Cap4+ sample treated by using various PSS concentrations were investigated as follows.

(2.1) PDDA-en-colOc immobilized on cotton fabric

In order to determine the quantities of PDDA-en-Oc nanocapsules immobilized on the cotton fabrics, the colored PD4-en-S10Oc10_t10 (colCap4+) nanocapsules were prepared by dissolving sudan red 7b in the *n*-octadecane core material. The colCap4+ nanocapsules were immobilized on the cotton fabrics using various concentrations of PSS binder to obtain Cat-cot/PSS/colCap4+ samples. The effect of PSS concentration on the quantities of immobilized colCap4+ nanocapsules was indirectly determined from the color strength (K/S value) of sudan red 7b containing in the Cat-cot/PSS/colCap4+ samples using the colorimeter. The Cat-cot sample was used to set the K/S values to zero (blank). The high K/S value referred to the high quantities of colored nanocapsules immobilized on cotton. Table 4.6 show the K/S values of Cat-cot/PSS/colCap4+ samples. It can be seen that the K/S values of Cat-cot/PSS/colCap4+ samples increased with the increase of PSS concentration used in the Cat-cot treatment prior to nanocapsule immobilization, indicating the increase of Cap4+ quantities immobilized on the Cat-cot/PSS surfaces.

Table 4.6 K/S values of Cat-cot/PSS/colCap4+ when using various PSS concentrations in the prior treatment

Sample	PSS concentration (mM)	K/S
Cat-cot/PSS1_t30/colCap4+_t30	1	0.0099 ± 0.0001
Cat-cot/PSS5_t30/colCap4+_t30	5	0.0152 ± 0.0003
Cat-cot/PSS10_t30/colCap4+_t30	10	0.0246 ± 0.0005
Cat-cot/PSS20_t30/colCap4+_t30	20	0.0301 ± 0.0007
Cat-cot/PSS30_t30/colCap4+_t30	30	0.0410 ± 0.0001
Cat-cot/PSS40_t30/colCap4+_t30	40	0.0459 ± 0.0003
Cat-cot/PSS50_t30/colCap4+_t30	50	0.0559 ± 0.0002

(2.2) Determination of dye adsorption

The surface properties of cotton fabrics before and after immobilization with the PD4-en-S10Oc10_t10 (Cap4+) nanocapsules were determined from dye adsorption behavior using two different kinds of synthetic dyes, i.e. cationic and anionic dyes. Figure 4.17 shows the methylene blue (MB) adsorption of Cat-cot/PSS (dash line) and the eosin B adsorption of Cat-cot/PSS/Cap4+ (solid line) as a function of PSS concentration used in the cotton treatment.

It was found that the Cat-cot/PSS precursors could effectively adsorb the cationic molecules of MB owing to the presence of negative PSS coated layer. The higher PSS concentrations used in the treatment, the higher quantity of MB adsorption were obtained due to the increase of negative sites on the Cat-cot/PSS surface. On the other hand, the MB could not be adsorbed by all of the Cat-cot/PSS/Cap4+ samples. These results indicated that the presence of positive sites on Cap4+ nanocapsules, resulting in the electrostatic repulsion between the Cap4+ immobilized on the cotton fabric and the positive MB molecules.

Since the surface properties of Cat-cot/PSS/Cap4+ samples could not determine from the MB adsorption, the adsorption of anionic eosin B was investigated. From Fig 4.17, it was found that the Cat-cot/PSS/Cap4+ samples could effectively adsorb the negative eosin B molecules. The eosin B adsorption of the Cat-cot/PSS/Cap4+ samples increased with the increase of PSS concentrations used in the prior treatment. These results were because the higher the PSS

concentrations used in the treatment, the higher quantity of PDDA-en-Oc adsorbed on the Cat-cot/PSS/Cap4+ samples was obtained as previously discussed, resulting in the higher positive sites for the eosin B adsorption. These results were significantly higher than those of the neat cotton and Cat-cot samples, i.e. 1.86 ± 0.16 and 16.48 ± 0.01 mg/g, respectively.

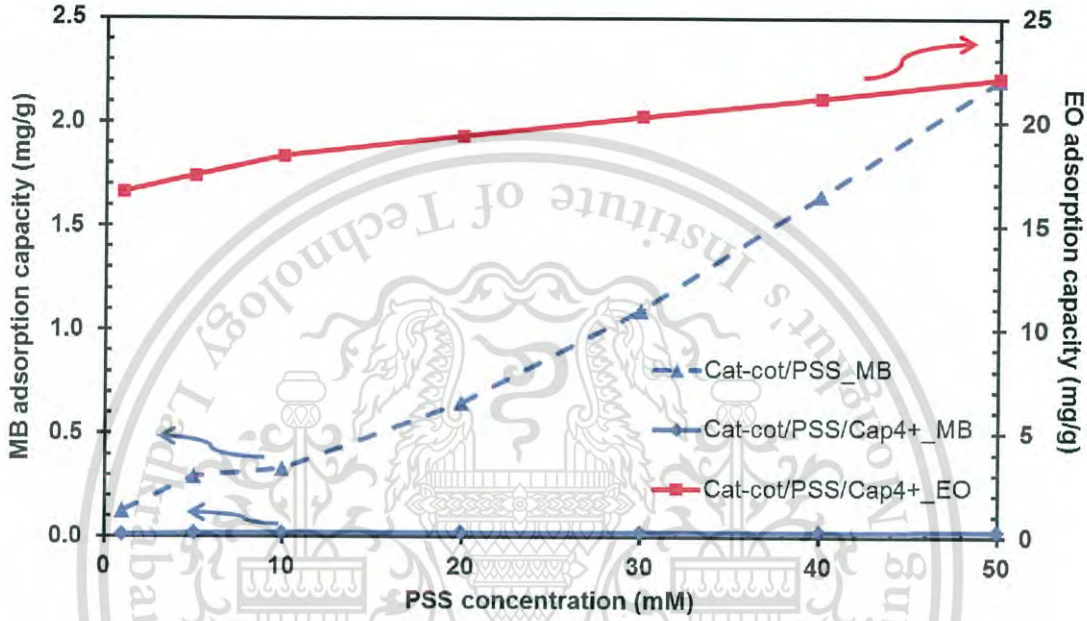

Figure 4.17 Adsorption capacities of Cat-cot/PSS for methylene blue (dash line) and Cat-cot/PSS/Cap4+ for eosin B (solid line) as a function of PSS concentration used in the treatment

From these results, the schematic structures of the PSS coated Cat-cot and Cap4+ immobilized Cat-cot/PSS samples when using various PSS concentrations were proposed as shown in Fig. 4.18(a) and Fig. 4.18(b), respectively. Since the PSS is strong polyelectrolyte, it completely dissociates in the aqueous solution forming as fully charged molecules. When the concentration of PSS polyelectrolyte used in the treatment was low, the stretched chains of PSS spontaneously formed in the solution because the intrachain charged repulsion was dominated over the interchain ones. It was, therefore, the PSS with the stretched chain conformation was adsorbed on the Cat-cot surface as shown in Fig. 4.18(a). The increase of PSS concentration in the treatment system brought about the increase of the interchain charged repulsion, resulting in a random coil conformation

of PSS molecules in the solution. The Cat-cot samples coated with the random coil PSS molecules possessed higher density of negatively charged surfaces than that with the stretched chain PSS. When the Cat-cot/PSS fabrics were soaked in the Cap4+ emulsion, the Cap4+ particles were spontaneously interacted with the PSS coated layer and immobilized on the Cat-cot/PSS fabrics as shown in Fig. 4.18(b). The higher density of negative charges on the Cat-cot/PSS surface, the higher amount of PD4-en-S10Oc10_t10 immobilized on the Cat-cot/PSS fabrics was obtained.

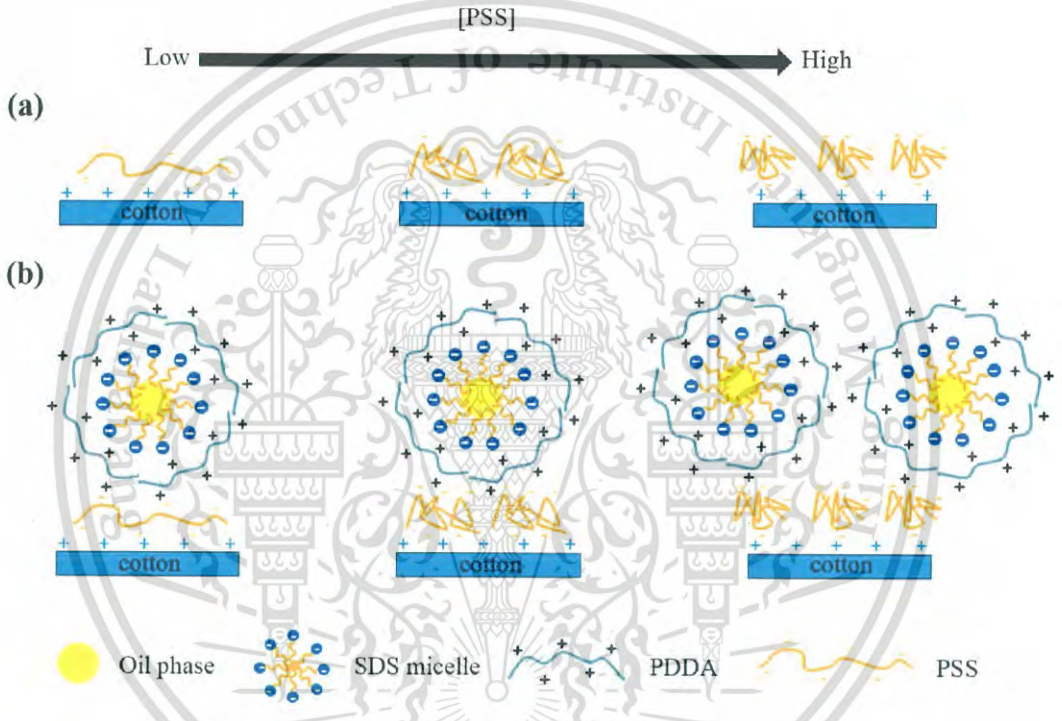

Figure 4.18 Schematic models of (a) Cat-cot/PSS and (b) Cat-cot/PSS/Cap4+ samples when using various PSS concentrations

(3) Effect of surface property of PDDA-en-Oc nanocapsules

The PDDA-en-Oc nanocapsules prepared by using various PDDA concentration possessed various surface property as mentioned previously in section 4.1.2. Therefore, the PD4-en-S10Oc10_t10 (Cap4+) nanocapsules having zeta potential value of (-40.29) mV was selected to immobilize on cotton fabric in comparison with the PD10-en-S10Oc10_t10 (Cap10+) nanocapsules having zeta potential value of (31.94) mV, in order to investigated the effect of surface property

of PDDA-en-Oc nanocapsules on the immobilized quantities of nanocapsules and surface properties of Cat-cot/PSS/Cap+ products.

(3.1) PDDA-en-colOc immobilized on cotton fabric

The colored *n*-octadecane nanocapsules, i.e. PD4-en-S10colOc10_t10 (colCap4+) and PD10-en-S10colOc10_t10 (colCap10+), were prepared and immobilized on the Cat-cot/PSS fabrics treated with various PSS concentrations, creating the Cat-cot/PSS/colCap+ samples. The quantities of nanocapsules having different zeta potential values immobilized on the Cat-cot/PSS/colCap+ samples were indirectly determined from the K/S value using the colorimeter. Table 4.7 shows the K/S values of Cat-cot/PSS/colCap4+ and Cat-cot/PSS/colCap10+ samples. It can be seen that the K/S values of Cat-cot/PSS/colCap4+ and Cat-cot/PSS/colCap10+ samples prepared by using equal PSS concentration were quite similar. These results suggested that both systems possessed the equivalent amount of Cap4+ and Cap10+ nanocapsules immobilized on the cotton samples. The higher PSS concentration used in the Cat-cot treatment prior to nanocapsule immobilization, the higher K/S values of Cat-cot/PSS/colCap4+ and Cat-cot/PSS/colCap10+ were obtained, indicating the increase of Cap4+ and Cap10+ quantities immobilized on the Cat-cot/PSS surfaces.

Table 4.7 K/S values of Cat-cot/PSS/colCap4+ and Cat-cot/PSS/colCap10+ when using various PSS concentrations in the prior treatments

Sample	K/S	
	Cap4+	Cap10+
Cat-cot/PSS1_t30/colCap+_t30	0.0099 ± 0.0001	0.0097 ± 0.0003
Cat-cot/PSS5_t30/colCap+_t30	0.0152 ± 0.0003	0.0148 ± 0.0010
Cat-cot/PSS10_t30/colCap+_t30	0.0246 ± 0.0005	0.0246 ± 0.0006
Cat-cot/PSS20_t30/colCap+_t30	0.0301 ± 0.0007	0.0288 ± 0.0008
Cat-cot/PSS30_t30/colCap+_t30	0.0410 ± 0.0001	0.0407 ± 0.0005
Cat-cot/PSS40_t30/colCap+_t30	0.0459 ± 0.0003	0.0456 ± 0.0013
Cat-cot/PSS50_t30/colCap+_t30	0.0559 ± 0.0002	0.0557 ± 0.0005

(3.2) Determination of dye adsorption

The surface properties of Cat-cot/PSS/Cap+ products immobilized with the nanocapsules having different zeta potential values, i.e. Cap4+ and Cap10+ were determined from dye adsorption behavior using both cationic (methylene blue, MB) and anionic (eosin B, EO) dyes. Figure 4.19 shows the MB adsorption and EO adsorption of Cat-cot/PSS/Cap4+ (dash line) and Cat-cot/PSS/Cap10+ (solid line) as a function of PSS concentration used in the prior treatment.

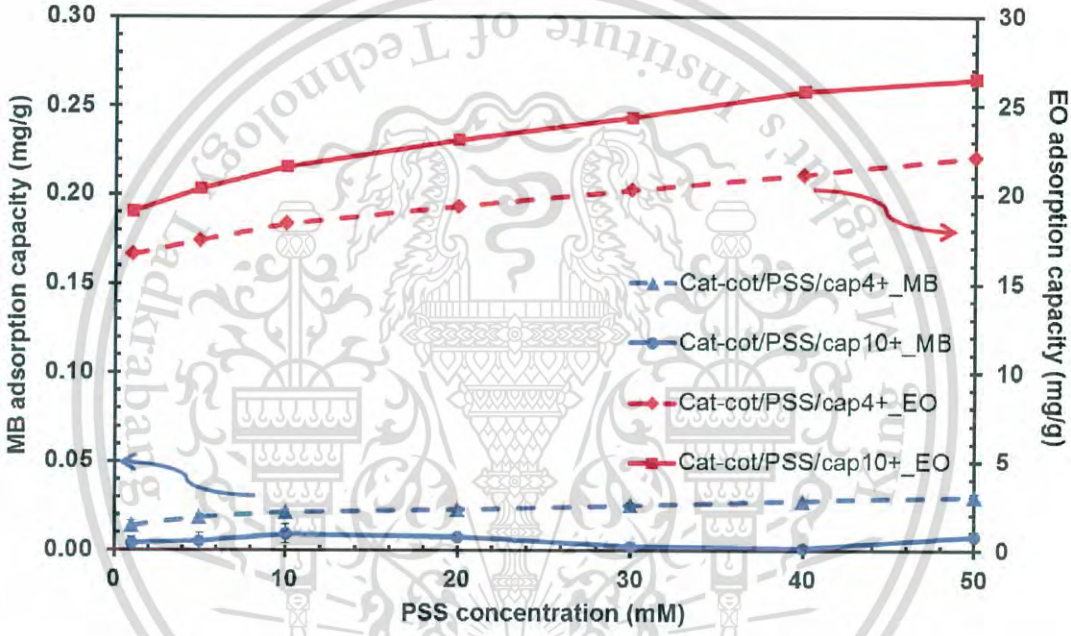

Figure 4.19 Adsorption capacities of Cat-cot/PSS/Cap+ using nanocapsules with different zeta potential value for methylene blue and eosin B as a function of PSS concentration used in the prior treatment

It was found that both Cat-cot/PSS/Cap+ could be effectively adsorbed the negative molecules of EO, indicating the presence of positive sites on the outermost surface of both of Cap4+ and Cap10+ nanocapsules immobilized on the cotton samples. However, the Cat-cot/PSS/Cap10+ sample adsorbed higher quantity of EO than the Cat-cot/PSS/Cap4+ sample. These results were considered to be because the presence of positive sites on outermost surface of Cap10+ was higher than the Cap4+. The higher PSS concentration used in the prior treatment, the higher quantity of EO adsorption was obtained from both of Cat-cot/PSS/Cap4+

and Cat-cot/PSS/Cap10+ due to the increase of nanocapsules quantities immobilized on cotton samples.

On the other hand, all of the Cat-cot/PSS/Cap10+ samples showed no MB adsorption. These results suggested that the Cat-cot/PSS/Cap10+ products possessed the highly positive charged surfaces due to the presence of Cap10+ nanocapsules coated on their surfaces. All of the Cat-cot/PSS/Cap4+ products could adsorb small amount of MB. These results considered to be because the PDDA positive outmost layer of Cap4+ could not overcome the negative charges of Oc-SDS inner micelle, thus its zeta potential value representing the net charge of particle in solution was in the range of negative value (-40.92 mV). Therefore, the Cap4+ could electrostatic interact with both negative and positive molecule, resulting in the abilities to adsorb both of cationic and anionic dyes. The higher PSS concentrations used in the prior treatment, the higher MB adsorption capacities of the Cat-cot/PSS/Cap4+ samples were obtained due to the increase of Cap4+ quantity on the Cat-cot/PSS/Cap4+ samples.

From these results, the schematic models of PDDA-en-Oc immobilized on the Cat-cot/PSS fabrics when using nanocapsules with different zeta potential values were proposed as shown in Fig. 4.20. The Cap4+ and Cap10+ nanocapsules were immobilized on the Cat-cot/PSS samples *via* the electrostatic interaction between the negative surface of PSS molecules coated on the Cat-cot fabrics and the positive sites on the outermost surface of both Cap4+ and Cap10+. Since the Cap10+ nanocapsules possessed higher amount of positive sites on its outermost surface than Cap4+, the Cat-cot/PSS/Cap10+ surface would own higher positive sites. The positive sites on the Cat-cot/PSS/Cap+ samples increased with the increase of PSS concentrations used in the prior process of cotton treatment.

From these results, it can be conclude that the different zeta potential values between Cap4+ and Cap10+ showed no significant effect on the quantities of immobilized PDDA-en-colOc on the cotton samples, but effect on the surface properties of Cat-cot/PSS/Cap10+ products.

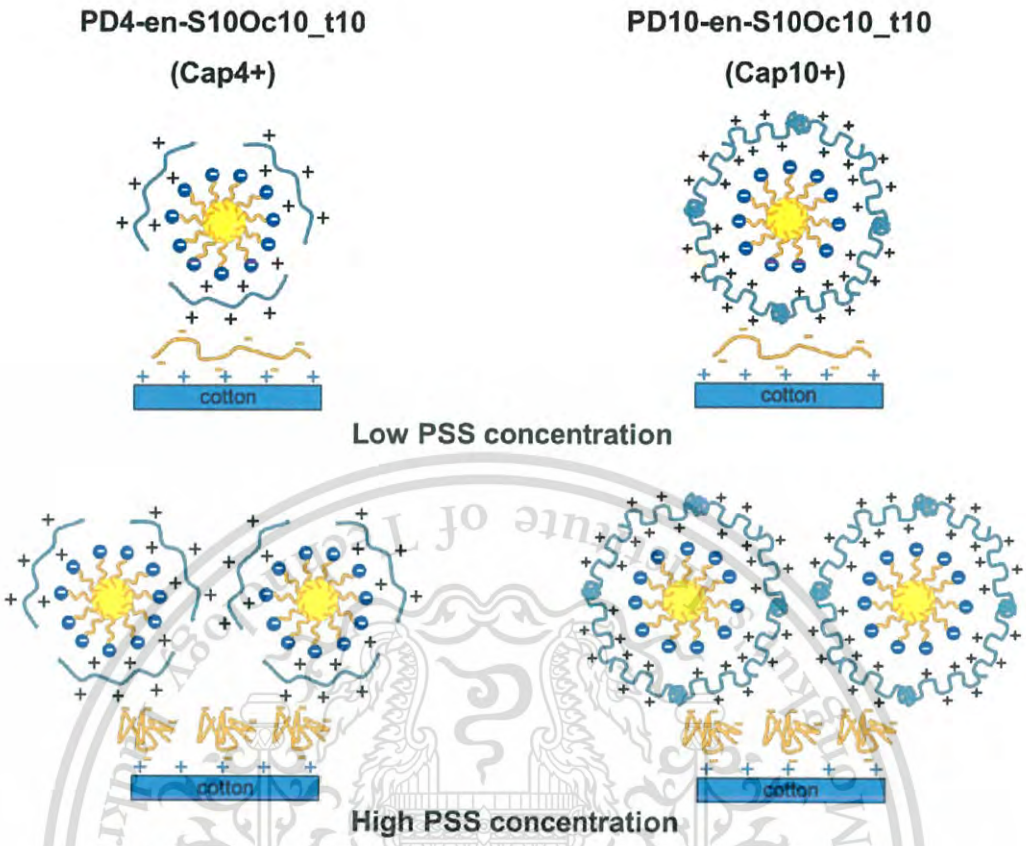

Figure 4.20 Schematic models of PDDA-en-Oc immobilized on Cat-cot/PSS fabrics when using capsules with different zeta potential value

4.2.2 Direct soaking in nanocapsules with negatively charged outermost shell

The alternative method for immobilization of nanocapsules on the cotton fabric is directly immersed the cationized cotton into the emulsion of nanocapsules with negatively charged outermost shell (2x(PD10-en-S10Oc10_t10), Cap-).

(1) Preparation of 2x(PD10-en-S10Oc10_t10) emulsion

In this part, the 2x(PD10-en-S10Oc10_t10) (Cap-) emulsions were prepared using various concentrations for creating the negatively charged outermost layer of nanocapsules. The zeta potential values of nanocapsules were determined as shown in Table 4.8.

Table 4.8 Zeta potential values of 2x(PD10-en-S10Oc10_t10) nanocapsules prepared by using various PSS concentrations

Sample	PSS concentration (mM)	Zeta potential (mV)
PD10-en-S10Oc10_t10	0	31.94 ± 0.22
2xPS4(PD10-en-S10Oc10_t10)	4	23.42 ± 0.89
2xPS8(PD10-en-S10Oc10_t10)	8	-12.94 ± 0.93
2xPS10(PD10-en-S10Oc10_t10)	10	-35.48 ± 1.00
2xPS14(PD10-en-S10Oc10_t10)	14	-40.16 ± 0.28
2xPS18(PD10-en-S10Oc10_t10)	18	-45.01 ± 3.09

From Table 4.8, it was found that the zeta potential values of 2x(PD10-en-S10Oc10_t10) nanocapsules gradually decreased from (32) mV to (-45) mV when increasing the PSS concentration used in the preparation. These results were attributed to the charge compensation between negative charges of PSS molecules and positive charges of PD10-en-S10Oc10_t10 outmost layer precursor. However, when the PSS concentration used in the encapsulation was lower than 10 mM, the zeta potential values of the as-prepared 2x(PD10-en-S10Oc10_t10) nanocapsules were in the range of (-30) – 30 mV. The zeta potential values in this range were considered to bring about the unstable emulsion system and then the flocculation was occurred.

From the above mentioned results, the 10 mM PSS solution was selected for further preparation of the 2x(PD10-en-S10Oc10_t10) (Cap-) nanocapsules in order to use for immobilization on cotton by direct soaking. It was because this preparation condition used low consumption of chemical reagent to obtain the nanocapsules without flocculation.

The PSS(PDDA-en-Oc) nanocapsules were directly immobilized on the Cat-cot fabrics by soaking the Cat-cot fabrics into the Cap- emulsion followed by rinsing in deionized water for 5 min in order to obtain the self-assembled PSS(PDDA-en-Oc) nanocapsules coated on cotton fabrics designated as Cat-cot/Cap- products. The surface morphologies of the Cat-cot/Cap- sample was shown in Fig. 4.21. It can be seen that the globular particles of Cap- nanocapsules were observed entirely coated on the fabric surface. This result indicated the successful immobilization of Cap- on the cotton fabric.

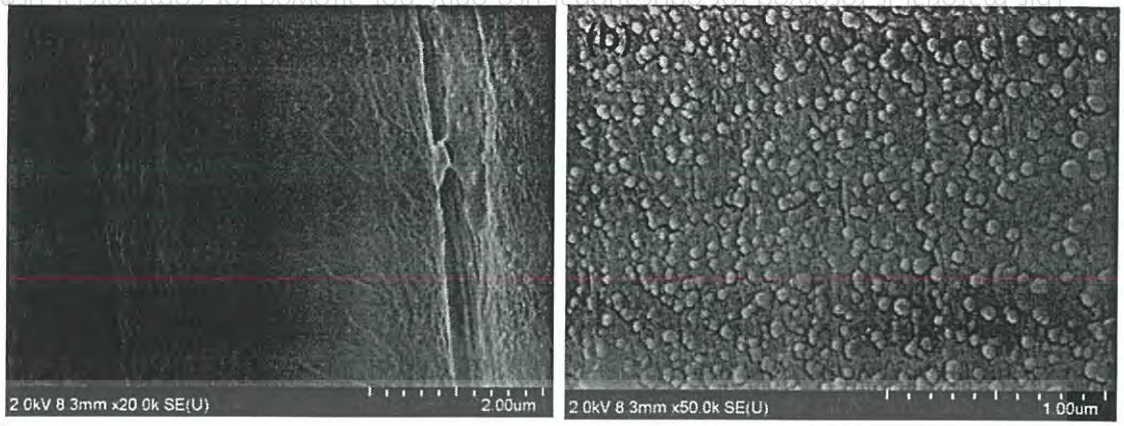

Figure 4.21 FE-SEM images of Cat-cot/Cap- sample at magnification (a) 20,000 X and (b) 50,000 X

(2) Effect of soaking time in 2x(PD10-en-S10Oc10_t10) emulsion

The effect of soaking time on the quantities of immobilized nanocapsule and surface properties of Cat-cot/Cap- samples were determined as follows.

(2.1) PEL-en-colOc immobilized on cotton fabrics

The effect of soaking time on the quantities of Cap- nanocapsules immobilized on the Cat-cot fabrics were indirectly determined by using colored nanocapsules (colCap-). The K/S values of sudan red 7b in the colCap- immobilized on the Cat-cot (Cat-cot/colCap-) samples as shown in Table 4.9. It can be seen that the K/S values increased with the increase of colCap- soaking time used in the preparation of Cat-cot/colCap- samples, indicating the increase of colCap- nanocapsules quantity.

Table 4.9 K/S values of Cat-cot/colCap- when using various soaking time

Sample	Soaking time (min)	K/S
Cat-cot/colCap-_t5	5	0.0185 ± 0.0004
Cat-cot/colCap-_t10	10	0.0204 ± 0.0005
Cat-cot/colCap-_t15	15	0.0215 ± 0.0001
Cat-cot/colCap-_t20	20	0.0220 ± 0.0002
Cat-cot/colCap-_t30	30	0.0235 ± 0.0002

(2.2) Determination of dye adsorption

The surface properties of Cat-cot/Cap- products were determined from dye adsorption behavior using cationic dyes, i.e. MB. Table 4.10 shows the MB adsorption capacity of Cat-cot/Cap- products obtained when using various soaking time in the 2x(PD10-en-S10Oc10_t10) (Cap-) immobilization.

Table 4.10 MB adsorption capacities of Cat-cot/Cap- products when using various soaking times in 2x(PD10-en-S10Oc10_t10) emulsion

Sample	Soaking time (min)	MB Adsorption capacity (mg/g)
Cat-cot	0	0.015 ± 0.002
Cat-cot/Cap-_t5	5	0.029 ± 0.005
Cat-cot/Cap-_t10	10	0.130 ± 0.002
Cat-cot/Cap-_t15	15	0.194 ± 0.002
Cat-cot/Cap-_t20	20	0.253 ± 0.003
Cat-cot/Cap-_t30	30	0.328 ± 0.002

It was found that the Cat-cot/Cap- products could effectively adsorb the cationic molecules of MB owing to the presence of negative surface from the Cap- nanocapsules coated on the fabric surfaces. The longer soaking time used in the treatment, the higher MB adsorption capacity was obtained, indicating the increase of negative sites from the Cap- nanocapsules immobilized on the Cat-cot surface. These results were in agreement with the previous data of K/S values.

4.3 Multi-cycle immobilization of PEL-en-Oc nanocapsules on fabrics

In order to increase the quantities of nanocapsules immobilized on the cotton fabrics, the Cat-cot fabric samples were treated by multi-cycle method. In this method, the Cat-cot fabrics were treated by stepwise soaking in 2 different procedures as follows.

4.3.1 Stepwise soaking in PSS solution and PDDA-en-Oc emulsion

In this procedure, the Cat-cot samples were soaked in the PSS solution and PDDA-en-Oc (Cap+) emulsion using various number of treatment cycles in order to increase the quantities of immobilized nanocapsules on the Cat-cot/PSS/Cap+ products.

From the above mentioned results in section 4.2.1, the Cat-cot/PSS10/Cap10+ sample was selected for using as the starting precursor in multicycle immobilization because the Cat-cot/PSS10/Cap10+ possessed high quantity of nanocapsules on cotton sample even using low PSS concentration, corresponding to the presence of high positive sites for further adsorption. The Cat-cot/PSS10/Cap10+ precursor was treated by stepwise soaking in PSS solution and PDDA-en-Oc emulsion using various soaking times. The optimum soaking time for PSS and Cap+ emulsion treatments were determined from dye adsorption behaviors using MB and EO dyes. Table 4.11 show the adsorption capacities of Cat-cot/PSS and Cat-cot/PSS10/Cap10+ samples for MB and EO dyes when using various soaking times in the treatments.

From Table 4.11, it was found that the longer PSS soaking time used in the treatment, the higher MB adsorption activities were obtained in the Cat-cot/PSS10 samples, indicating the increase of PSS molecules coated on the Cat-cot/PSS10 surfaces. When the PSS soaking time was increased from 5 to 10 min, the MB adsorption activity would be clearly increased from 0.251 to 0.288 mg/g. However, the MB adsorption activities of Cat-cot/PSS samples were slightly increased after prolonged PSS soaking from 10 to 30 min. These results indicated that the first 10 minutes of PSS soaking was the effective period for interaction between PSS molecules and Cat-cot samples. Therefore, the Cat-cot/PSS10_t10 sample obtained from 10 min PSS soaking was used for further Cap10+ immobilization. The Cat-cot/PSS10_t10 samples were soaked in the Cap10+ emulsion for various soaking times in order to determine the optimum Cap10+ soaking time from the dye adsorption behavior. It was found that all Cat-cot/PSS10/Cap10+ samples hardly adsorbed the MB cationic dye, suggesting the successful immobilization of positively charged Cap10+ on the cotton surfaces. Therefore, the quantities of Cap10+ nanocapsules immobilized on the Cat-cot/PSS10_t10 samples were indirectly determined from EO adsorption. The increase of EO adsorption was obtained when

increasing the Cap10+ soaking time used in the treatment owing to the increase of Cap10+ quantity adsorbed on the Cat-cot/PSS10_t10 samples. The EO adsorption capacities of Cat-cot/PSS10/Cap10+ samples were clearly increased from 20.43 to 20.80 mg/g when increasing the Cap10+ soaking time from 5 to 10 min. However, when the Cat-cot/PSS10_t10 samples were soaked in the Cap10+ emulsion for longer than 10 min, the EO adsorption capacities of Cat-cot/PSS10_t10/Cap10+ samples would be slightly increased. These results suggested that the optimum soaking time for immobilization of Cap10+ nanocapsules on the Cat-cot/PSS10_t10 samples was 10 min.

Table 4.11 MB and EO adsorption capacities of Cat-cot/PSS and Cat-cot/PSS/Cap+ samples prepared by using various soaking times

Sample	MB Adsorption capacity (mg/g)	EO Adsorption capacity (mg/g)
Cat-cot/PSS10_t5	0.251 ± 0.007	n/a
Cat-cot/PSS10_t10	0.288 ± 0.002	n/a
Cat-cot/PSS10_t15	0.306 ± 0.004	n/a
Cat-cot/PSS10_t20	0.319 ± 0.004	n/a
Cat-cot/PSS10_t30	0.331 ± 0.002	n/a
Cat-cot/PSS10_10/Cap10+_t5	0.007 ± 0.005	20.430 ± 0.016
Cat-cot/PSS10_t10/Cap10+_t10	0.008 ± 0.004	20.800 ± 0.012
Cat-cot/PSS10_t10/Cap10+_t15	0.007 ± 0.002	20.909 ± 0.009
Cat-cot/PSS10_t10/Cap10+_t20	0.010 ± 0.002	21.005 ± 0.008
Cat-cot/PSS10_t10/Cap10+_t30	0.008 ± 0.004	21.106 ± 0.011

It can be concluded from the above mentioned results that the optimum soaking time for both PSS and Cap+ treatments were 10 min-soaking time. The optimum soaking times were used further in multi-cycle immobilization process.

The multi-cycle immobilization was performed by alternate soaking the Cat-cot fabric into the PSS solution and PDDA-en-Oc emulsion for 1 - 5 cycles. The surface morphology of Cat-cot/(PSS10/Cap10+)_x5 product obtained from 5 cycles treatment was shown in Fig. 4.22. It can be seen that the surface of treated fabric was coated with a rough layer consisting the globular particles of Cap10+.

However, the Cap10+ coating layer in this sample was observed as worm-like clusters due to the aggregation of globular particles in the PSS binder layer. This result revealed the increase of immobilized Cap10+ quantity on the cotton fabric.

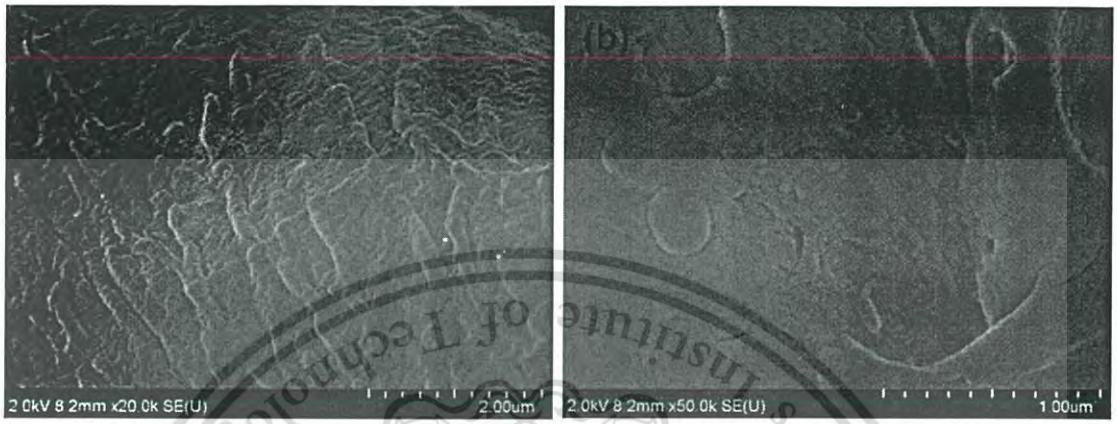

Figure 4.22 FE-SEM images of Cat-cot/(PSS10/Cap10+)_x5 at magnification (a) 20,000X and (b) 50,000X

In addition, the presence of Cap10+ nanocapsules on the cotton fabric treated by multi-cycle immobilization was further confirmed by using the colored Cap10+ nanocapsules (colCap10+). The quantities of colCap10+ nanocapsules multi-cycle immobilized on the cotton samples (1 - 5 cycles) could be indirectly determined from the K/S values as shown in Table 4.12. The higher number of treatment cycle (PSS10/colCap10+), the higher K/S values of Cat-cot/(PSS10/colCap10+) samples were obtained due to the increase of colCap10+ content. These results revealed the successful addition of Cap10+ quantity immobilized on the cotton fabrics by increasing the treatment cycle of Cat-cot stepwise soaking in PSS solution and PDDA-en-Oc emulsion.

Table 4.12 K/S values of Cat-cot/(PSS10/colCap10+) products prepared by multi-cycle immobilization process

Sample	Number of Cap10+ coated layer	K/S
Cat-cot/(PSS10/colCap10+)_x1	1	0.0243 ± 0.0004
Cat-cot/(PSS10/colCap10+)_x2	2	0.0289 ± 0.0004
Cat-cot/(PSS10/colCap10+)_x3	3	0.0343 ± 0.0004
Cat-cot/(PSS10/colCap10+)_x4	4	0.0423 ± 0.0003
Cat-cot/(PSS10/colCap10+)_x5	5	0.0517 ± 0.0002

4.3.2 Stepwise soaking in PSS(PDDA-en-Oc) and PDDA-en-Oc emulsion

An addition method for increase the quantity of nanocapsules immobilized on the cotton fabrics has been proposed by stepwise soaking the Cat-cot fabric in two emulsion systems having nanocapsules with negatively charged and positively charged outermost shell layer, i.e. PSS(PDDA-en-Oc) (Cap-) and PDDA-en-Oc (Cap+), respectively. According to the preparation of Cat-cot/Cap- mentioned in section 4.2.2, the Cat-cot/Cap-_t10 possessed the high quantity of Cap- nanocapsules on the cotton sample even using short soaking time. Therefore, the Cat-cot samples were alternately soaked in the Cap- for 10 min and Cap+ for 10 min in multi-cycle immobilization process.

The nanocapsules immobilization *via* multi-cycle stepwise treatment was performed by alternate soaking the Cat-cot fabric into the 2x(PD10-en-S10Oc10_t10) (Cap-) emulsion and PD10-en-S10Oc10_t10 (Cap10+) emulsion for 1 - 5 layers. The surface morphology of Cat-cot/(Cap-/Cap10+)_x5 was shown in Fig. 4.23. It can be seen that the surface of treated fabric was coated with a rough layer of globular aggregates of nanocapsules. This result presented the successful immobilization of nanocapsules on the cotton fabric by multi-cycle immobilization process.

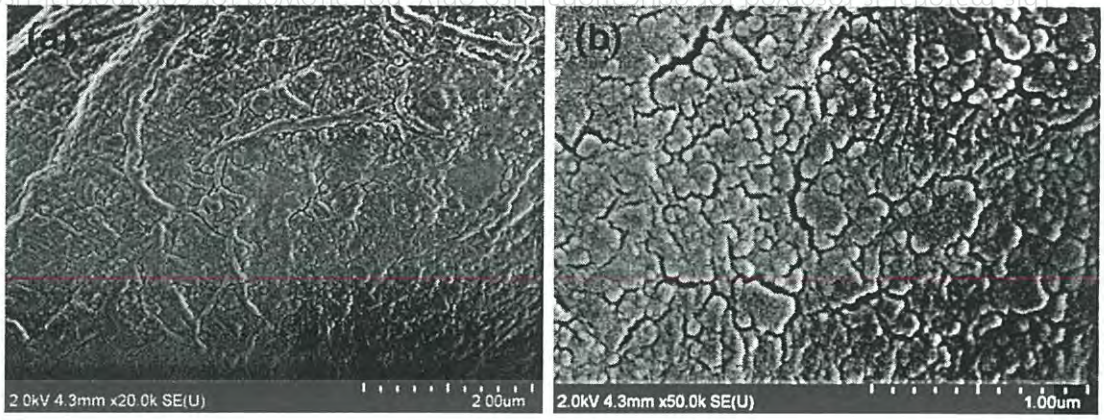

Figure 4.23 FE-SEM images of Cat-cot/(Cap-/Cap10+)_x5 at magnification (a) 20,000X and (b) 50,000X

In addition, the colored Cap- (colCap-) and colored Cap10+ (colCap10+) nanocapsules were prepared and then multi-cycle immobilized on the Cat-cot for 1 - 5 layers creating the Cat-cot/(colCap-/colCap10+) products. The K/S values of Cat-cot/(colCap-/colCap10+) products were determined in order to confirm the presence of nanocapsules on the treated cotton samples as shown in Table 4.13. It can be seen that the higher K/S values were obtained when using the higher number of treatment cycle for colCap immobilization. These results affirmed that the effective addition of nanocapsules content immobilized on the cotton fabrics was obtained by multi-cycle stepwise soaking in Cap- and Cap10+ emulsions.

Table 4.13 K/S values of Cat-cot/(colCap-/colCap10+) products prepared by multi-cycle immobilization process

Sample	Number of treatment cycle	K/S
Cat-cot/colCap-_t10	1	0.0204 ± 0.0005
Cat-cot/(colCap-/colCap10+)_x2	2	0.0414 ± 0.0009
Cat-cot/(colCap-/colCap10+)_x3	3	0.0623 ± 0.0015
Cat-cot/(colCap-/colCap10+)_x4	4	0.0765 ± 0.0006
Cat-cot/(colCap-/colCap10+)_x5	5	0.0951 ± 0.0009

4.4 Thermo-regulating property

The treated cotton samples containing different amount of PEL-en-Oc nanocapsules were used for evaluating the thermo-regulating property in comparison with the neat cotton. After the untreated and treated cotton samples were chilled at 5 °C for 3 min, they were kept in the chamber at temperature of about 50 °C and monitored their temperature change during 1 – 10 min from the thermal images. Figure 4.24 to 4.29 show the thermal images of untreated and treated cotton samples after taking out from the chilling system for 1, 2, 3, 5, 7 and 10 min. In the thermal image, the temperature is represented by color in which the blue color respectively represents cooler temperature than yellow and red. It can be seen that the surface temperatures of all treated cotton samples were lower than those of untreated samples, indicating the action of thermo-regulating property of PEL-en-Oc nanocapsules immobilized on the cotton samples. When the surrounding temperature increased, the *n*-octadecane in the nanocapsules absorbed heat from the surrounding area, resulting in phase transition of *n*-octadecane from solid to liquid (Melting process). This action could retard the temperature change of treated cotton until all of *n*-octadecane in the nanocapsules immobilized on the samples were melted.

The neat cotton could maintain the cold temperature for 3 min due to the thermal insulation property of cotton fabric. On the other hand, the treated cotton could maintain the cold temperature for longer period of time. The longer duration of thermo-regulating effect was obtained when the treated cotton samples immobilized with the higher quantity of *n*-octadecane nanocapsules. However, the duration of thermo-regulating effect in the treated cotton consisted of Cap- layers, i.e. Cat-cot/Cap-_t10, Cat-cot/(Cap-/Cap10+)_x3 and Cat-cot/(Cap-/Cap10+)_x5, was shorter than those consisted of PSS/Cap10+ layers having the equivalent number of nanocapsule layers. These results were considered to be because the latent heat of Cap- was lower than the Cap10+ as mentioned in section 4.1.3, resulting in the decline of thermo-regulating effect in the Cap- nanocapsules immobilized cotton.

In addition, the surface temperature of neat cotton and treated cotton after taking out from the chilling system for 1 min were detected from the thermal images by FLIR infrared thermography camera as shown in Appendix A.3. The temperature

differences between neat cotton and treated cotton samples (ΔT) were calculated and then summarized in Table 4.14.

The higher quantity of *n*-octadecane nanocapsules immobilized on the treated cotton, the higher ΔT was obtained due to the higher heat absorption from the surrounding area. The amount of heat absorption not only depended on the quantity of *n*-octadecane nanocapsules immobilized on the treated cotton, but also their latent heat value. Therefore, the duration and ΔT of thermo-regulating action obtained in the treated cotton were listed as follows:

Cat-cot/Cap-_t10 < Cat-cot/(PSS10/Cap10+)_x1 <
Cat-cot/(Cap-/Cap10+)_x3 < Cat-cot/(PSS10/Cap10+)_x3 <
Cat-cot/(Cap-/Cap10+)_x5 < Cat-cot/(PSS10/Cap10+)_x5

The Cat-cot/(PSS10/Cap10+)_x5 sample exhibited the longest thermo-regulating action with the highest temperature difference between neat cotton and treated cotton samples, in which its ΔT was about 2.5 °C for longer than 10 min.

Table 4.14 K/S values of treated cotton samples and their temperature differences (ΔT) between neat and treated cotton after taking out from the chilling system for 1 min

Samples	K/S	ΔT (°C)
Cat-cot/(PSS10/Cap10+)_x1	0.0243 ± 0.0004	2.13 ± 0.21
Cat-cot/(PSS10/Cap10+)_x3	0.0343 ± 0.0004	2.23 ± 0.10
Cat-cot/(PSS10/Cap10+)_x5	0.0517 ± 0.0002	2.50 ± 0.15
Cat-cot/Cap-_t10	0.0204 ± 0.0005	2.06 ± 0.06
Cat-cot/(Cap-/Cap10+)_x3	0.0623 ± 0.0015	2.20 ± 0.10
Cat-cot/(Cap-/Cap10+)_x5	0.0951 ± 0.0009	2.34 ± 0.06

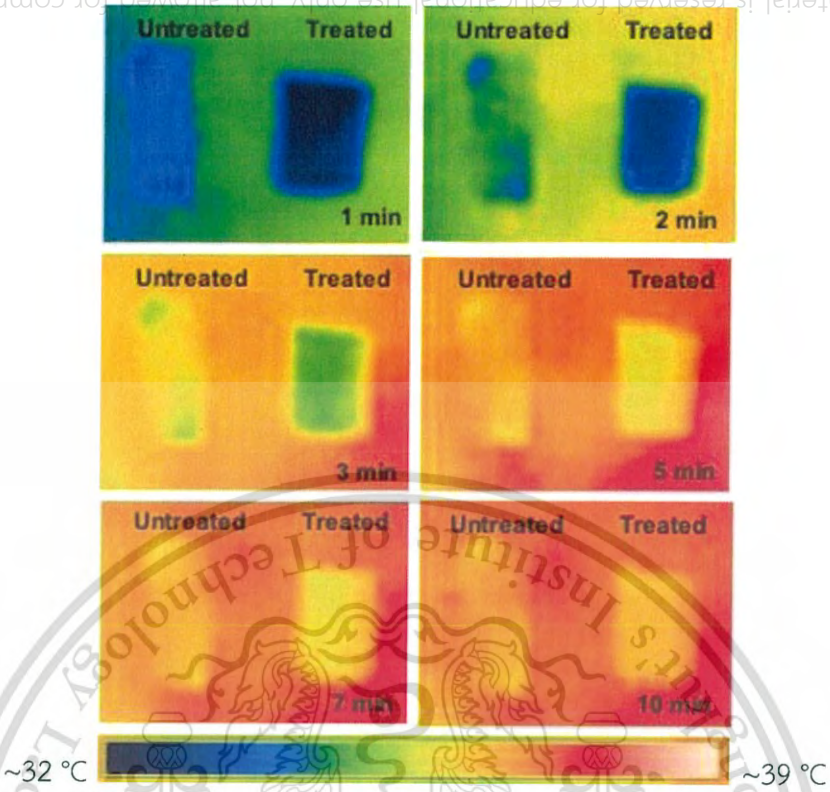

Figure 4.24 Thermal images of Cat-cot/(PSS10/Cap10+)_x1 sample

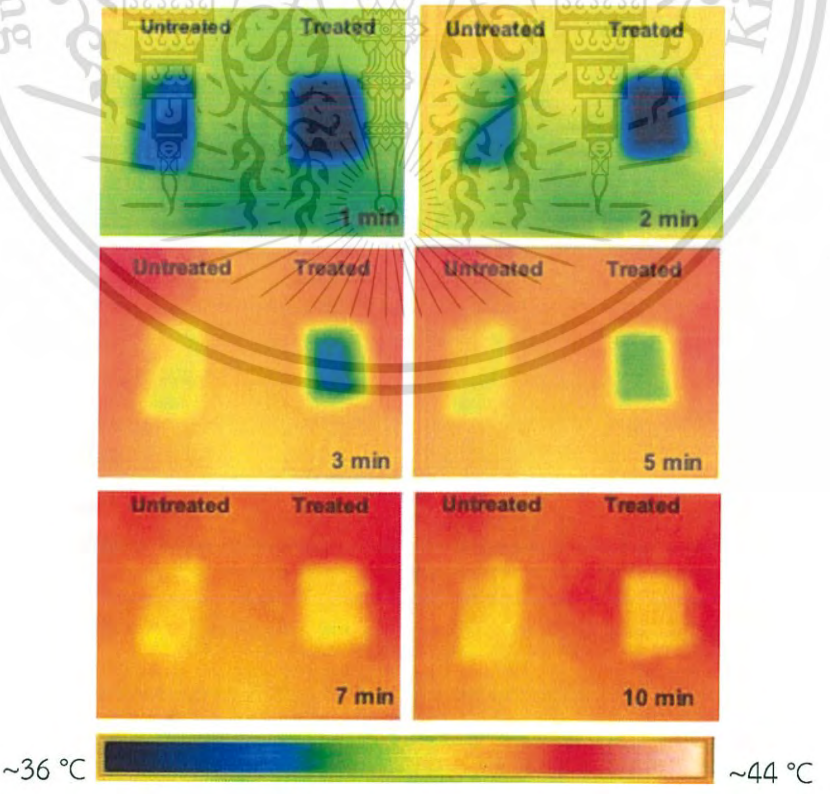

Figure 4.25 Thermal images of Cat-cot/(PSS10/Cap10+)_x3 sample

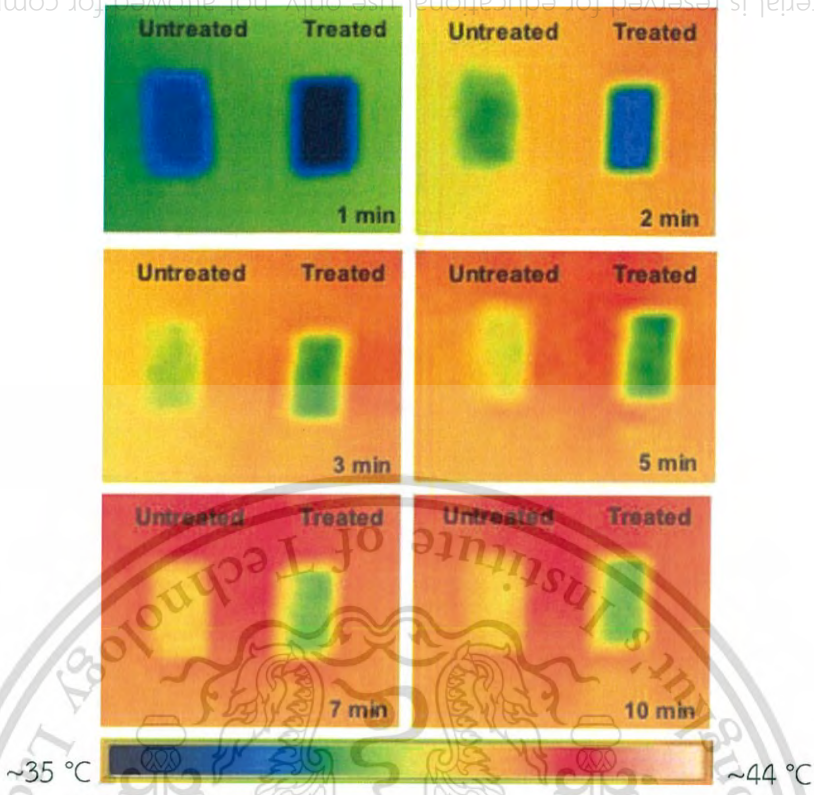

Figure 4.26 Thermal images of Cat-cot/(PSS10/Cap10+)_x5 sample

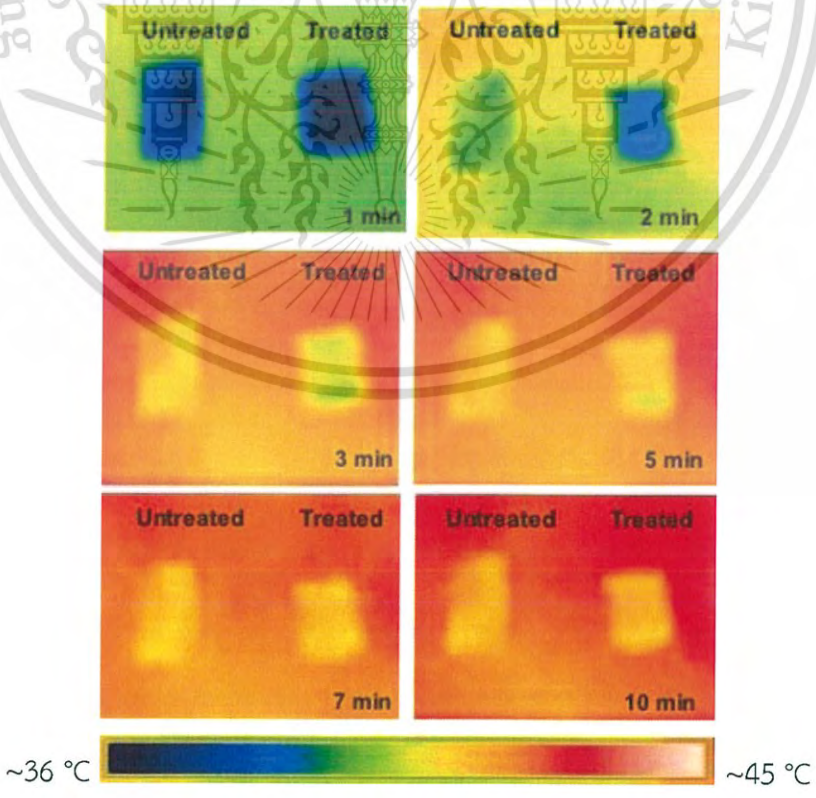

Figure 4.27 Thermal images of Cat-cot/Cap-_t10 sample

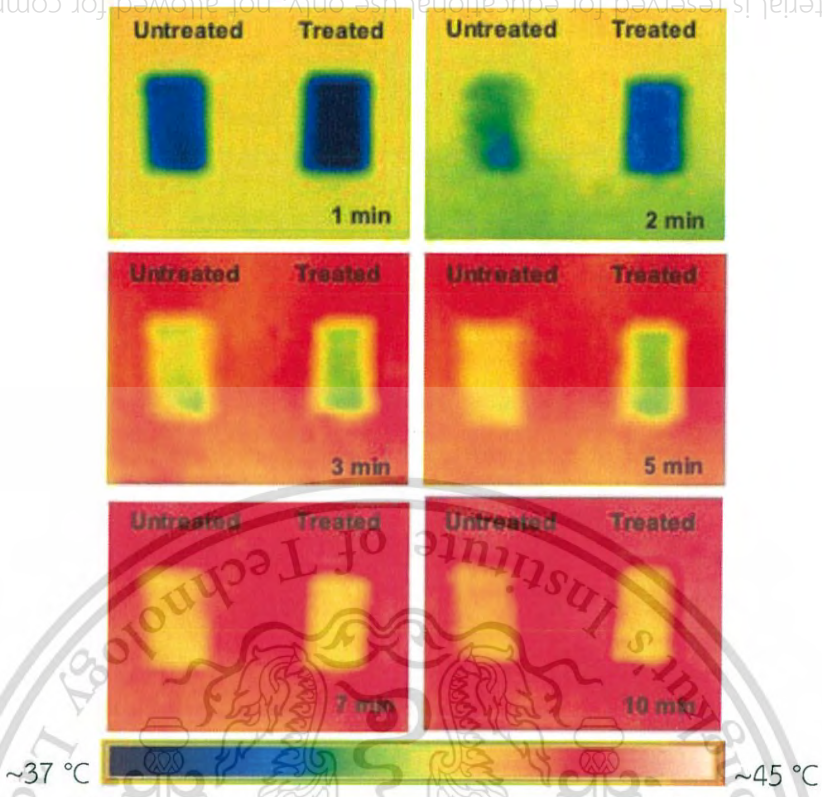

Figure 4.28 Thermal images of Cat-cot/(Cap-/Cap10+)_x3 sample

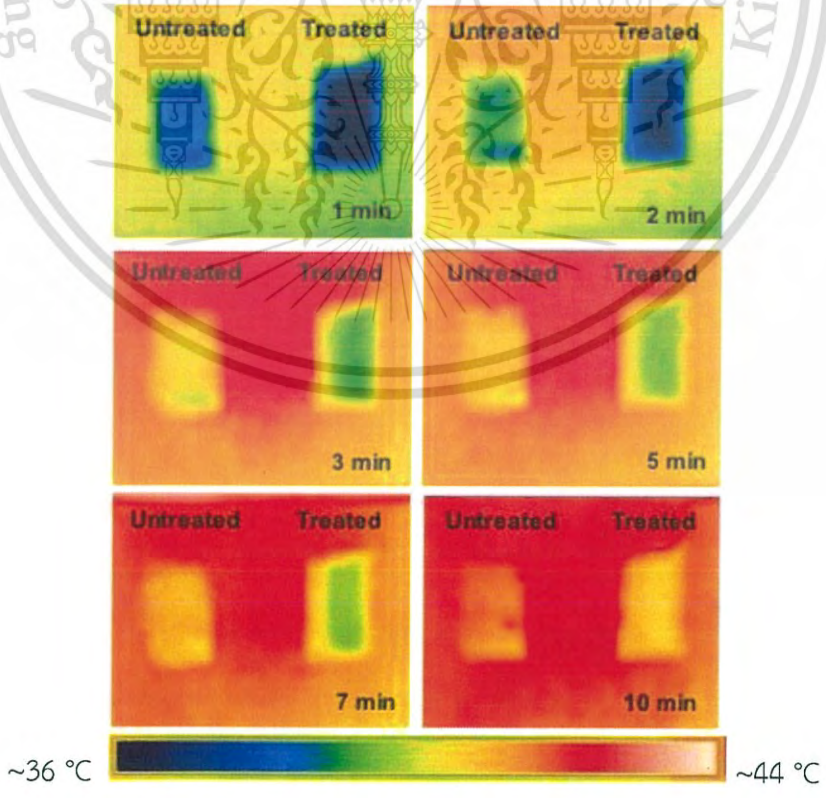

Figure 4.29 Thermal images of Cat-cot/(Cap-/Cap10+)_x5 sample

4.5 Breathability determination

Sweating is an important thermo-regulation process, in which the human body uses to lose heat when the body temperature starts to increase. Sweat commonly evaporates through the air gaps between yarns of clothing fabrics. If the sweat unable to remove and accumulate in the clothing, the wearers feel discomfort. In order to determine the sweat removing ability of clothing or breathability, the water vapor transmission rate (WVTR) was measured. The entry level WVTR ratings of breathable fabrics should be in the range of 2,000 - 3,000 g/m^2/day as reported elsewhere [140], in which the high WVTR rate obtained in the cotton sample due to its high breathability property.

The WVTR of PEL-en-Oc immobilized cotton samples prepared by different treatment procedures were shown in Fig. 4.30 and Table 4.15.

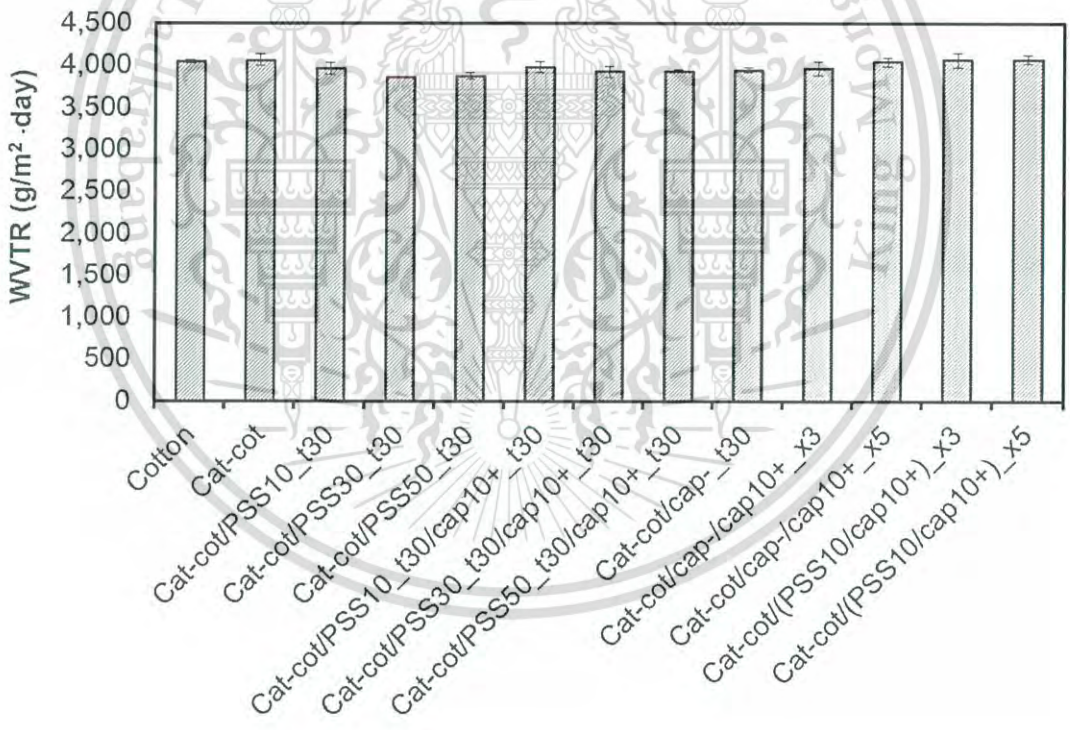

Figure 4.30 WVTR of untreated and treated cotton samples

From Fig. 4.30 and Table 4.15, it can be seen that the WVTR values of all treated cotton samples were in the range of 3,860 - 4,080 g/m^2/day, in which they were higher than the common value suggested for the breathable fabrics. These

results indicated that the immobilization processes proposed in this research did not significantly effect on breathability of cotton fabric.

Table 4.15 Water vapor transmission rate values of untreated and treated cotton fabrics

Sample	WVTR ($g/m^2/day$)
Cotton	4,042 ± 21
Cat-cot	4,060 ± 71
Cat-cot/PSS10_t30	3,961 ± 71
Cat-cot/PSS30_t30	3,857 ± 11
Cat-cot/PSS50_t30	3,872 ± 42
Cat-cot/PSS10_t30/Cap10+_t30	3,980 ± 63
Cat-cot/PSS30_t30/Cap10+_t30	3,923 ± 64
Cat-cot/PSS50_t30/Cap10+_t30	3,929 ± 15
Cat-cot/(PSS10/Cap10+)_x3	3,946 ± 27
Cat-cot/(PSS10/Cap10+)_x5	3,959 ± 82
Cat-cot/Cap-_t30	4,039 ± 53
Cat-cot/Cap-/Cap10+_x3	4,062 ± 85
Cat-cot/Cap-/Cap10+_x5	4,071 ± 53

However, the WVTR values of cotton samples treated with PSS or PSS/Cap+ were lower than those of the starting cotton and Cat-cot samples. These results were because the presence of PSS treatment layer partially covered the air gaps among the cotton yarns, thus, the water vapor might be partially blocked. On the others hand, the WVTR values of Cat-cot samples treated with Cap- or Cap-/Cap10+ were close to the WVTR values of neat cotton and Cat-cot samples suggesting that the breathabilities of these treated cotton samples did not change after immobilization with the Cap- and Cap-/Cap+ nanocapsules. These results might be because these samples were coated with very tiny globular nanocapsules, therefore, the air gaps among the cotton yarns were not blocked.

4.6 Washing durability

The efficiencies of immobilization techniques proposed in this research were evaluated from washing durability. The washing durabilities of colored nanocapsules immobilized on cotton samples were determined from the reduction percentages of their K/S values after washing and rinsing for 5, 10 and 15 cycles, in which the K/S values corresponded to the quantities of colored nanocapsules immobilized on the cotton samples. The treated cotton samples consisted of PSS/colCap10+, colCap- or colCap-/colCap10+ layers containing different amount of colored nanocapsules were selected for testing. Table 4.16 shows the reduction percentages of K/S values of treated cotton samples after washing and rinsing.

Table 4.16 Reduction percentages of K/S values of colored nanocapsules immobilized on various cotton samples after washing and rinsing for 5, 10 and 15 cycles

Sample	% Reduction		
	5 wash	10 wash	15 wash
Cat-cot/(PSS10/Cap10+)_x1	11.98 ± 1.02	32.10 ± 0.61	35.46 ± 1.11
Cat-cot/(PSS10/Cap10+)_x5	10.80 ± 0.88	19.77 ± 0.39	22.58 ± 0.27
Cat-cot/Cap-_t10	15.50 ± 2.49	38.27 ± 0.97	44.03 ± 1.36
Cat-cot/Cap-/Cap10+_x5	32.73 ± 3.35	50.16 ± 0.42	54.29 ± 0.68

It can be seen that the higher number of washing cycle, the higher reduction percentage was obtained in all samples, indicating that the colored nanocapsules immobilized on the cotton fabrics were gradually detached during washing. The reductions of immobilized nanocapsules was mainly occurred during the first 10 washing and rinsing cycles in all treated cotton samples, in which it might be due to the detachment of loosely immobilized nanocapsules. The reduction percentages obtained in the 15-washed samples were slightly higher than those in the 10-washed samples, indicating the well adhesion of remaining nanocapsules.

Considering the PSS/colCap10+ immobilized cotton samples, the detachment of colCap10+ nanocapsules from the cot/PSS10_t30/Cap10+_t30 with 1 set of PSS/colCap10+ was higher than the Cat-cot/(PSS10/Cap10+)_x5 samples with 5 sets of PSS/colCap10+. These results were considered to be because the increase of

number of PSS layers could promote the electrostatic interaction of PSS attached between Cap+ and Cat-cot.

For the samples without PSS layer, the detachment of colCap- and/or colCap10+ nanocapsules from the Cat-cot/Cap-/Cap10+_x5 with 5 layers of colored nanocapsules was higher than the Cat-cot/Cap-_t30 with 1 layer of colCap-. These results suggested that the adhesion between Cat-cot and colCap- was stronger than the adhesion between colCap- and colCap10+ nanocapsules. Since the colCap- nanocapsules could electrostatically interact not only with the external surfaces of Cat-cot threads, but also their internal surfaces, therefore, the colCap- nanocapsules in Cat-cot/Cap-_t30 exhibited more washing durability.

Comparing between two treatment systems, the cotton samples prepared by stepwise soaking in PSS and colCap10+ showed higher washing durability than those prepared by direct soaking in colCap- and stepwise soaking in colCap- and colCap10+. The presence of PSS binder was considered to play an important role in the efficiency of nanocapsule immobilization because the PSS binder possessed a large number of highly charged functional groups which can promote the adhesion between Cat-cot and colCap10+ or two layers of colCap10+ nanocapsules. In addition, the immobilized colCap10+ nanocapsules might be embedded among the molecular chains of PSS binder, in which these molecular chains could hinder the detachment of immobilized nanocapsules.

Chapter 5
Conclusions and Recommendations

5.1 Conclusions

This research successfully prepared the polyelectrolyte nanoencapsulated *n*-octadecane (PEL-en-Oc) nanocapsules having the average particle size and latent heat of fusion in the range of 101 – 256 nm and 99 – 152 J/g, respectively. The polyelectrolyte encapsulation of *n*-octadecane could enhance the thermal stability of *n*-octadecane and prevent its leakage and loss during the phase transition process. In addition, various effective methods for immobilization the PEL-en-Oc nanocapsules on the cotton fabrics have been developed. The cotton fabrics immobilized with the PEL-en-Oc nanocapsules could exhibit the thermo-regulating property with long-lasting performance and preserved the high breathability of cotton. The effects of conditions used for nanocapsules preparation and immobilization on the properties of nanocapsules and treated cotton were concluded as follows.

5.1.1 Polyelectrolyte encapsulated *n*-octadecane

The polyelectrolyte encapsulated *n*-octadecane (PEL-en-Oc) having the different shell structures were successfully prepared, i.e. single-layer shell of PDDA polyelectrolyte (PDDA-en-Oc) and multilayer shell of PDDA and PSS (PSS(PDDA-en-Oc) and PDDA(PSS(PDDA-en-Oc)). In the PDDA-en-Oc preparation, the increase of PDDA concentration played an important role in the conformation of PDDA molecules formed as the capsules' shell, resulting in the increases of shell thickness and capsule size. In addition, the increase of PDDA concentration could improve the efficiency of *n*-octadecane encapsulation, bringing about the increase PDDA-en-Oc nanocapsules quantity. The higher amount of encapsulated nanocapsules, the higher latent heat quantity was obtained during the phase transition of *n*-octadecane. The highest encapsulation efficiency was obtained at about 65.99 % when the 10 mM PDDA was used in the encapsulation process, in which it possessed the highest latent heat of about 151.97 J/g.

In the multilayer shell nanocapsules, the properties of polyelectrolytes used as the outermost shell layer played an important role in the average particle size and latent heat quantity of (PSS(PDDA-en-Oc) and PDDA(PSS(PDDA-en-Oc) nanocapsules. The nanocapsules with multilayer shell possessed different surface charges depending on the type of outermost polyelectrolyte shell. The increase of number of shell layer used in encapsulation process could enhance the thermal stability of (PSS(PDDA-en-Oc) and PDDA(PSS(PDDA-en-Oc) nanocapsules, however, the average particle size and latent heat quantity of PEL-en-Oc nanocapsules were decreased. The PDDA(PSS(PDDA-en-Oc) nanocapsules having 3 layers of polyelectrolyte shell (PDDA/PSS/PDDA) exhibited the highest thermal stability.

5.1.2 PEL-en-Oc nanocapsules immobilized on cotton fabrics

Various facile treatment methods were successfully developed for immobilization the PEL-en-Oc nanocapsules on the cotton fabrics, i.e. (1) stepwise coating with the PSS binder and PDDA-en-Oc nanocapsules having positively charged outermost shell and (2) direct coating with the PEL-en-Oc nanocapsules having negatively charged outermost shell. The higher concentrations of PSS binder used for stepwise coating with the PSS binder and PDDA-en-Oc nanocapsules created the higher negative sites on the treated cotton, resulting in the higher quantity of immobilized PDDA-en-Oc nanocapsules. The increase of immobilized PDDA-en-Oc quantity on the cotton fabrics brought about the increase of their positive surface charges. In addition, the increase of number of PSS/PDDA-en-Oc treatment cycles could enhance the quantity of immobilized nanocapsules. The increase of treatment time for immobilization of PSS(PDDA-en-Oc) nanocapsules having negatively charged outermost shell on the cotton samples could increase the quantity of PEL-en-Oc nanocapsules, resulting in the increase of negative sites on cotton samples. In addition, the quantity of PEL-en-Oc nanocapsules immobilized on the cotton fabric could be increased by stepwise soaking the cotton samples in the PEL-en-Oc nanocapsules having oppositely charged outermost shell.

The cotton samples immobilized with the PEL-en-Oc nanocapsules showed the thermo-regulating action, in which the duration of the thermo-regulating action was depended mainly on the quantity of PEL-en-Oc nanocapsules immobilized on the cotton fabrics and their heat storage capacity. In addition, the

immobilization process proposed in this research did not significant effect on the breathability of cotton fabrics. In the simulated washing test, the presence of PSS binder could enhance the washing durability of PEL-en-Oc nanocapsules immobilized cotton.

The effective methods for *n*-octadecane encapsulation and immobilization on the cotton fabrics proposed in this study were facile polyelectrolyte assisted finishing systems performed at ambient temperature using low concentrations of non-toxic chemicals, fulfilling the concept of green chemistry.

5.2 Recommendations

(1) The adhesion force between PEL-en-Oc nanocapsules and cotton fabrics should be analyzed in order to investigate the durability of nanocapsules immobilized on the cotton fabrics.

(2) The processes of nanocapsules immobilization should be applied and developed for finishing on other natural and/or synthetic fabrics.

(3) The processes of oil-phase encapsulation and immobilization on the cotton fabrics should be applied and developed for larger production scale.

References

[1] Monllor, P., Bonet, A.M., and Cases, F. (2007). Characterization of the behaviour of flavour microcapsules in cotton fabrics. *Eur Polym J, 43*, 2481–2490.

[2] Sohn, S.O., Lee, S.M., Kim, Y.M., Yeum, J.H., Choi, J.H., and Ghim, H.D. (2007). Aroma finishing of PET fabrics with PVAc nanoparticles containing lavender oil. *Fiber Polym, 8*(2), 163-167

[3] Lee, A.R., and Yi, E. (2013). Investigating performance of cotton and lyocell knit treated with microcapsules containing Citrus unshiu oil. *Fiber Polym, 14*(12), 2088-2096.

[4] Fouda, M.M.G., and Fahmy, E. (2011). Multifunctional finish and cellulosic fabrics cellulose fabric. *Carbohyd Polym, 86*(2), 625-629.

[5] Zhang, S., and Horrocks, R. (2003). Substantive intumescent flame retardants for functional fibrous polymers. *J Mater Sci, 38*(10), 2195-2198.

[6] Gonçalves, A.G., Jarrais, B., Pereira, C., Morgado, J., Freire, C., Pereira, M.F.R. (2012). Functionalization of textiles with multi-walled carbon nanotubes by a novel dyeing-like process. *J Mater Sci, 47*(13), 5263-5275.

[7] Sánchez, P., Sánchez-Fernandez, M.V., Romero, A., Rodríguez, J.F., Sánchez-Silva, L. (2010). Development of thermo-regulating textiles using paraffin wax microcapsules. *Thermochim Acta, 498*(1-2), 16-21.

[8] Zhang, X.X., Wang, X.C., Tao, X.M., and Yick, K.L. (2005). Energy storage polymer/MicroPCMs blended chips and thermo-regulated fibers. *J Mater Sci, 40*(14), 3729-3734.

[9] Koo, K., Park, Y., Choe, J., and Kim, E. (2008). The application of microencapsulated phase change materials to nylon fabric using direct dual coating method. *J Appl Polym Sci, 108*(4), 2337-2344.

[10] Miró Specos, M.M., García, J.J., Tornesello, J., Marino, P., Della Vecchia, M., Defain Tesoriero, M.V., and Hermida, L.G. (2010). Microencapsulated citronella oil for mosquito repellent finishing of cotton textiles. *T Roy Soc Trop Med H, 104*, 653-658.

[11] Abdel-Mohdy, F.A., Fouda, M.M.G., Rehan, M.F., and Ali, A.S. (2009). Repellency of controlled-release treated-cotton fabrics based on permethrin and bioallethrin against mosquitoes. *J Text Inst, 100*(8), 695-701.

[12] Iamphaojeen, Y., and Siriphannon, P. (2012). Immobilization of zinc oxide nanoparticles on cotton fabrics using poly 4-styrenesulfonic acid polyelectrolyte. *Int J Mater Res, 103*(5), 643-647.

[13] Kathirvelu, S., D'Souza, L., and Dhurai, B. (2010). Study of stain-eliminating textiles using ZnO nanoparticles. *J Tex Inst, 101*(6), 520-526.

[14] Ladhari, N., Baouab, M.H.V., Dekhil, A.B., Bakhrouf, A., and Niquett, P. (2007). Antibacterial activity of quaternary ammonium salt grafted cotton. *J Text Inst, 98*(3), 209-218.

[15] Available : http://www.thenational.ae/news/uae-news/environment/sudden-change-from-hot-to-cold-can-harm-health

[16] Sun, G., and Zhang, Z. (2002). Mechanical strength of microcapsules made of different wall materials. *Int J Pharm, 242*(1-2), 307-311.

[17] Pause, B. (2000). Textiles with improved thermal capabilities through the application of phase change material (PCM) microcapsules. *Melliand Textilberichte, 81*(9), 753–754.

[18] Nelson, G. (2001). Microencapsulation in textile finishing. *Rev Prog Color Relat Top, 31*, 57–64.

[19] Pause, B. (2003). Nonwoven protective garments with thermo-regulating properties. *J Ind Text, 33*(2), 93–99.

[20] Ying, B., Kwok, Y.L., Li, Y., Zhu, Q.Y., and Yeung, C.Y. (2004). Assessing the performance of textiles incorporating phase change materials. *Polym Test, 23*, 541–549.

[21] Bendkowska, W., Tysiak, J., Grabowski, L., and Blejzyk, A. (2005). Determining temperature regulating factor for apparel fabrics containing phase change material. *Int J Cloth Sci Tech, 17*(3-4), 209–214.

[22] Ying, B., Kwok, Y.L., Li, Y., Yeung, C.Y., and Song, Q.W. (2004). Thermal regulating functional performance of PCM garments, *Int J Cloth Sci Tech, 16*(1/2), 84-96.

[23] Zhang, X.X. (2001). Heat-storage and thermo-regulated textiles and clothing. In Tao, X.M. (Ed.), *Smart fibres, fabrics and clothing* (pp. 34–57). UK: Woodhead Publishing

[24] Gries, T. (2003). Smart textiles for technical applications. *Technische Textilen/Technical Textiles, 46*(2), E66

[25] Thakare, A.M., Sangwan, A., and Yadav, S. (2005). Providing comfort through phase change materials, *Man Made Textiles in India 48*(6):239–242.

[26] Mondal, S. (2008). Phase change materials for smart textiles – An overview. *Appl Therm Eng, 28*, 1536–1550.

[27] Shin, Y., Yoo, D., and Son, K. (2005). Development of thermoregulating textile materials with microencapsulated phase change materials (pcm). ii. preparation and application of pcm microcapsules. *J Appl Polym Sci, 96*, 2005-2010.

[28] Sarier, N., and Onder, E. (2012). Organic phase change materials and their textile applications: An overview. *Thermochim Acta, 540*, 7–60.

[29] Atul, Sharma., Tyagi, V.V., Chen, C.R., and Buddhi, D. (2011). Review on thermal energy storage with phase change materials and applications. *Renew Sust Energ Rev, 15*, 3813–3832.

[30] Demirbas, M.F. (2006). Thermal energy storage and phase changing materials: an overview. *Energ Source B, 1*(1), 85–95.

[31] Atkinson, C.M.L., Larkin, J.A., and Richardson, M.J. (1969). Enthalpy changes in molten *n*- alkanes and polyethylene. *J Chem Thermodyn, 1*(5), 435–440.

[32] Zongrong, L., and Chung, D.D.L. (2001). Calorimetric evaluation of phase change materials for use as thermal interface materials. *Thermochim Acta, 366*, 135–147.

[33] Sharma, S.D., and Sagara, K. (2005). Latent heat storage materials and systems: a review. *Int J Green Energy, 2*, 1–56.

[34] Morikawa, J., and Hashimoto, T. (2000). Simultaneous measurement of heat capacity and thermal diffusivity in solid–solid and solid–liquid phase transitions of *n*-alkane. *Thermochim Acta, 352–353*, 291–296.

[35] Alvarado, J.L., Marsh, C., Sohn, C., Vilceus, M., Hock, V., Phetteplace, G., and Newell, T. (2006). Characterization of supercooling suppression of microencapsulated phase change material by using DSC. *J Therm Anal Calorim, 86*(2), 505–509.

[36] Domanska, U., and Stankiewicz, D.W. (1991). Enthalpies of fusion and solid–solid transition of even-numbered paraffins $C_{22}H_{46}$, $C_{24}H_{50}$ and $C_{26}H_{54}$ and $C_{28}H_{58}$. *Thermochim Acta, 179*, 265–271.

[37] Gines, J.M., Arias, M.J., Rabasco, A.M., Novak, C., RuizConde, A., and SanchezSoto, P.J. (1996). Thermal characterization of polyethylene glycols applied in the pharmaceutical technology using differential scanning calorimetry and hot stage microscopy. *J Therm Anal, 46*(1), 291–304.

[38] Craig, D.Q.M., and Newton, J.M. (1991). Characterisation of polyethylene glycols using differential scanning calorimetry. *Int J Pharm, 74*(1 and 2), 33–41.

[39] Constantinescu, M., Dumitrache, L., Constantinescu, D., Anghel, E.M., Popa, V.T., Stoica, A., and Olteanu, M. (2010). Latent heat nano composite building materials. *Eur Polym J, 46*, 2247–2254.

[40] Meng, Q., and Hu, J. (2008). A poly(ethylene glycol)-based smart phase change material. *Sol Energ Mater Sol C, 92*, 1260–1268.

[41] Feldman, D., and Shapiro M.M. (1989). Fatty acids and their mixtures as phase-change materials for thermal energy storage, *Sol Energ Mat, 18*, 201–216.

[42] Suppes, G.J., Goff, M.J., and Lopes, S. (2003). Latent heat characteristics of fatty acid derivatives pursuant phase change material applications, *Chem Eng Sci, 58*(9), 1751–1763.

[43] Feldman, D., Shapiro, M.M., and Banu, D. (1986). Organic phase change materials for thermal energy storage. *Sol Energ Mat, 13*(1), 1–10.

[44] Feldman, D., Banu, D., and Hawes, D. (1995). Development and application of organic phase change mixtures in thermal storage gypsum wallboard. *Sol Energ Mater Sol C, 36*, 147–157.

[45] Hasan, A. (1994). Thermal energy storage system with stearic acid as phase change material. *Energ Convers Manage, 35*, 843–856.

[46] Cedeno, F.O., Prieto, M.M., Espina, A., and Garcia, J.R. (2001). Measurements of temperature and melting heat of some pure fatty acids and their binary and ternary mixtures by differential scanning calorimetry. *Thermochim Acta, 369*, 39–50.

[47] Rozanna, D., Chuah, T.G., Salmiah, A., Choong, T.S.Y., and Saari, M. (2005). Fatty acids as phase change materials (PCMs) for thermal energy storage: a review. *Int J Green Energy, 1*(4), 495–513.

[48] Zhang, J.J., Zhang, J.L., He, S.M., Wu, K.Z., and Liu, X.D. (2001). Thermal studies on the solid–liquid phase transition in binary system of fatty acids. *Thermochim Acta, 369*, 157–160.

[49] Nagano, K., Mochida, T., Takeda, S., Doman´ski, R., and Rebow, M. (2003). Thermal characteristics of manganese(II) nitrate hexahydrate as a phase change material for cooling systems. *Appl Therm Eng, 23*(2), 229–241.

[50] Canbazoğlua, S., Şahinaslana, A., Ekmekyaparb, A., Aksoya, Ý.G., and Akarsua, F. (2005). Enhancement of solar thermal energy storage performance using sodium thiosulfate pentahydrate of a conventional solar water heating system. *Energ Buildings, 37*(3), 235–242.

[51] Saito, A., Okawa, S., Shintani, T., and Iwamoto, R. (2001). On the heat removal characteristics and the analytical model of a thermal energy storage capsule using gelled Glauber's salt as the PCM. *Int J Heat Mass Transf, 44*(24), 4693–4701.

[52] Biswas, D.R. (1977). Thermal energy storage using sodium sulphate decahydrate and water. *Sol Energ, 19*, 99–100.

[53] Marks, S. (1980). An investigation of the thermal energy storage capacity of Glauber's salt with respect to thermal cycling. *Sol Energ, 25*(3), 255–258.

[54] Furbo, S. (1982). *Heat storage units using a salt hydrate as storage medium based on the extra water principle*. Report no. 116. Technical University of Denmark

[55] Karthik, K., Ramachandran, T., Shumugasundaram, O.L., Balasubramaniam, M., and Ragavendra, T. (Spring 2012). Microencapsulation of PCMs in textiles: a review. *JTATM, 7*(3), 1-10.

[56] Jamekhorshid, A., Sadrameli, S.M., and Farid, M. (2014). A review of microencapsulation methods of phase change materials (PCMs) as a thermal energy storage (TES) medium. *Renew Sust Energ Rev, 31*, 531–542.

[57] Zhao, C.Y., and Zhang, G.H. (2011). Review on microencapsulated phase change materials (MEPCMs): Fabrication, characterization and applications. *Renew Sust Energ Rev, 15*, 3813–3832.

[58] Gibbs, B.F., Kermasha, S., Alli, I., and Mulligan, C.N. (1999). Encapsulation in the food industry: a review. *Int J Food Sci Nutr, 50*, 213–214.

[59] Sarier, N., and Onder, E. (2007). The manufacture of microencapsulated phase change materials suitable for the design of thermally enhanced fabrics. *Thermochim Acta, 452*(2), 149–160.

[60] Tseng, Y.H., Fang, M.H., Tsai, P.S., and Yang, Y.M. (2005). Preparation of microencapsulated phase-change materials (MCPCMs) by means of interfacial polycondensation. *J Microencapsul, 22*, 37–46.

[61] Su, J.F., Wang, L.X., Ren, L., Huang, Z., and Meng, X.W. (2006). Preparation and characterization of polyurethane microcapsules containing *n*-octadecane with styrene–maleic anhydride as a surfactant by interfacial polycondensation. *J Appl Polym Sci, 102*, 4996–5006.

[62] Siddhan, P., Jassal, M., and Agrawal, A.K. (2007). Core content and stability of *n*-octadecane-containing polyurea microencapsules produced by interfacial polymerization. *J Appl Polym Sci, 106*, 786–792.

[63] Zhang, H., and Wang, X. (2009). Synthesis and properties of microencapsulated *n*- octadecane with polyurea shells containing different soft segments for heat energy storage and thermal regulation. *Sol Energy Mater Sol Cells, 93*, 1366–1376.

[64] Liang, C., Lingling, X., Hongbo, S., and Zhibin, Z. (2009). Microencapsulation of butyl stearate as a phase change material by interfacial polycondensation in a polyurea system. *Energy Convers Manag, 50*, 723–729.

[65] Su, J.F., Wang, L.X., and Ren, L. (2007). Synthesis of polyurethane microPCMs containing *n*-octadecane by interfacial polycondensation: influence of styrene-maleic anhydride as a surfactant. *Colloids Surf A: Physicochem Eng Asp, 299*, 268–275.

[66] Su, J., Ren, L., and Wang, L. (2005). Preparation and mechanical properties of thermal energy storage microcapsules. *Colloid Polym Sci, 284*, 224–228.

[67] Wei, J., Li, Z., Liu, L., and Liu, X. (2013). Preparation and characterization of novel polyamide paraffin MEPCM by interfacial polymerization technique. *J Appl Polym Sci, 127*, 4588–4593.

[68] Cho, J.S., Kwon, A., and Cho, C.G. (2002). Microencapsulation of octadecane as a phase-change material by interfacial polymerization in an emulsion system. *Colloid Polym Sci, 280*, 260-266.

[69] Choi, J.L., Kim, J.H., and Yang, H. (2001). Preparation of microcapsules containing phase change materials as heat transfer media by in-situ polymerization. *J Ind Eng Chem, 7*, 358–362.

[70] Zhang, X.X., Tao, X.M., Yick, K.L., and Wang, X.C. (2004). Structure and thermal stability of microencapsulated phase-change materials. *Colloid Polym Sci, 282*, 330–336.

[71] Zhang, X.X., Tao, X.M., Yick, K.L., and Fan, Y.F. (2005). Expansion space and thermal stability of microencapsulated *n*-octadecane. *J Appl Polym Sci, 97*, 390–396.

[72] Fan, Y.F., Zhang, X.X., Wu, S.Z., and Wang, X.C. (2005). Thermal stability and permeability of microencapsulated *n*-octadecane and cyclohexane. *Thermochim Acta, 429*, 25–29.

[73] Boh, B., Knez, E., and Staresinic, M. (2005). Microencapsulation of higher hydrocarbon phase change materials by in situ polymerization. *J Microencapsul, 22*, 715–735.

[74] Su, J., Wang, L., and Ren, L. (2006). Fabrication and thermal properties of microPCMs: used melamine–formaldehyde resin as shell material. *J Appl Polym Sci, 101*, 1522–1528.

[75] Rao, Y., Lin, G., Luo, Y., Chen, S., and Wang, L. (2007). Preparation and thermal properties of microencapsulated phase change material for enhancing fluid flow heat transfer. *Heat Transf Asian Res, 36*, 28–37.

[76] Salaün, F., and Vroman, I. (2008). Influence of core materials on thermal properties of melamine–formaldehyde microcapsules. *Eur Polym J, 44*, 849–860.

[77] Yu, F., Chen, Z.H., and Zeng, X.R. (2009). Preparation, characterization, and thermal properties of microPCMs containing *n*-dodecanol by using different types of styrene–maleic anhydride as emulsifier. *Colloid Polym Sci, 287*, 549–560.

[78] Zhang, H., and Wang, X. (2009). Fabrication and performances of microencapsulated phase change materials based on *n*-octadecane core and resorcinol-modified melamine–formaldehyde shell. *Colloids Surf A Physicochem Eng Asp, 332*, 129–138.

[79] Li, W., Zhang, X.X., Wang, X.C., and Niu, J.J. (2007). Preparation and characterization of microencapsulated phase change material with low remnant formaldehyde content. *Mater Chem Phys, 106*, 437–442.

[80] Zhang, X.X., Fan, Y.F., Tao, X.M., and Yick, K.L. (2004). Fabrication and properties of microcapsules and nanocapsules containing *n*-octadecane. *Mater Chem Phys, 88*, 300–307.

[81] Fang, Y., Kuang, S., Gao, X., and Zhang, Z. (2008). Preparation and characterization of novel nanoencapsulated phase change materials. *Energ Convers Manage, 49*, 3704–3707.

[82] Baek, K.H., Lee, J.Y., and Kim, J.H. (2007). Core/shell structured PCM nanocapsules obtained by resin fortified emulsion process. *J Dispers Sci Technol, 28*, 1059–1065.

[83] Alkan, C., Sarl, A., Karaipekli, A., and Uzun, O. (2009). Preparation, characterization, and thermal properties of microencapsulated phase change material for thermal energy storage. *Sol Energy Mater Sol Cells, 93,* 143–147.

[84] Alay, S., Göde, F., and Alkan, C. (2010). Preparation and characterization of poly(methyl- methacrylate-coglycidyl methacrylate)/*n*-hexadecane nanocapsules as a fiber additive for thermal energy storage. *Fibers Polym, 11*, 1089–1093.

[85] Alay, S., Alkan, C., and Göde, F. (2011). Synthesis and characterization of poly(methyl methacrylate)/*n*-hexadecane microcapsules using different cross-linkers and their application to some fabrics. *Thermochim Acta, 518*, 1–8.

[86] Sarl, A., Alkan, C., and Karaipekli, A. (2010). Preparation, characterization and thermal properties of PMMA/*n*-heptadecane microcapsules as novel solid-liquid microPCM for thermal energy storage. *Appl Energy, 87*, 1529–1534.

[87] Ma, S., Song, G., Li, W., Fan, P., and Tang, G. (2010). UV irradiation-initiated MMA polymerization to prepare microcapsules containing phase change paraffin. *Sol Energy Mater Sol Cells, 94*(10), 1643–1647.

[88] Alay, S., Göde, F., and Alkan, C. (2011). Synthesis and thermal properties of poly(*n*-butyl acrylate)/*n*-hexadecane microcapsules using different cross-linkers and their application to textile fabrics. *J Appl Polym Sci, 120*, 2821–2829.

[89] Sarı, A., Alkan, C., Karaipekli, A., and Uzun, O. (2009). Microencapsulated *n*-octacosane as phase change material for thermal energy storage. *Sol Energy, 83*, 1757–1763.

[90] Chen, Z.H., Yu, F., Zeng, X.R., Zhang, Z.G. (2012). Preparation, characterization and thermal properties of nanocapsules containing phase change material *n*-dodecanol by miniemulsion polymerization with polymerizable emulsifier. *Appl Energ, 91*, 7–12.

[91] Sánchez, L., Sánchez, P., Carmona, M., de Lucas, A., and Rodríguez, J. (2008). Influence of operation conditions on the microencapsulation of PCMs by means of suspension-like polymerization. *Colloid Polym Sci, 286*, 1019–1027.

[92] Sánchez-Silva, L., Carmona, M., de Lucas, A., Sánchez, P., and Rodríguez, J.F. (2010). Scale-up of a suspension-like polymerization process for the microencapsulation of phase change materials. *J Microencapsul, 27*, 583–593.

[93] Sánchez-Silva, L., Rodríguez, J.F., Romero, A., Borreguero, A.M., Carmona, M., and Sánchez, P. (2010). Microencapsulation of PCMs with a styrene-methyl methacrylate copolymer shell by suspension-like polymerisation. *Chem Eng J, 157*, 216–222.

[94] You, M., Zhang, X., Wang, J., and Wang, X. (2009). Polyurethane foam containing micro- encapsulated phase-change materials with styrene–divinybenzene co-polymer shells. *J Mater Sci, 44*, 3141–3147.

[95] Borreguero, A.M., Carmona, M., Sanchez, M.L., Valverde, J.L., and Rodriguez, J.F. (2010). Improvement of the thermal behaviour of gypsum blocks by the incorporation of microcapsules containing PCMS obtained by suspension polymerization with an optimal core/coating mass ratio. *Appl Therm Eng, 30*, 1164–1169.

[96] Li, W., Song, G., Tang, G., Chu, X., Ma, S., and Liu, C. (2011). Morphology, structure and thermal stability of microencapsulated phase change material with copolymer shell. *Energy 36*:785–791

[97] Wang, H., Wang, J.P., Wang, X., Li, W., and Zhang, X. (2013). Preparation and properties of microencapsulated phase change materials containing two-phase core materials. *Ind Eng Chem Res, 52*, 14706–14712.

[98] Huang, J., Wang, T., Zhu, P., and Xiao, J. (2013). Preparation, characterization, and thermal properties of the microencapsulation of a hydrated salt as phase change energy storage materials. *Thermochim Acta, 557*, 1–6.

[99] You, M., Wang, X., Zhang, X., Zhang, L., and Wang, J. (2011). Microencapsulated *n*-octadecane with styrene–divinybenzene co-polymer shells. *J Polym Res, 18*, 49–58.

[100] Sánchez, L., Sánchez, P., de Lucas, A., Carmona, M., and Rodriguez, J. (2007). Microen- capsulation of PCMs with a polystyrene shell. *Colloid Polym Sci, 285*, 1377–1385.

[101] McClements, D.J. (2004). *Food Emulsions: Principles, Practices, and Techniques*, (2nd ed.). Boca Raton, FL: CRC Press

[102] Guzey, D., and McClements, D.J. (2006). Formation, stability and properties of multilayer emulsions for application in the food industry. *Adv Colloid Interface Sci, 128–130*, 227–248.

[103] McClements, D.J. (2005). Theoretical analysis of factors affecting formation and stability of multilayered colloidal dispersions. *Langmuir, 21*, 9777–9785.

[104] Schönhoff, M. (2003). Layered polyelectrolyte complexes: physics of formation and molecular properties. *J Phys Condens Matter, 15*, R1781–1808.

[105] Becher, P. (1965). *Emulsions: theory and practice*. New York: Reinhold

[106] Bibette, J., Leal-Calderon, F., and Poulin, P. (1999). Emulsions: basic principles. *Rep Prog Phys, 62*, 969-1033.

[107] Israelachvili, J.N. (1992). *Intermolecular and Surface Forces*. London: Academic Press

[108] Available : http://www.gcsescience.com/o77.htm

[109] Available : http://sci-tech.ksc.kwansei.ac.jp/~ozaki/en/resproj/research-field/nirtop/nirmisci/

[110] Available : http://www.stevenabbott.co.uk/PracticalSurfactants/CMCValues.html

[111] Michaels, M.A. (2006). *Quantitative model for the prediction of hydrodynamic size of nonionic reverse micelles*. (Master's thesis). Virginia Commonwealth University, Virginia, USA.

[112] Dobrynina, A.V., and Rubinsteinb, M. (2005). Theory of polyelectrolytes in solutions and at surfaces. *Prog Polym Sci, 30*, 1049–1118.

[113] Armstrong, R.W., and Strauss, U.P. (1969). Polyelectrolyte. In Mark, H.F., Gaylord, N.G., and Bikales, N.M. (Ed.). *Encyclopedia of polymer science and technology* (Vol.7, pp. 439-504). New York: Wiley-Interscience

[114] Cohen Stuart, M.A. (1988). Polyelectrolyte adsorption. *J Phys, 49*, 1001–1008.

[115] Cohen Stuart, M.A., Fleer, G.J., Lyklema, J., Norde, W., and Scheutjens, J.M.H.M. (1991). Adsorption of ions, polyelectrolytes and proteins. *Adv Colloid Interface Sci, 34*, 477–535.

[116] Fleer, G.J., Cohen Stuart, M.A., Scheutjens, J.M.H.M., Cosgrove, T., and Vincent, B. (1993). *Polymers at interfaces* (pp. 343–373). London: Chapman & Hall

[117] Poptoshev, E., Schoeler, B., and Caruso, F. (2004). Influence of solvent quality on the growth of polyelectrolyte multilayers. *Langmuir, 20*(3), 829–834.

[118] Decher, G., Hong, J.D., and Schmitt, J. (1992). Buildup of ultrathin multilayer films by a self-assembly process: III. Consecutively alternating adsorption of anionic and cationic polyelectrolytes on charged surfaces. *Thin Solid Films, 210*, 831–835.

[119] Steitz, R., Leiner, V., Siebrecht, R., von Klitzing, R. (2000). Influence of the ionic strength on the structure of polyelectrolyte films at the solid/liquid interface. *Colloids Surf A Physicochem Eng Asp, 163*, 63–70.

[120] Kato, N., Schuetz, P., Fery, A., and Caruso, F. (2002). Thin multilayer films of weak polyelectrolytes on colloid particles. *Macromolecules, 35*(26), 9780–9787.

[121] Schönhoff, M. (2003). Self-assembled polyelectrolyte multilayers. *Curr Opin Colloid Interface Sci, 8*. 86–95.

[122] Sukhorukov, G.B., Antipov, A.A., Voigt, A., Donath, E., and Mohwald, H. (2001). pH- controlled macromolecule encapsulation in and release from polyelectrolyte multilayer nanocapsules. *Macromol Rapid Commun, 22*(1), 44–46.

[123] Dobrynin, A.V. (2001). Effect of solvent quality on polyelectrolyte adsorption at an oppositely charged surface. *J Chem Phys, 115*, 8145–8153.

[124] Bryant, Y.G., and Colvin, D.P. (1998). *Fibre with reversible enhanced thermal storage properties and fabrics made therefrom*. USP 4756958

[125] Salaün, F., Devaux, E., Bourbigot, S., and Rumeau, P. (2010). Thermoregulating response of cotton fabric containing microencapsulated phase change materials. *Thermochim Acta, 506*, 82–93.

[126] Wang, Q., and Hauser, P.J. (2009). New characterization of layer-by-layer self-assembly deposition of polyelectrolytes on cotton fabric. *Cellulose, 16*, 1123–1131.

[127] Hyde, K., Dong, H., and Hinestroza, J.P. (2007). Effect of surface cationization on the conformal deposition of polyelectrolytes over cotton fibers. *Cellulose, 14*, 615–623.

[128] Uğur, Ş.S., Sarıışık, M., Aktaş, A.H., Uçar, M.Ç., and Erden, E. (2010). Modifying of cotton fabric surface with nano-ZnO multilayer films by Layer-by-Layer deposition method. *Nanoscale Res Lett, 5*, 1204–1210.

[129] Joshi, M., Khanna, R., Shekhar, R., and Jha, K. (2011). Chitosan nanocoating on cotton textile substrate using layer-by-layer self-Assembly technique. *J Appl Polym Sci, 119*, 2793–2799.

[130] Ali, S.W., Rajendran, S., and Joshi, M. (2010). Effect of process parameters on Layer-by-layer self-assembly of polyelectrolytes on cotton substrate. *Polym Polym Compos, 18*(5), 237-250.

[131] Wang, Q., and Hauser, P.J. (2010). Developing a novel UV protection process for cotton based on layer-by-layer self-assembly. *Carbohydr Polym, 81*, 491–496.

[132] Ristić, N., and Ristić, I., (2012). Cationic modification of cotton fabrics and reactive dyeing characteristics. *J Eng Fiber Fabr, 7*(4), 113-121.

[133] Öztürk, H.B., and Bechtold, T. (2007). Effect of NaOH treatment on the inter brillar swelling and dyeing properties of lyocell (TENCEL®) fibres. *Fibres Text East Eur, 15*(5-6), 114-117.

[134] Ramkumar, S.S., Purushothaman, A., Hake, K.D. and McAlister D.D. (2007). Relationship Between Cotton Varieties and Moisture Vapor Transport of Knitted Fabrics. *J Eng Fiber Fabr*, 2, 10-18.

[135] González-Martín, M.L., Janczuk, B., Bruque, J.M. and Dorado-Calasanz, C. (1994). Adsorption of sodium dodecyl sulphate on cassiterite surface. *Can J Chem Eng*, 72, 551–553.

[136] Canselier J.R., Delmas, H., Wilhelm, A.M. and Abismail, B. (2002). Ultrasound emulsification—An overview. *J Dispersion Sci Technol*, 23, 333–349.

[137] Miller, M.D. and Bruening M.L., (2005). Correlation of the swelling and permeability of polyelectrolyte multilayer films. *Chem Mater*, 17, 5375–5381.

[138] Wei, J., Kawaguchi, Y., Hirano, S. and Takeuchi, H. (2005). Study on a PCM heat storage system for rapid heat supply. *Appl Therm Eng*, 25, 2903-2920.

[139] Saric, S.P. and Schofield, R.K. (1946). The dissociation constants of the carboxyl and hydroxyl groups in some insoluble and sol-forming polysaccharides. *Proc R Soc Lond Series A Math Phys Eng Sci*, 185, 431–447.

[140] Available : http://www.skis.com/Buying-Guide-for-Womens-Ski-Pants/buying-guide-9-17-2012,default,pg.html#Breathability_Rating

Appendix

Appendix A : Calculations

A.1 Determination of dye adsorption capacity

a. UV-Visible spectrophotometer (UV-Vis)

Absorbencies of the dye solutions were measured by UV-Visible spectrophotometer at λ_{max} 664.5 nm and 530 nm for methylene blue (MB) and eosin B (EO), respectively. The standard calibration curves of MB and EO were shown in Fig. A.1(a) and A.1(b), respectively. Therefore, the dye concentration was calculated by linear regression equation from the standard calibration curve as shown in Table A.1.

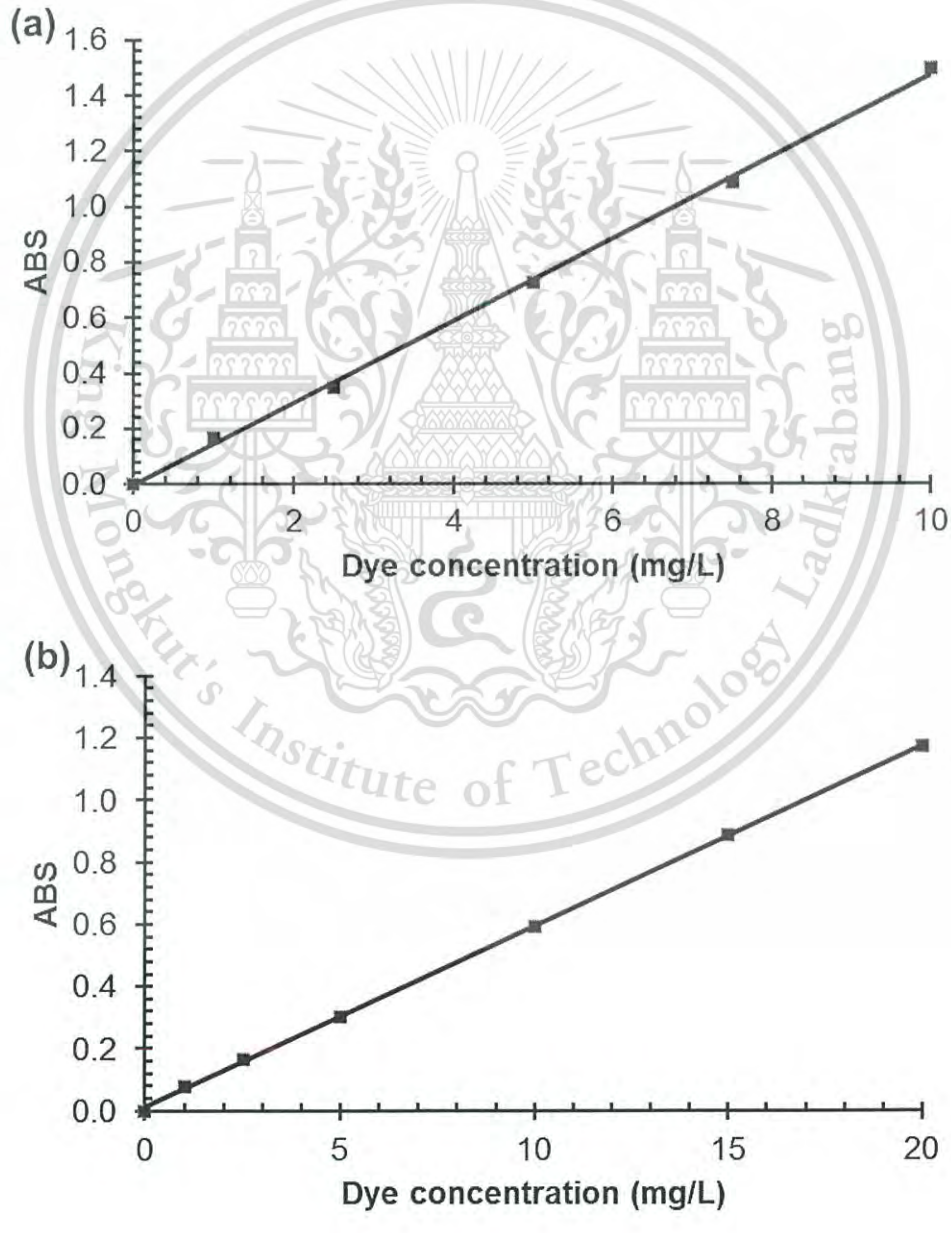

Figure A.1 Standard calibration curves of (a) MB and (b) EO

Table A.1 The linear regression equations from the standard calibration curve of MB and EO

Dye	Linear regression equation	R^2
Methylene blue (MB)	y = 0.1477x - 0.0029	0.99881
Eosin B (EO)	y = 0.0581x + 0.0121	0.99975

where y = UV-Vis absorbance

x = Final dye concentration (mg/L).

The dye adsorption capacities of cotton sample (mg/g) were calculated by equation (A.1):

$$\text{Adsorption capacities} = \frac{V(C_i - C_f)}{m} \qquad \text{(A.1)}$$

where C_i = Initial dye concentration (mg/L)

C_f = Final dye concentration (mg/L)

V = Volume of dye solution (L)

m = Weight in grams of cotton sample (g)

For example,

The absorbance value of EO dye solution after soaked by the 0.0197 g Cat-cot/PSS10_t30/colCap10+_t30 sample was 0.447. (y = 0.447; m = 0.0197 g; C_i = 50 mg/L; V = 0.010 L)

y = 0.0581x + 0.0121

x = (0.447-0.0121)/0.0581

$x = C_f$ = 7.48 mg/L

EO adsorption capacities = $(V \times (C_i - C_f))/ m$

= $(0.010 \times (50 - 7.48)) / 0.0197$

= 21.58 mg/g

Therefore, the EO adsorption capacity of Cat-cot/PSS10_t30/colCap10+_t30 sample was 21.58 mg/g.

A.2 Calculation of color strength (K/S value)

The color strength (K/S value) at λ_{max} 530 nm was calculated using the Kubelka-Munk equation as shown in equation (A.2).

$$\frac{K}{S} = \frac{(1-R)^2}{2R} \qquad \text{(A.2)}$$

where K = Sorption coefficient (cm^{-1})

S = Scattering coefficient (cm^{-1})

R = Reflectance of the cotton sample at 530 nm

For example,

The reflectance of the Cat-cot/PSS10_t30/colCap10+_t30 sample was 0.6621. (R = 0.6621; K/S_{blank} = 0.061699)

$$\frac{K}{S} = \frac{(1-R)^2}{2R}$$

K/S_{sample} = ((1 – 0.6621) x (1 – 0.6621)) / (2 x 0.6621)

= 0.0862

K/S = K/S_{sample} – K/S_{blank}

= 0.0862 – K/S_{blank}

= 0.0862 - 0.0617

= 0.0245

Therefore, the K/S value of Cat-cot/PSS10_t30/colCap10+_t30 sample was 0.0245.

A.3 Calculation of temperature differences (ΔT)

The thermal images of neat and treated cotton samples after taking out from the chilling system for 1 min (Fig. A.2 – A.7) were used for calculation their temperature differences (ΔT) using equation (A.3), in which the surface temperatures of neat cotton were Sp1, Sp2 and Sp3 and treated cotton were Sp4, Sp5 and Sp6.

$$\Delta T = T_{neat,avg} - T_{sample} \qquad (A.3)$$

where $T_{neat,avg}$ = The average values of the surface temperature of neat cotton (°C)

T_{sample} = The surface temperature of treated cotton (°C)

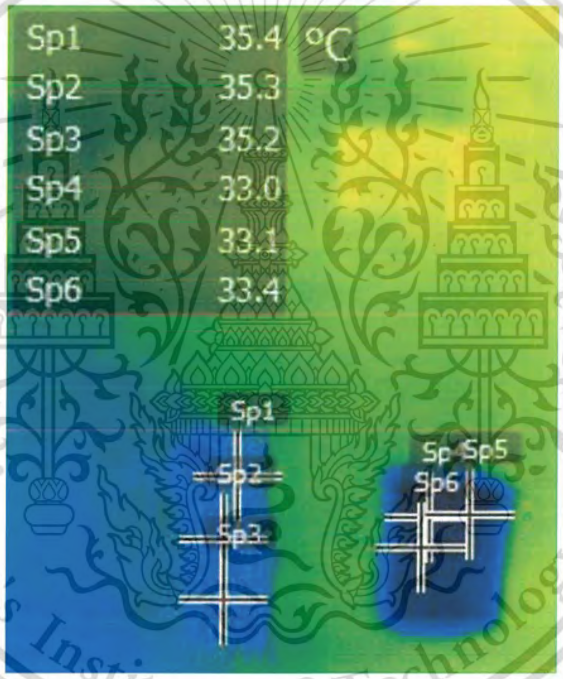

Figure A.2 Surface temperature of neat cotton and Cat-cot/(PSS10/Cap10+)_x1 sample

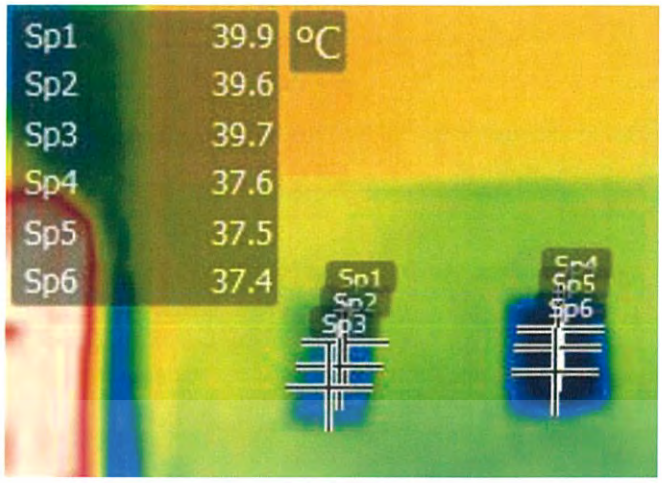

Figure A.3 Surface temperature of neat cotton and Cat-cot/(PSS10/Cap10+)_x3 sample

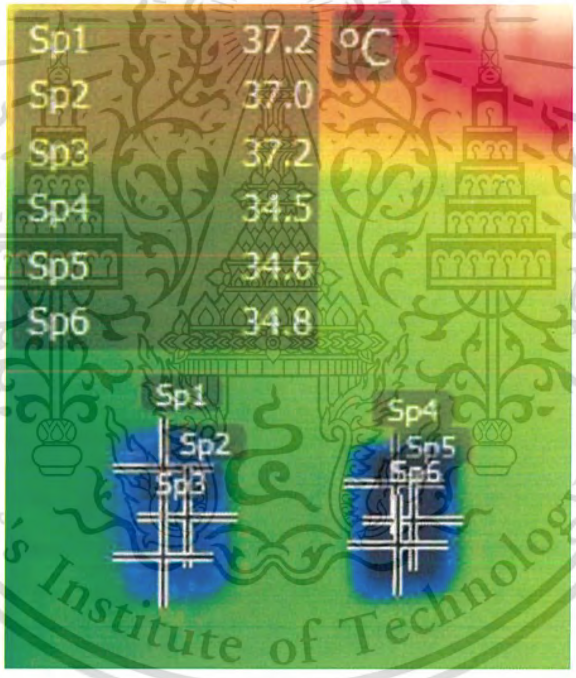

Figure A.4 Surface temperature of neat cotton and Cat-cot/(PSS10/Cap10+)_x5 sample

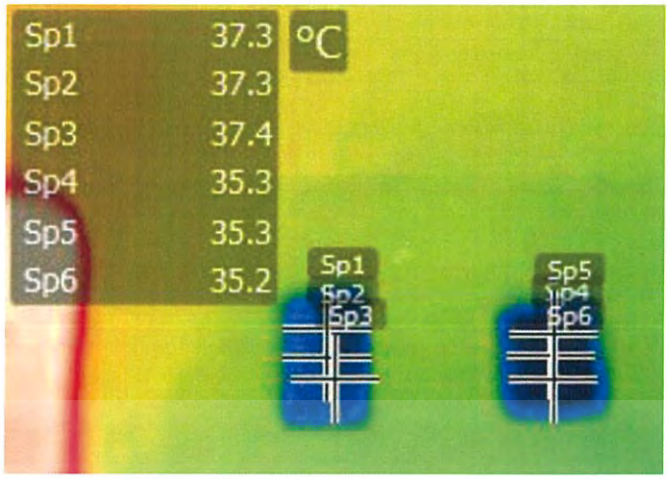

Figure A.5 Surface temperature of neat cotton and Cat-cot/Cap-_t10 sample

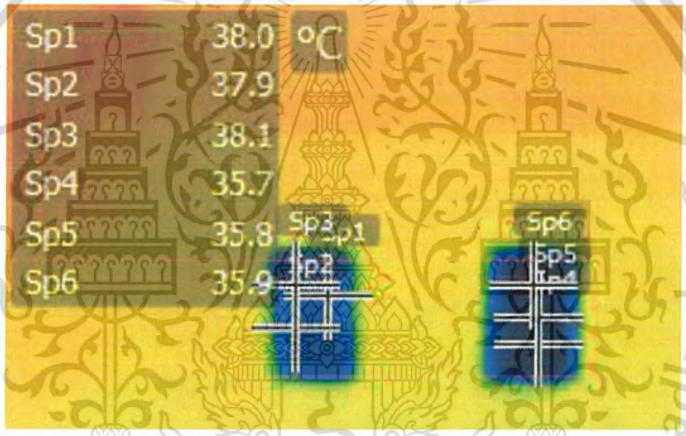

Figure A.6 Surface temperature of neat cotton and Cat-cot/(Cap-/Cap10+)_x3 sample

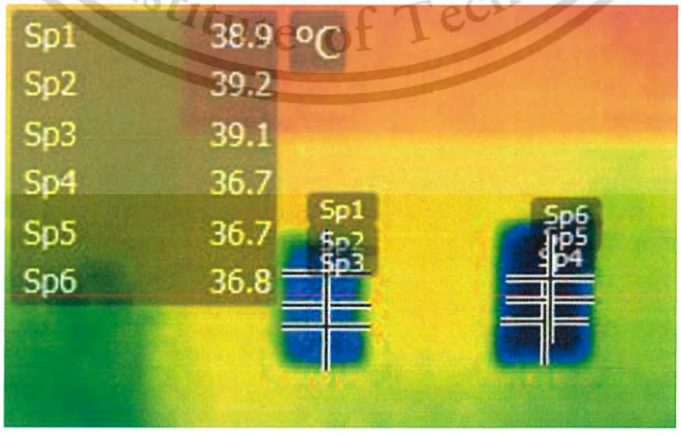

Figure A.7 Surface temperature of neat cotton and Cat-cot/(Cap-/Cap10+)_x5 sample

For example,

From Fig. A.2 (Left sample), the surface temperatures of neat cotton were recorded from 3 different positions, i.e. 35.4, 35.3 and 35.2 °C, in which they were averaged to obtained $T_{neat,avg}$ as shown below.

$$T_{neat,avg} = (35.4 + 35.3 + 35.2) / 3 = 35.3 \text{ °C}$$

The surface temperatures of Cat-cot/(PSS10/Cap10+)_x1 sample were also recorded from 3 different positions, i.e. 33.0, 33.1 and 33.4 °C as shown in Fig. A.2 (Right sample). The ΔT values of each position were calculated as follows:

$$\Delta T = T_{neat,avg} - T_{sample}$$
$$= 35.3 - 33.0$$
$$= 2.3 \text{ °C}$$

A.4 Calculation of water vapor transmission rate (WVTR)

The WVTR in g/m^2/day was calculated from the loss in mass of water in the test tube using equation (A.4).

$$WVTR = \frac{24M}{At} \quad (A.4)$$

where M = The loss in mass of water in the test tube (g)
A = Area of test tube (m^2)
t = Time used in the measurement (hr)

For example,

The loss in mass of water of the Cat-cot/PSS10_t30/colCap+_t30 sample was 0.5314 g. (M = 0.5314 g; A = 0.00013279 m^2; t = 24 hr)

$$WVTR = 24M / At$$
$$= (24 \times 0.5314) / (0.00013279 \times 24)$$
$$= 4{,}002 \text{ g/m}^2\text{/day}$$

Appendix B : Photographs

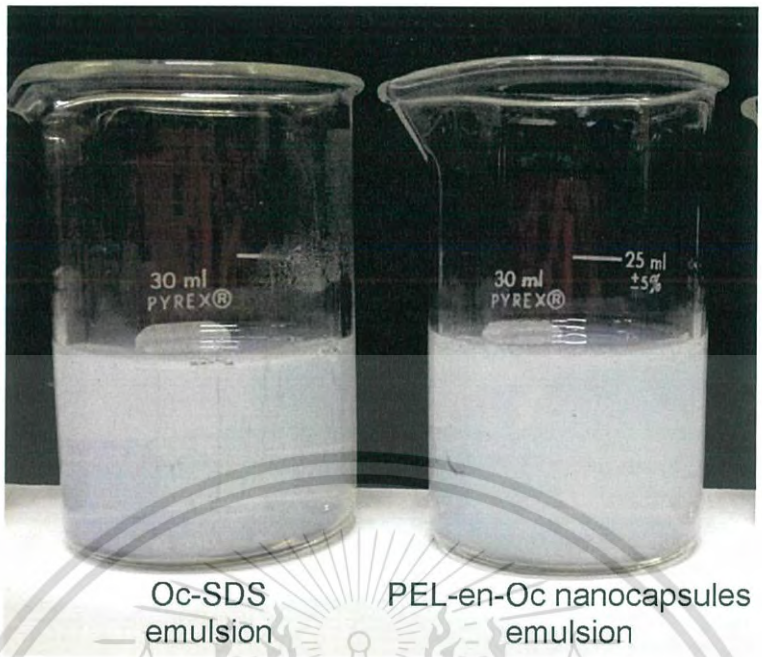

Figure B.1 Photograph of Oc-SDS emulsion and PEL-en-Oc nanocapsules emulsion

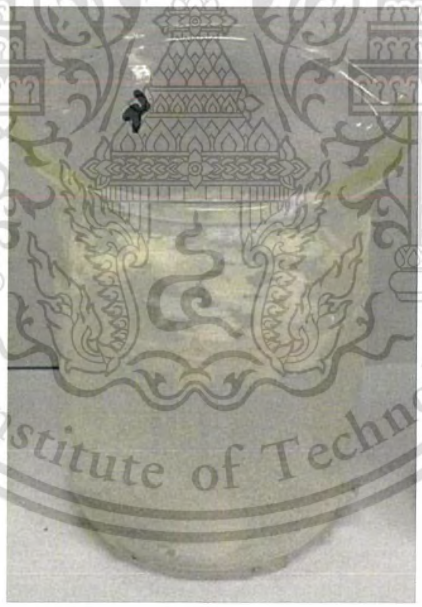

Figure B.2 Photograph of flocculation phenomena

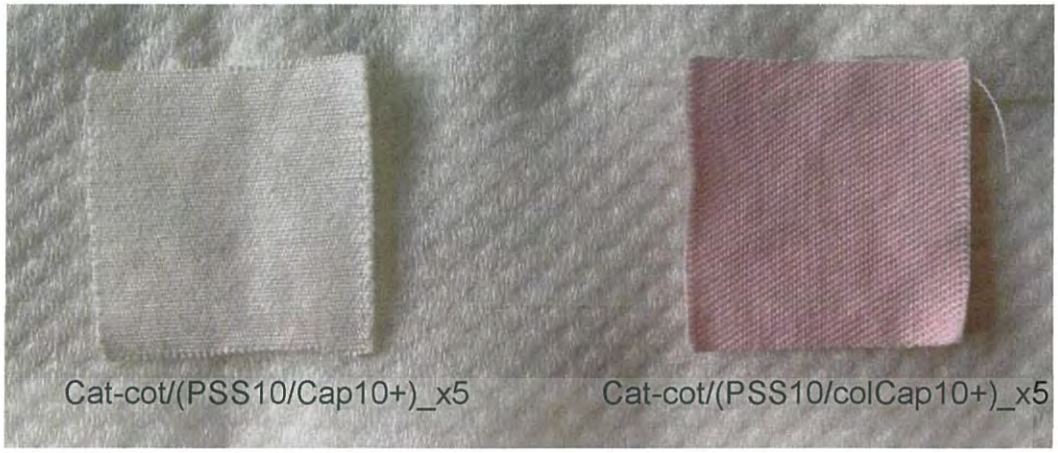

Figure B.3 Photograph of Cat-cot/(PSS10/Cap10+)_x5 and Cat-cot/(PSS10/colCap10+)_x5 samples

Appendix C : DSC and TGA thermograms

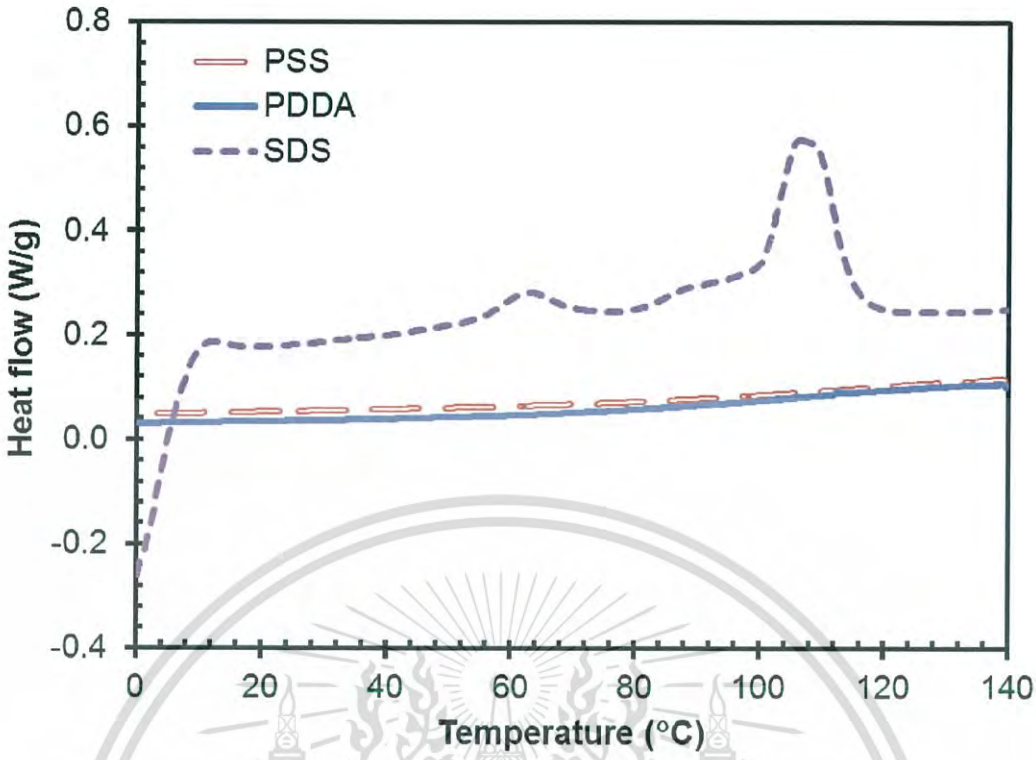

Figure C.1 DSC thermograms of SDS, PDDA and PSS

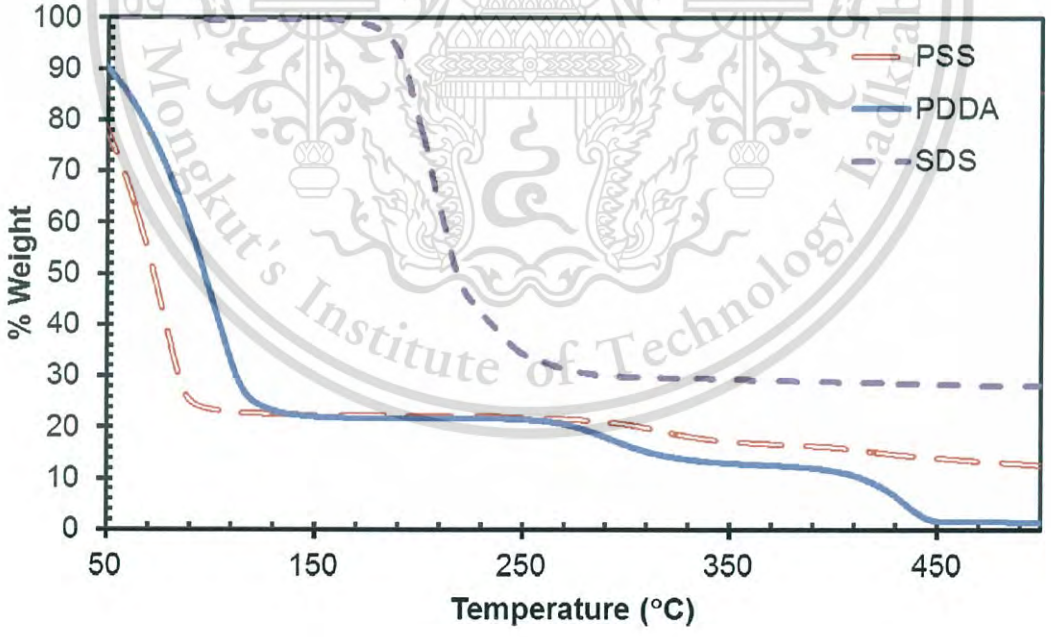

Figure C.2 TGA thermograms of SDS, PDDA and PSS

Appendix D : K/S values

Table D.1 K/S values of Cat-cot/PSS when using various PSS concentrations in the treatment

Sample	PSS concentration (mM)	K/S
Cat-cot/PSS1_t30	1	0.0082 ± 0.0004
Cat-cot/PSS5_t30	5	0.0117 ± 0.0007
Cat-cot/PSS10_t30	10	0.0159 ± 0.0010
Cat-cot/PSS20_t30	20	0.0185 ± 0.0004
Cat-cot/PSS30_t30	30	0.0212 ± 0.0009
Cat-cot/PSS40_t30	40	0.0241 ± 0.0009
Cat-cot/PSS50_t30	50	0.0278 ± 0.0009

Appendix E : Dye adsorption capacities

Table E.1 MB adsorption capacities of Cotton, Cat-cot, Cat-cot/PSS and Cat-cot/PSS/Cap4+ when using various PSS concentrations

Sample	PSS concentration (mM)	MB Adsorption capacity (mg/g)	
		Before capsule immobilization	After capsule immobilization
Cotton	-	1.304 ± 0.004	n/a
Cat-cot	0	0.015 ± 0.002	n/a
Cat-cot/PSS1_t30	1	0.129 ± 0.002	0.014 ± 0.002
Cat-cot/PSS5_t30	5	0.293 ± 0.006	0.019 ± 0.001
Cat-cot/PSS10_t30	10	0.331 ± 0.002	0.022 ± 0.001
Cat-cot/PSS20_t30	20	0.649 ± 0.002	0.023 ± 0.001
Cat-cot/PSS30_t30	30	1.095 ± 0.004	0.025 ± 0.001
Cat-cot/PSS40_t30	40	1.645 ± 0.004	0.028 ± 0.001
Cat-cot/PSS50_t30	50	2.205 ± 0.002	0.031 ± 0.002

Table E.2 EO adsorption capacities of Cat-cot/PSS/Cap4+ when using various PSS concentrations

Sample	PSS concentration (mM)	EO Adsorption capacity (mg/g)
Cat-cot/PSS1_t30/Cap4+_t30	1	16.641 ± 0.015
Cat-cot/PSS5_t30/Cap4+_t30	5	17.419 ± 0.008
Cat-cot/PSS10_t30/Cap4+_t30	10	18.362 ± 0.012
Cat-cot/PSS20_t30/Cap4+_t30	20	19.328 ± 0.012
Cat-cot/PSS30_t30/Cap4+_t30	30	20.249 ± 0.009
Cat-cot/PSS40_t30/Cap4+_t30	40	21.124 ± 0.018
Cat-cot/PSS50_t30/Cap4+_t30	50	22.106 ± 0.015

Table E.3 MB adsorption capacities of Cat-cot/PSS/Cap4+ and Cat-cot/PSS/Cap10+ when using various PSS concentrations

Sample	MB Adsorption capacity (mg/g)	
	Cap4+	Cap10+
Cat-cot/PSS1_t30/Cap+_t30	0.014 ± 0.002	0.004 ± 0.003
Cat-cot/PSS5_t30/Cap+_t30	0.019 ± 0.001	0.005 ± 0.005
Cat-cot/PSS10_t30/Cap+_t30	0.022 ± 0.001	0.009 ± 0.005
Cat-cot/PSS20_t30/Cap+_t30	0.023 ± 0.001	0.008 ± 0.002
Cat-cot/PSS30_t30/Cap+_t30	0.025 ± 0.001	0.003 ± 0.002
Cat-cot/PSS40_t30/Cap+_t30	0.028 ± 0.001	0.002 ± 0.002
Cat-cot/PSS50_t30/Cap+_t30	0.031 ± 0.002	0.008 ± 0.003

Table E.4 EO adsorption capacities of Cat-cot/PSS/Cap4+ and Cat-cot/PSS/Cap10+ when using various PSS concentrations

Sample	EO Adsorption capacity (mg/g)	
	Cap4+	Cap10+
Cat-cot/PSS1_t30/Cap+_t30	16.641 ± 0.015	19.064 ± 0.007
Cat-cot/PSS5_t30/Cap+_t30	17.419 ± 0.008	20.351 ± 0.021
Cat-cot/PSS10_t30/Cap+_t30	18.362 ± 0.012	21.572 ± 0.009
Cat-cot/PSS20_t30/Cap+_t30	19.328 ± 0.012	23.088 ± 0.016
Cat-cot/PSS30_t30/Cap+_t30	20.249 ± 0.009	24.334 ± 0.009
Cat-cot/PSS40_t30/Cap+_t30	21.124 ± 0.018	25.835 ± 0.006
Cat-cot/PSS50_t30/Cap+_t30	22.106 ± 0.015	26.494 ± 0.022

Author Biography

Name	Miss Yuwanda Iamphaojeen
Date of Birth	July 14, 1987
Address	78/2 M.5 Nawamin Road, Bungkum, Bangkok 10240, THAILAND
E-mail	yuwanda.iam@gmail.com
Education	
2005 – 2009	B.Sc. in Industrial Chemistry, GPA 3.27, Faculty of Science, King Mongkut's Institute of Technology Ladkrabang, Thailand Special project topic: Surface Modification of High Strength Polyethylene Fiber Sheets with Calcium Silicate for Medical Applications
2009 – 2011	M.Sc. in Polymer Technology, GPA 4.00, Faculty of Science, King Mongkut's Institute of Technology Ladkrabang, Thailand Thesis topic: Immobilization of Zinc Oxide Nanoparticles on Cotton fabrics using Poly 4-Styrenesulfonic acid Polyelectrolyte
Scholarships	
2009 - 2011	Scholarship from Faculty of Science, King Mongkut's Institute of Technology Ladkrabang for M.Sc. degree in Polymer Technology
2011 - 2014	Scholarship from the Royal Golden Jubilee Ph.D Program, Thailand Research Fund
Awards	
2011	Award from Professor Dr. Tab Nilanidhi's Foundation for outstanding academic excellence awards in Master of Science
2012	Qualified the quarter-finals of Sci & Tech Innovation and Sustainability Awards 2012: Energy and Environmental Technology for Sustainable Society Title: Immobilization of ZnO nanoparticles on cotton fabric by environmental friendly process
2015	Award from RGJ-Ph.D. Congress XVI for outstanding oral presentation

Academic Publications

- Iamphaojeen, Y. and Siriphannon, P., (2011). Growth of ZnO nanoparticles on poly 4-styrenesulfonic acid modified cotton fabrics and UV protection property, KKU Science Journal, 39(3), 459-465.

- Iamphaojeen, Y. and Siriphannon P., (2012). Immobilization of zinc oxide nanoparticles on cotton fabrics using poly 4-styrenesulfonic acid polyelectrolyte. International Journal of Materials Research, 103(5), 643-647. http://dx.doi.org/10.3139/146.110726

- Iamphaojeen, Y. and Siriphannon P., (2014). Nanoencapsulation of *n*-octadecane phase change material in self-assembled polyelectrolyte by soft solution technique. International Journal of Polymeric Materials and Polymeric Biomaterials, 63(17), 918-922. http://dx.doi.org/10.1080/00914037.2014.886229

- Iamphaojeen, Y., Manian A. P., Wright T., Caven B., Bechtold T. and Siriphannon P., (2016). Polyelectrolyte assisted immobilization of oil-based nanocapsules on cotton fabric. Australian Journal of Chemistry, 69, 811-816. http://dx.doi.org/10.1071/CH15746

Conferences

- Iamphaojeen Y. and Siriphannon P., (2011, March 17-18). Growth of nano-ZnO seeds immobilized on cotton fabrics using poly 4-styrenesulfonic acid. 5th SWU Academic Conference, Srinakharinwirot University, Bangkok, THAILAND.

- Siriphannon, P., and Iamphaojeen, Y., (2012, Sep 23-26). Growth of nano-zno seeds immobilized on cotton fabrics using poly 4-styrenesulfonic acid. 15th International Conference on Advances in Materials & Processing Technologies, Wollongong, AUSTRALIA.

- Iamphaojeen, Y. and Siriphannon P., (2016, March 13-17). Effect of polyelectrolyte multilayers shell on thermal properties of *n*-octadecane phase change material nanocapsule. 251st American Chemical Society National Meeting & Exposition, San Diego, California, USA.

Experience

Apr 2008 - May 2008 Trainee at the Toyota Motor Thailand Co., Ltd.– Samutprakarn, THAILAND

Jun 2009 - Aug 2009	Research assistant for the development project of Nippon Paint (Thailand) Co.,Ltd, THAILAND
Jun 2011 - Aug 2011	Teaching assistant of General Chemistry Laboratory at King Mongkut's Institute of Technology Ladkrabang, THAILAND
Mar 2014 - Aug 2014	Research abroad at Research Institute of Textile Chemistry and Textile Physics, University of Innsbruck, AUSTRIA